Investigation of the Repairability of Thermoplastic Composite Structures Through Conduction Welding

Calvin Zachary Bijl

A thesis submitted to the Faculty of Graduate Studies in partial fulfillment of the requirements for the degree of Master of Applied Science

Graduate Program in Mechanical Engineering

Lassonde School of Engineering

York University

Toronto, Ontario, Canada

Abstract

Thermoplastic composites are gaining prominence in various industries for their recyclability and superior mechanical properties. This thesis investigates the use of thermoplastic composites, emphasizing their notable capability for repair and joining through conduction welding, a cost-effective fusion bonding technique that eliminates the necessity for adhesives or mechanical fasteners in the assembly of composite materials. By applying this method, the repairability of thermoplastic composite samples is assessed through the application of variously sized repair patches welded to open hole tensile samples. Furthermore, this research investigates the optimization of welding parameters, such as temperature and compaction pressure, aiming to produce high shear strength joints produced by this technique. The findings of these studies highlight the potential of conduction welding as an effective and economical approach for the assembly and repair of thermoplastic composites, suggesting its promise for wider adoption in composite manufacturing and repair processes.

Dedication and Acknowledgements

Firstly, I would like to thank my supervisor, Dr. Garrett Melenka, for his invaluable guidance and support over the last two years. His open-door policy and readiness to offer advice whenever I encountered challenges have been a cornerstone of my journey. Dr. Melenka has consistently pushed me to expand my boundaries and has provided numerous opportunities for professional development, for which I am deeply grateful. The time and patience he has invested in assisting me with this thesis have been crucial to my success and this work would not have been possible without his help every step of the way.

I also wish to extend my gratitude to my lab mates, whose presence made this journey both enjoyable and enriching. The numerous late nights and weekends dedicated to our research were not only productive but also genuinely enjoyable, thanks to our collective efforts and camaraderie. I am thankful for the constant exchange of ideas and the support provided throughout this process. The sense of community and mutual assistance within our lab significantly contributed to the completion of my thesis. Thank you to everyone for being an essential part of this experience and for making it memorable.

Table of Contents

Table of Figures

List of Tables

List of Abbreviations

ANOVA	Analysis Of Variance
DIC	Digital Image Correlation
DSC	Differential Scanning Calorimetry
FEM	Finite Element Method
GMA	Glycidyl Methacrylate
IRT	Infrared Thermography
LM-PAEK	Low-Melt Poly-Aryl-Ether-Ketone
NDI	Non-Destructive Inspection
PAN	Polyacrylonitrile
PEEK	Poly-Ether-Ether-Ketone
PEKK	Poly-Ether-Ketone-Ketone
PMMA	Poly-Methyl Methacrylate
SCF	Stress Concentration Factor
TPC	Thermoplastic Composite
TPU	Thermoplastic Polyurethane
UHMWPE	Ultra-High Molecular Weight Polyethylene
UTS	Ultimate Tensile Strength

List of Variables

C_p	Specific Heat Capacity
L_c	Characteristic Length
T_∞	Boundary Temperature
T_i	Initial Temperature
A	Surface area of the susceptor
Ac	Cross sectional surface area
E	Elastic Modulus
f	Frequency of the magnetic field
F	Force
$H(I)$	Magnetic field intensity
I	Applied Current
k	Thermal Conductivity
P	Power
Q	Heat Generated
R	Electrical Resistance
α	Thermal Diffusivity
ε	Strain
ρ	Density
σ	Stress
τ	Fourier Number
ω	Frequency of oscillations

Chapter 1: Introduction

1.1 Motivation

With the relentless pursuit of efficiency and performance increases, composite materials, particularly fiber-reinforced polymers, have emerged as critical materials in this endeavor. Driven by the need for components that are both stronger and lighter, engineers have increasingly utilized these materials, exploiting their exceptional strength-to-weight ratios [1], [2]. The implementation of composites has been further enhanced by their tailorable mechanical properties. This is achieved through strategic fiber orientation utilizing their impressive tensile strength to resist loading in desired directions. This approach not only enhances strength where it is most needed but also allows for the removal of material in non-critical areas, further reducing the overall weight of the structure. These innovations in material science have been pivotal in advancing industries such as aerospace, automotive, and energy [3]. A prime example is the adoption of composites in aircraft, significantly enhancing airframe strength and reducing weight. Modern aircraft such as the Boeing 787 is comprised of 50% composite materials enabling this aircraft to achieve a 20% weight reduction compared to traditional aluminum designs [4], [5], [6]. Another example of composite material use is the energy generation industry utilizing composite materials to manufacture wind turbine blades [7].

Despite the clear advantages that composite materials possess there is one inherent downside, their lack of recyclability [7], [8]. Traditional composite materials are predominantly made with thermosetting epoxy resins which undergo irreversible chemical reactions during their curing process [9]. This process restricts the matrix from being remelted or being dissolved in a solvent.

Because of the lack of viable recycling techniques, composites at the end of their lifecycle are commonly discarded to landfills [10], [11].

In contrast, thermoplastic composite materials offer an alternative to this waste. Thermoplastics, being polymers that can be reheated and reshaped multiple times, facilitate not only repeated remolding but also allow for the dissolution and recovery of embedded fibers[12], [13]. This recyclability positions thermoplastic composites as a more environmentally friendly option while also offering other benefits such as rapid processing times, higher fracture toughness, and higher impact resistance [14], [15], [16].

In addition to their inherent recyclability, thermoplastic composites can take advantage of their ability to be remelted to be welded together in a process called fusion bonding [17], [18]. This process introduces the potential for repairs to be made to composites structures extending the lifecycle of these materials and reducing their environmental footprint.

The repair of traditional composite materials presents a host of challenges stemming from their complex damage mechanisms and their irreversible curing process [2]. The inherent thermal resistance of thermosets, while beneficial in some use cases, makes it impossible to repair these materials by remelting the polymer matrix. Because of this, structural adhesives are commonly used when attempting to repair a thermoset composite [19]. However, this comes with other challenges such as extensive surface preparation, long curing times and weakened overall strength in the structure [20], [21].

In contrast, thermoplastic composites offer new and innovative solutions to the challenges faced when attempting composite repairs. The ability for these materials to be reheated and reshaped multiple times allows for new repair methodologies such as the fusion bonding method. Fusion

bonding, also called plastic welding, takes advantage of the remeltability of thermoplastics to soften the matrix material in a damaged area to reform the matrix into a single cohesive structure again [6], [22]. With fusion bonding, repairs can be performed quickly without the use of adhesives eliminating the need for surface preparation and long cycle times [20] . This innovative method is also being investigated for its use in the joining of composite structures, removing the need for adhesives or bolts. These characteristics, combined with the potential for recycling, positions thermoplastic composites as a promising new material. The subsequent sections of this thesis will delve deeper into the properties of thermoplastic composites, exploring how their unique characteristics can be leveraged to overcome the traditional obstacles in composite material repair.

1.2 Objective

The objective of this thesis is to investigate the repairability of thermoplastic composites utilizing a subclass of fusion bonding called conduction welding, which is a low-cost plastic welding technique. To complete this objective, the thesis will detail two studies. In both studies the samples used will be a thermoplastic composite made from carbon fiber and a novel liquid thermoplastic resin, manufactured via resin infusion. The first study focuses on the effectiveness of repair patches applied using conduction welding, and a second study focusing on the optimization of the conduction welding process to address current gaps in the literature.

In the first study, various sizes of repair patches, ranging from 12.5 mm by 12.5 mm to 50 mm by 25 mm are applied to damaged composite samples. Undamaged samples will be used as a control specimen and will allow for the calculation of the percentage of recovered strength for the repaired samples, ultimately revealing the repairs effectiveness. The damage is standardized across samples by drilling a hole in the center of the samples, ensuring consistent comparison. Testing involves

tension experiments using a universal testing machine and Digital Image Correlation (DIC) for detailed strain analysis.

The second study aims to optimize critical welding parameters such as temperature, welding time, and contact pressure to enhance bonding strength. Lap shear joints are fabricated and tested to identify the best processing conditions to enable high strength joints. The study also employs optical microscopy for analyzing the void content at the bonding interface, contributing to the optimization process. This optimization will not only further enhance the effectiveness of repairs but also provide a general guideline for other researchers investigating the use of conduction welding.

The results from these studies will demonstrate the effectiveness of the conduction welding process for joining thermoplastic composites. In addition, the results will demonstrate the strength of repair patches applied utilizing this method. Through these results, this thesis hopes to fill the gaps in the current literature on this topic and provide areas for future researchers to investigate.

1.3 Thesis Outline

This thesis is organized into five chapters, each discussing various aspects of composite materials with a focus on novel thermoplastic composites. Chapter 2 begins the discussion with a comprehensive literature review of current research in the field of composite materials. The chapter begins with a review of the fundamentals of composites, their material properties, and classifications. Next it discusses various manufacturing methods for composite materials. It also looks at current literature in the field of fusion bonding and its applications for joining and repair of thermoplastic composites. Furthermore, various mechanical testing methods are discussed, and digital image correlation (DIC) is introduced as an effective means of measuring deformation

during mechanical testing. Finally, this chapter focuses on identifying gaps in the current literature with regards to fusion bonding of thermoplastic composites and proposes a study to fill these gaps. The gaps identified in this section will then be addressed in chapters three and four.

Chapter 3 focuses on a research study that aims to evaluate the effectiveness of various repair patches applied to tensile composite samples. A novel liquid thermoplastic is utilized to fabricate tensile samples which are then damaged, and subsequently repaired with three different sizes of repair patches. These repair patches are applied using a low-cost method called conduction welding, implemented through a heated press. Samples are then tested using a universal testing cell and DIC is used to generate full field strain maps of the samples. A detailed discussion of the results is performed, and the effectiveness of the repairs is compared against other literature.

Chapter 4 focuses on the improvement of the conduction welding process utilized in Chapter 3 and aims to fill the gaps in the literature regarding optimal processing parameters. A study of the effects that welding temperature and compaction pressure have on the lap shear strength of conduction welded joints is performed. Utilizing statistical analysis, the findings of this study are examined and the influence of the variables on the resulting strength of the joints is discussed. Finally, optical microscopy is utilized to inspect the cross sections of the welded joints, providing insights into the bonding surface and the critical role temperature plays in the welding quality.

Chapter 5 summarizes and concludes the work done in this thesis and details future work to be undertaken in this field.

1.4 References

[1] A. K. Kaw, *Mechanics of composite materials*. Taylor & Francis, 2006.

[2] K. B. Katnam, L. F. M. Da Silva, and T. M. Young, "Bonded repair of composite aircraft structures: A review of scientific challenges and opportunities," *Progress in Aerospace Sciences*, vol. 61, pp. 26–42, Aug. 2013, doi: 10.1016/J.PAEROSCI.2013.03.003.

[3] J. P. Carey, *Handbook of Advances in Braided Composite Materials*. Elsevier, 2017. doi: 10.1016/C2014-0-03943-3.

[4] J. L. B.S.Kukreja, "Composites in the Aircraft Industry." Accessed: Jan. 11, 2024. [Online]. Available: https://www.appropedia.org/Composites_in_the_Aircraft_Industry

[5] Composites World, "Boeing sets pace for composite usage in large civil aircraft." Accessed: Nov. 02, 2023. [Online]. Available: https://www.compositesworld.com/articles/boeing-sets-pace-for-composite-usage-in-large-civil-aircraft

[6] J. Barroeta Robles, M. Dubé, P. Hubert, and A. Yousefpour, "Repair of thermoplastic composites: an overview," *Advanced Manufacturing: Polymer and Composites Science*, vol. 8, no. 2. Taylor and Francis Ltd., pp. 68–96, 2022. doi: 10.1080/20550340.2022.2057137.

[7] L. Mishnaevsky, K. Branner, H. Petersen, J. Beauson, M. McGugan, and B. Sørensen, "Materials for Wind Turbine Blades: An Overview," *Materials*, vol. 10, no. 11, p. 1285, Nov. 2017, doi: 10.3390/ma10111285.

[8] Y. Yang, R. Boom, B. Irion, D. J. van Heerden, P. Kuiper, and H. de Wit, "Recycling of composite materials," *Chemical Engineering and Processing: Process Intensification*, vol. 51, pp. 53–68, Jan. 2012, doi: 10.1016/j.cep.2011.09.007.

[9] Painter Paul C. and Coleman Michael M., *Essentials of Polymer Science and Engineering*. 2009.

[10] Chris Martin, "Wind Turbine Blades Can't Be Recycled, So They're Piling Up in Landfills," Bloomberg.

[11] N. Ramawat, N. Sharma, P. Yamba, and M. A. T. Sanidhi, "Recycling of polymer-matrix composites used in the aerospace industry-A comprehensive review," *Mater Today Proc*, Jun. 2023, doi: 10.1016/j.matpr.2023.05.386.

[12] D. S. Cousins, Y. Suzuki, R. E. Murray, J. R. Samaniuk, and A. P. Stebner, "Recycling glass fiber thermoplastic composites from wind turbine blades," *J Clean Prod*, vol. 209, pp. 1252–1263, Feb. 2019, doi: 10.1016/j.jclepro.2018.10.286.

[13] A. D. La Rosa, D. R. Banatao, S. J. Pastine, A. Latteri, and G. Cicala, "Recycling treatment of carbon fibre/epoxy composites: Materials recovery and characterization and

environmental impacts through life cycle assessment," *Compos B Eng*, vol. 104, pp. 17–25, Nov. 2016, doi: 10.1016/j.compositesb.2016.08.015.

[14] R. Stewart, "Thermoplastic composites-recyclable and fast to process," 2011. [Online]. Available: www.reinforcedplastics.com

[15] M. Kayaaslan, T. Coskun, U. M. Unlu, and O. S. Sahin, "Effects of thickness, fibre orientation and fabric textile on the low-velocity impact performances of thermoset and thermoplastic composites," *Journal of Thermoplastic Composite Materials*, vol. 36, no. 11, pp. 4408–4429, Nov. 2023, doi: 10.1177/08927057231158536.

[16] P. Bajurko, "Comparison of damage resistance of thermoplastic and thermoset carbon fibre-reinforced composites," *Journal of Thermoplastic Composite Materials*, vol. 34, no. 3, pp. 303–315, Mar. 2021, doi: 10.1177/0892705719844550.

[17] A. Yousefpour, M. Hojjati, and J. P. Immarigeon, "Fusion bonding/welding of thermoplastic composites," *Journal of Thermoplastic Composite Materials*, vol. 17, no. 4, pp. 303–341, Jul. 2004, doi: 10.1177/0892705704045187.

[18] C. Ageorges, L. Ye, and M. Hou, "Advances in fusion bonding techniques for joining thermoplastic matrix composites: a review," *Compos Part A Appl Sci Manuf*, vol. 32, no. 6, pp. 839–857, Jun. 2001, doi: 10.1016/S1359-835X(00)00166-4.

[19] S. Budhe, M. D. Banea, S. de Barros, and L. F. M. da Silva, "An updated review of adhesively bonded joints in composite materials," *Int J Adhes Adhes*, vol. 72, pp. 30–42, Jan. 2017, doi: 10.1016/j.ijadhadh.2016.10.010.

[20] W. P. Seneviratne, J. S. Tomblin, and B. L. Saathoff, "Influence of various surface preparation techniques on resistance welded and adhesively bonded unidirectional thermoplastic composite joints."

[21] S. Omairey, N. Jayasree, and M. Kazilas, "Defects and uncertainties of adhesively bonded composite joints," *SN Applied Sciences*, vol. 3, no. 9. Springer Nature, Sep. 01, 2021. doi: 10.1007/s42452-021-04753-8.

[22] J. P. Reis, M. de Moura, and S. Samborski, "Thermoplastic composites and their promising applications in joining and repair composites structures: A review," *Materials*, vol. 13, no. 24. MDPI AG, pp. 1–33, Dec. 02, 2020. doi: 10.3390/ma13245832.

Chapter 2: Literature Review

2.1 Introduction

Composite materials have seen increasing usage in recent years in many industries, such as the aerospace industry for rockets, the aviation industry for aircraft wings and fuselages, and automotive for car chassis and panels [1], [2]. From the usage in these industries, the current size of the composite material market is an estimated $117.47 billion in 2023 and is expected to grow to $216.04 billion by 2031 [3]. The steady growth in the industry is due to the ideal mechanical properties that composite materials exhibit with respect to their strength-to-weight ratio. High strength-to-weight ratios allow engineers to design very light yet incredibly strong structures. Another advantage that composites provide is their tailorable material properties. This is done by designing a laminate that takes advantage of the fibre's tensile strength to resist loading in specific directions. By doing this, designers and engineers can create materials that are able to resist loads in some directions and remove material in others, ultimately leading to stronger and lighter end products.

Traditionally, composite material markets have been dominated by the use of thermoset composites. These types of composites represent a market size of $55.3 billion in 2023 and are heavily favored in the industry because of their durability, high temperature and corrosion resistance, and wide range of manufacturing techniques [4]. However, thermoset composites possess one fundamental limitation: their lack of recyclability [5]. During the curing process of thermosets, an irreversible chemical reaction occurs, which cross-links the polymer chains. This cross-linking process restricts the polymer from being dissolved with solvents or being remelted and reshaped with heat [6].

Thermoplastics are a class of polymers that do not undergo crosslinking and, as a result, can be remelted and solidified multiple times with negligible impacts on their mechanical properties. Using these thermoplastic materials to create composites offers an alternative with many potential benefits, such as recyclability, repairability, rapid processing times, higher fracture toughness, higher impact resistance, and higher strength-to-weight ratios [7], [8], [9]. This remeltability has also allowed for the development of new welding techniques and the ability to repair composite materials that were previously impossible with thermosets. In a study by Ogugua et al. [10] the life cycle impact of the fabrication of thermoplastic and thermoset composites is compared. It is found that thermoplastic composites can reduce the global warming potential by roughly 30% compared to traditional thermoset composites. The authors also conclude that this reduction in global warming potential can be improved upon by considering various thermoplastic recycling techniques that were not included in their life cycle assessment. Another dramatic reduction in environmental impact could be seen by reclaiming the embedded fibres for reuse. This is because fibre production accounts for almost 30% of the total energy demand while manufacturing composite materials. By taking products at the end of their life and recovering fibre and matrix materials to be reused for other applications, the environmental impact of these materials decreases dramatically [11], [12]. The inherent capability of these composites to be re-melted not only offers another method to reduce their carbon footprint but also introduces repairability as a significant benefit [13]. Various damage mechanisms such as matrix cracking, delamination, and fibre fracture can be more easily addressed with thermoplastics by re-melting the matrix material. Through new fields of study focused on their reparability, the lifespan of composite materials can be extended, eliminating the need for replacement and again lowering the overall carbon footprint created. Because of these benefits, the thermoplastic composite market has been growing in recent years,

reaching a market size of $19.22 billion in 2023 and is expected to grow to $24.29 billion in 2027 [14].

This work aims to determine the repairability of thermoplastic composite structures and test their mechanical properties with various repair patch sizes applied via conduction welding. This is done to explore the viability of this welding process and determine the optimal repair patch size. This chapter will begin by discussing essential topics in the field of thermoplastic composite materials. It will analyze current and past literature to give a thorough background on the fundamental principles of composite materials. A comprehensive review of composite material manufacturing methods and classifications will be discussed, along with composite material repairs and mechanical testing methods. An analysis of composite material testing through digital image correlation will also be investigated. Finally, this chapter will aim to identify gaps in the current academic literature and propose studies to fill these gaps.

2.2 Composite Materials

A composite material is characterized by the combination of two or more components at a macroscopic scale. The goal of combining these materials is to get a new material with mechanical properties greater than either of the individual components. Typically, a composite comprises a reinforcing element and a matrix component.

The reinforcement element provides the material's overall strength and is the primary component in load bearing. The reinforcement materials are typically made of fibres with high specific tensile strength and can withstand large loads in tension but have zero compressive strength on their own. Many types of fibrous reinforcement materials, such as glass, carbon, and aramid, are used today.

These fibres come in many different shapes and sizes, which can be seen in Figure 2-1, such as continuous unidirectional fibres (a), woven fibres (b), and chopped randomly oriented fibres (c).

The matrix component holds the reinforcement material in place and distributes applied loads to the fibres. Polymer matrix materials are commonly used as they provide an even distribution of an applied load while offering excellent environmental and chemical resistance. Combining these two materials allows composite materials to have exceptional strength-to-weight ratios.

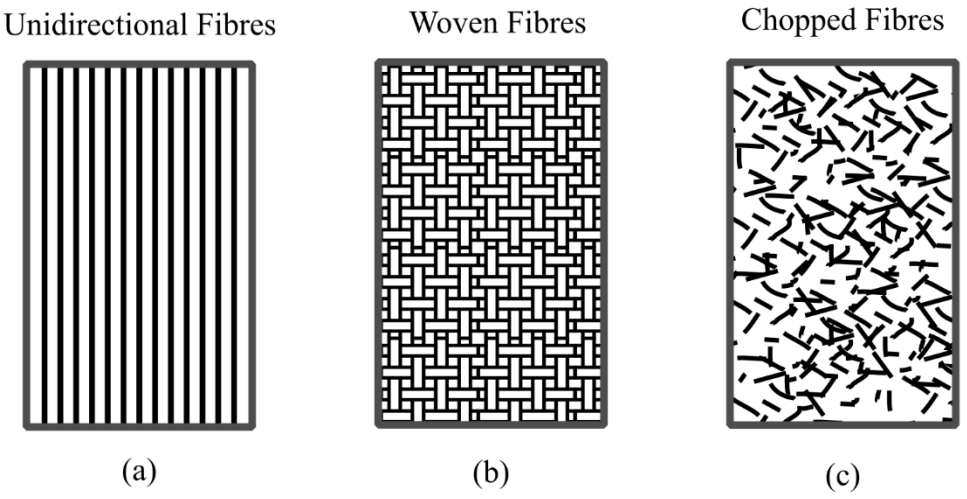

Figure 2-1: Comparative diagram of composite materials showcasing (a) unidirectional fibres with fibres aligned in one direction, (b) plain woven fibres illustrating a textile weave pattern for strength in two directions, and (c) chopped fibres in random orientations for isentropic reinforcement

2.2.1 Reinforcement Materials

Reinforcement materials used in composite structures are most commonly fibres such as glass, carbon, aramid, or natural fibres. These fibres are individually small, measuring between 5 and 20 microns in diameter [15], [16]. Fibres are bundled together in the thousands to form tows of fibres, which can be placed unidirectionally or woven together to form textiles or braids. Glass fibres, used in Fibreglass composites, are made by drawing molten glass through fine orifices [17].

Carbon fibres can be manufactured from two different precursor materials, pitch or polyacrylonitrile (PAN). Pitch is a viscoelastic hydrocarbon precursor made from crude oil, coal, or plant materials and fibers are created by melt spinning threads of this viscoelastic precursor. Next a series of heat treatments are performed to crosslink the fibers and remove any nonorganic material [18]. PAN based carbon fibers are created from precursor material of PAN, where the PAN fibres are extruded to the desired diameter and then subjected to a series of heat treatments and chemical processes to achieve the desired strength and stiffness [19]. Pitch based carbon fibers are known to be more expensive and have a lower ultimate tensile strength compared to PAN fibers but often have a higher stiffness and are commonly known as high modulus fibers [20]. Aramid fibres are synthesized from aromatic polyamide and are naturally abrasive and impact-resistant [21]. Natural fibres like jute, flax, and hemp are derived from plant sources [22].

Fibres are chosen based on their material properties, which include tensile strength, stiffness, and low weight. Fibre orientation must also be decided as composite materials have the unique property of being anisotropic. Because fibres are best at resisting loads in tension, the mechanical properties of a composite are primarily dictated by the angle at which the fibres are aligned, and careful consideration must be given to their orientation to be able to resist loads. The applications of these reinforcement fibres are vast, ranging from aerospace components, where lightweight and high strength are crucial, to automotive parts, sporting goods, and even everyday consumer products. In Table 2-1, a summary of the specific strengths and weaknesses of composite fibres can be seen.

Table 2-1: Reinforcement material strengths and weaknesses[21]

Fibre Material	Strengths	Weaknesses
Carbon Fibres	• Excellent strength-to-weight ratio • High stiffness • Excellent corrosion resistance • Excellent fatigue resistance	• High cost • Brittle fractures
Glass Fibres	• Low cost • Good impact resistance	• Lower specific strength than alternatives
Aramid Fibres	• High abrasion resistance • High impact resistance	• High UV sensitivity • Difficulty machining
Natural Fibres (e.g., Jute, Flax, Hemp)	• Sustainable material • Biodegradable • Low cost	• Lower mechanical properties than alternatives • Moisture absorption • Variability in mechanical properties

2.2.2 Matrix Materials

Matrix materials are used in composite structures to bind the reinforcement fibres in place, ensuring an even distribution of stress and adding unique mechanical properties such as corrosion resistance, ultraviolet radiation resistance, and moisture resistance. Among the commonly used matrix materials are polymers like epoxy, polyester, vinyl ester, nylon, polypropylene, and Poly-methyl methacrylate (PMMA) [23]. These polymers can be divided into two categories, thermoset polymers and thermoplastic polymers, and these classifications will be discussed in detail in the next section.

In terms of applications, epoxy resins such as Bisphenol-A or Glycidylamine are often favored in the aerospace and automotive sectors due to their superior mechanical properties and temperature resistance [23]. Polyesters find extensive use in boat hulls and other marine applications, as well as gel coats on the surface of composite parts due to their moisture resistance and low cost [24]. Thermoplastics like nylon and polypropylene are prevalent in consumer goods, while PMMA is a popular choice for optical applications like eyeglass lenses and windows [25], [26]. High-performance thermoplastics like poly-ether-ether-ketone (PEEK) and poly-ether-ketone-ketone (PEKK) are generally used in engineering applications that require high-strength plastics. These engineering materials are also biocompatible and are used in dental and medical applications [27].

Each matrix material comes with its benefits and challenges, and the specific requirements of the intended application often dictate the choice. A table of the advantages and disadvantages of each of these polymer matrix materials can be seen below in Table 2-2.

Table 2-2: Polymer matrix materials strengths and weaknesses [28]

Matrix Material	Strengths	Weaknesses
Bisphenol - A Epoxy (Thermoset)	• High mechanical strength • Good chemical resistance	• Brittle fracture • Temperature sensitivity • No recyclability
Glycidylamine Epoxy (Thermoset)	• Low viscosity • High Temperature Resistance	• No recyclability • Relatively expensive
Polyester (Thermoset)	• Cost-effective • Good flexibility	• Lower chemical resistance than epoxy • Can shrink during curing
Vinyl ester (Thermoset)	• Superior corrosion resistance • Good fatigue resistance	• More expensive than polyester • Can be brittle
Nylon (Thermoplastic)	• High strength and toughness • Good wear resistance	• Moisture absorption can affect properties • Can be expensive
Polypropylene (Thermoplastic)	• Lightweight • Good chemical resistance	• Lower melting point • Lower Durability
PMMA (Thermoplastic)	• Clear and transparent • UV resistant	• Can be brittle • Not resistant to solvents
PEEK (Thermoplastic)	• High-temperature resistance • Excellent mechanical properties	• Expensive • Difficult to process
PEKK (Thermoplastic)	• Similar to PEEK but better moldability • Biologically inert	• Expensive • Limited availability

2.3 Composite Material Classification

Two primary polymer classifications can be used in fibre-reinforced polymer composites: a thermoset polymer and a thermoplastic polymer. In this section, their differences will be discussed. Below in Figure 2-2, an example of a (a) thermoset and a (b) thermoplastic used in everyday life can be seen. Figure 2-2 (a) shows a circuit board which is made using glass fibres and a thermosetting phenolic resin, and Figure 2-2 (b) shows a 3d printed part which takes advantage of thermoplastics re-meltable nature to extrude resin into a complex 3-dimensional shape.

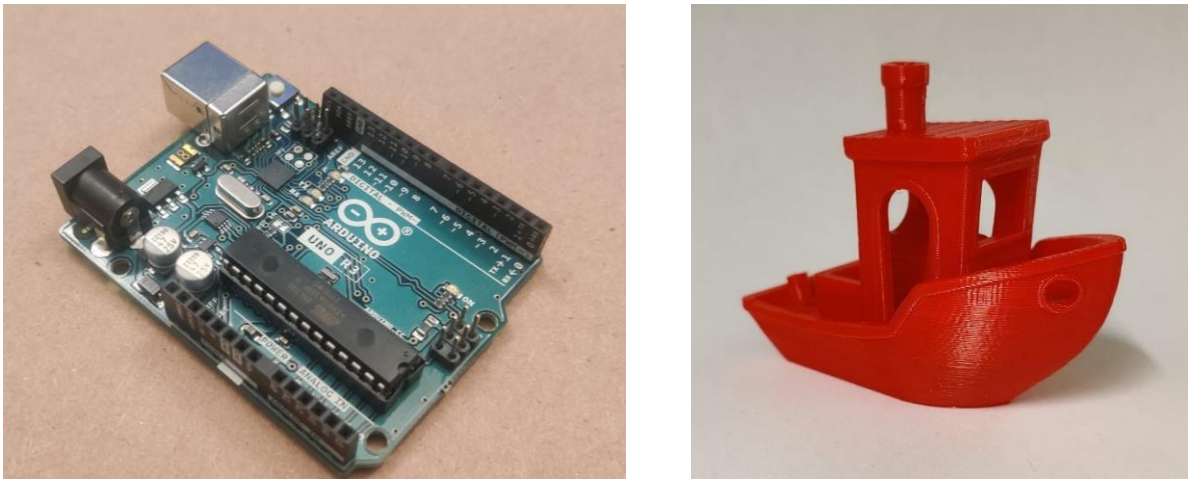

(a) (b)

Figure 2-2: Examples of thermoset and thermoplastics that are seen in everyday life. (a) shows an example of a thermoset resin used to create the base of a circuit board. (b) shows a thermoplastic resin extruded into a 3d shape to make a common 3d print

2.3.1 Thermoset Composites

A thermoset polymer is a class of polymer that undergoes an irreversible chemical reaction during solidification [6]. This chemical reaction is usually done by applying heat, ultraviolet light, or a chemical initiator [29]. Because of the wide range of curing processes available for thermoset composites they allow for a wide range of manufacturing techniques to be used in their production.

During the hardening process, polymer chains begin forming and perform a process called cross-linking, in which the polymer chains form an interwoven three-dimensional structure [6], [28]. This interwoven structure locks the polymer chains with covalent bonds and prevents the polymer from returning to the liquid state. Therefore, thermosets cannot be reshaped or remelted once the polymer is cured.

This cross-linking process is advantageous for thermoset polymers because it gives the cured product high strength and rigidity. The inability to return to the liquid phase means these polymers exhibit excellent heat resistance as they do not soften when exposed to high temperatures. Thermoset polymers also exhibit high chemical resistance, allowing them to be used in situations requiring exposure to corrosive substances.

However, because of this irreversible cross-linking process, recycling and disposal of thermoset polymers remains challenging [5], [11], [12]. According to current market estimates the total consumption of polymer composite materials in 2023 was approximately 13.6 million metric tons. With a majority of these materials being thermoset polymer composite that resist heat and chemical recycling techniques such as pyrolysis or solvent decomposition, these materials are ultimately destined for landfills at the end of their lifecycle [30], [31].

2.3.2 Thermoplastic Composites

Thermoplastic polymers are classified as polymers with long molecular chains held together by weak atomic forces [6], [28]. One of the critical differences between thermoplastics and thermosets is that they can be remelted and reprocessed multiple times without significantly degrading their mechanical properties [28]. The recyclability of thermoplastics is another key advantage of this polymer, as its ability to be reused allows for a much more sustainable material. The re-meltability

of thermoplastics also allows for rapid manufacturing techniques such as injection moulding or extrusion, making them highly useful in our modern world.

To further classify this type of material, the chemical structure of a thermoplastic needs to be understood as it dramatically affects the material's overall properties. The two morphologies present in thermoplastics are either an amorphous structure or a crystalline structure. A simplified diagram showing these two molecular arrangements is shown below in Figure 2-3 (a) and (b).

Amorphous polymers have randomly packed polymer chains with no long-term order. As a result, these polymers have a higher free volume inside the polymer, have lower strengths than crystalline polymers, and are less resistant to chemical dissolution. Amorphous polymers also have unique melting characteristics, as no definitive melting point exists. These types of polymers gradually transition from solid to viscous polymer melt over a range of temperatures, which is referred to as the glass transition. The glass transition temperature is commonly defined as the midpoint of the transition region and can be measured using differential scanning calorimetry (DSC) to measure the specific heat versus temperature [6].

Conversely, crystalline polymers have an ordered structure where the polymer chains neatly pack themselves together to form lamella. Lamela allows for long-range order in the polymer and lowers the free volume in the polymer. This neatly ordered structure, however, can be compromised at the end of polymer chains, or chains can form unwanted loops outside of the crystal structure. Because of this phenomenon, there can still be amorphous regions in a crystalline polymer, and therefore, there is always a degree to which a polymer is crystalline, ranging from 0% to 100 %. Therefore, crystalline polymers are called semi-crystalline. Semi-crystalline polymers tend to have higher strengths and melting temperatures than amorphous polymers while also being more resistant to chemicals [6], [28]. The melting characteristics of semi-crystalline polymers are also unique, as

there is a glass transition temperature and a melting temperature. The glass transition temperature indicates the transition of the amorphous regions from solid to viscous and, like amorphous polymers, there is a range of temperatures at which this occurs. The melting point of these polymers indicates the crystalline regions of the polymer transitioning from solid to viscous and has a sharper defined temperature at which this occurs. This is a result of the higher energy needed to break apart the neatly ordered structure of the crystalline polymer [6].

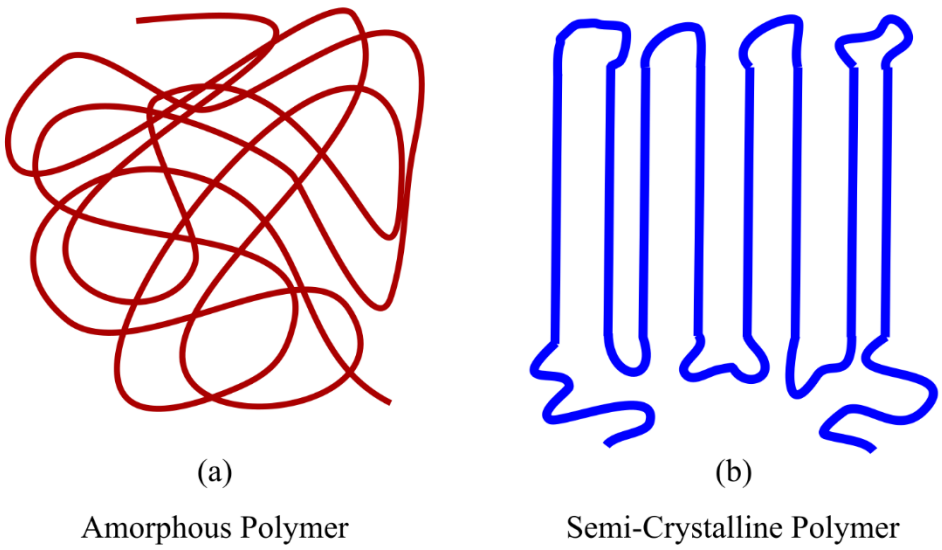

Figure 2-3: Polymer chain structure where (a) depicts amorphous polymer structures showing randomly ordered polymer chain with no long-range order. (b) A semi crystalline polymer structure with repeating lamella packed together forming long-range order.

2.3.3 Liquid Thermoplastic Composites

Liquid thermoplastic composites represent a groundbreaking advancement in polymer technology, pioneered by Arkema with the introduction of Elium® resin [32]. This innovative material aims to address the challenges associated with the manufacturability of traditional thermoplastic composites, removing the requirements for high temperatures and pressures to be used to process thermoplastics into a composite material. Elium® resin starts as a liquid monomer solution that

can be transformed into a solid, PMMA-based thermoplastic through a process of free radical polymerization, initiated at room temperature and pressure by the addition of a peroxide initiating compound. This unique characteristic significantly reduces the energy and equipment requirements for manufacturing allowing for easier production of thermoplastic composites.

The viscosity of the Elium® resin is compared with that of traditional thermoset infusion epoxies in Table 2-3. With its viscosity a mere 100 centipoise before curing, Elium® resin is exceptionally well-suited to replace thermoset resins for use in established composite manufacturing methods, such as resin infusion, resin transfer molding, and hand layups [33]. This resin also helps expand the environmental benefits of thermoplastic composites as it combines the recyclability of thermoplastics with the ease of processing typically associated with thermoset composites [12].

Table 2-3: Viscosity of infusion resins at room temperature compared to Elium® resin

Epoxy Resin System	Room Temperature Viscosity (cps)	Reference
Elium® Resin	100-300	[34]
System 4500 Infusion Epoxy	320	[35]
SikaBiresin® CR72	400-600	[36]
PRO-SET INF-114 / INF-210	200-300	[37]
IN2 Epoxy Infusion Resin	200 - 450	[38]

The significance of Elium® in the composite materials sector is highlighted by various research studies examining its mechanical properties. These studies have consistently shown that Elium® resin matches or surpasses the strength of conventional thermosets, providing a reliable and high-performance option for a wide range of applications [33], [39], [40], [41], [42], [43]. One such study by Bhudolia et al. [33] examines the flexural properties of composites manufactured with Elium®/carbon fiber and compares it to epoxy/carbon fiber composites. In this study the flexural

properties of both composites are found to be approximately 820 MPa with less than a 3% deviation between the two composites. This paper highlights the similar mechanical properties that Elium® resin has to traditional thermoset epoxies while retaining the advantages of recyclability and reform ability that comes with a thermoplastic matrix.

In another study by Bhudolia et al. [39] the impact resistance of Elium® resin composites was compared to epoxy composites. In this study various impact energies were studied ranging from 25 J to 52 J and the composite samples response and resulting structural integrity were measured. The structural integrity measured from the load deflection curve showed a 53% increase for the Elium® composites compared to the epoxy composites when tested. This result highlights the exceptional impact resistance that thermoplastics exhibit compared to thermosets.

The introduction of liquid thermoplastic composites like Elium® by Arkema represents a significant step forward in material science, bridging the gap between sustainability and manufacturability in the composites industry.

2.4 Composite Material Manufacturing Methods

The manufacturing of FRP composites can be achieved through a variety of different processes. Each manufacturing method has its own unique advantages and disadvantages which should be evaluated when determining how a specific component should be manufactured. Below in Figure 2-4, a diagram of some of the manufacturing techniques, such as (a) hand layups, (b) resin infusions, (c) automated tape laying, or (d) 3D printing can be seen.

The advent of liquid thermoplastic resins presents a unique alternative to thermosetting resins when manufacturing composite materials [32]. This is because the typical challenges associated with manufacturing thermoplastic composites such as high pressures and temperatures are

eliminated. With this novel class of resin, thermoplastic composites can be manufactured using simple and established manufacturing methods such as hand layups and vacuum resin infusion techniques typically reserved for thermoset matrix materials.

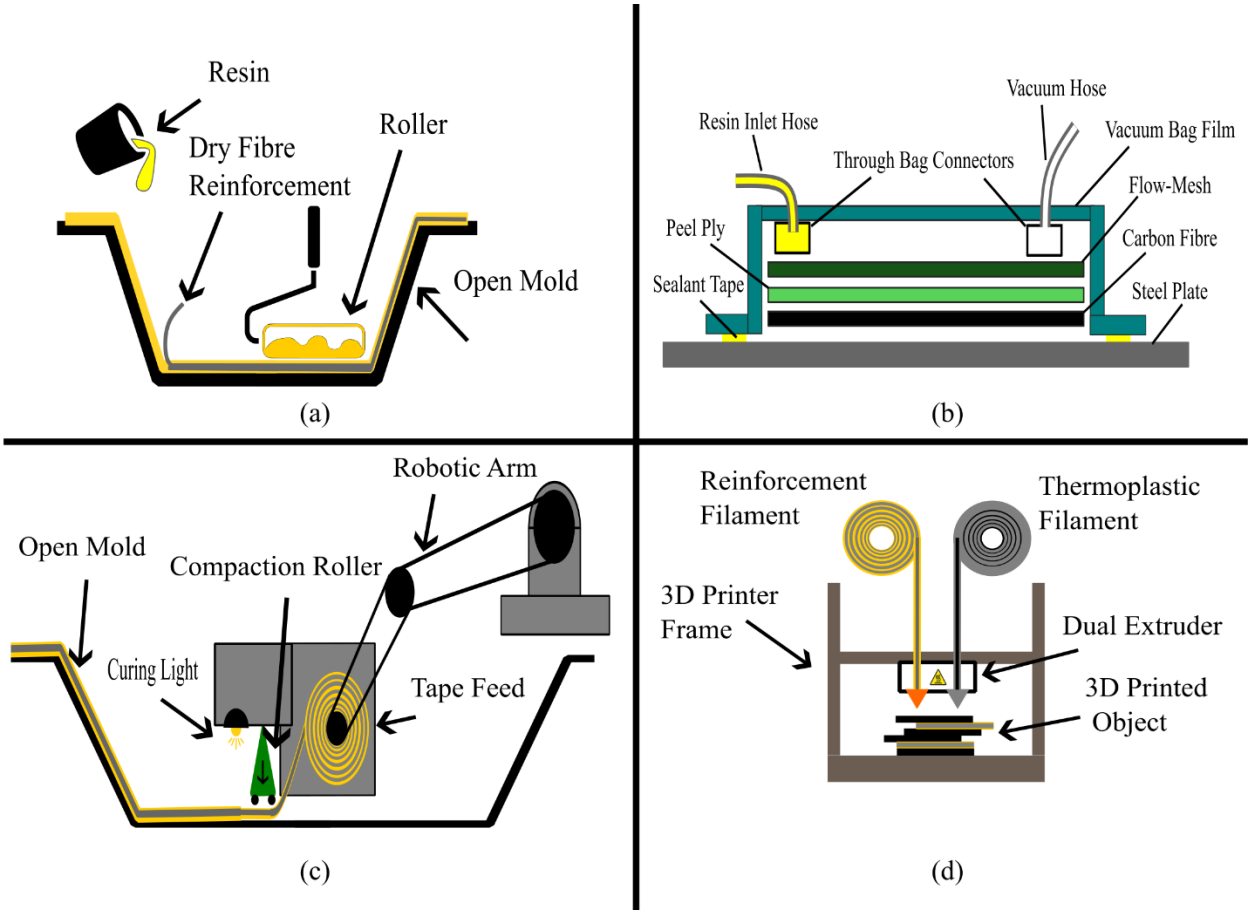

Figure 2-4: Diagram of composite material fabrication techniques: (a) Hand Lay-Up Process, where resin is manually applied to dry fibres in an open mold. (b) Resin infusion, where a vacuum is applied to a laminate in a mold to compact the layers and remove air then resin is drawn into the mold infusing the fibres. (c) Automated Tape Laying, utilizing a robotic arm to place pre-impregnated tapes on a mold and a curing light to initiate polymerization. (d) 3D Printing with Continuous Fibre Reinforcement, where a dual extruder simultaneously deposits thermoplastic and reinforcement filaments to create a composite object.

2.4.1 Hand Layup

The hand layup technique is one of the simplest production methods for creating composite materials. Resin is poured into a mold and spread evenly with rollers or a brush. Next, the dry fibrous material is placed into the mold, and the resin is drawn through the fibres. After the resin has evenly coated all the fibrous material, another layer of fibres is placed on top, and this process is repeated until the desired laminate thickness is achieved. Depending on final part requirements, sometimes a vacuum bag can be placed on top of the final layer of the laminate and a vacuum is drawn. This can help apply compaction to the laminate reducing the void content and ultimately increasing the mechanical properties of the final part. This technique is widely used for its simplicity when creating small production volume composite parts [44], [45].

Advantages of this process include the lack of specialized tooling required, the curing process does not require an oven, and this method accommodates large part sizes quite easily. Disadvantages of this production method are that part quality and strength can vary from part to part reducing the repeatability of this process. Hand layups can also have longer production times than other methods, such as heated tool molding or automated fibre placement.

2.4.2 Vacuum Assisted Resin Infusion

Vacuum-assisted resin infusion is a slightly more complex method of composite manufacturing compared to hand layups, but it is used to ensure high-quality parts with minimal void content. Like the hand layup process, dry fibres are placed into a mold at the desired orientations, but no resin is applied. A peel ply is placed over the final lamina, and then a flow mesh is placed on top of the peel ply to allow resin to flow through and into the laminate. A vacuum bag is placed overtop and a vacuum is drawn to remove all the air inside the laminate. All leaks in the system must be eliminated from the vacuum bag and then resin is allowed to be drawn into the mold [44], [45].

This manufacturing method's advantages stem from the elimination of voids in the laminate, which results in a higher fibre ratio in the final part, ultimately producing a stronger laminate. It has been seen that an increase in the void content by 1% can reduce the interlaminar shear stress by 7% [46]. Void content also impacts other material properties such as the ultimate tensile strength and the stiffness of the laminate [47], [48].

Some disadvantages of this process are that it requires more equipment and adds more disposable vacuum bagging materials, ultimately increasing cost. It also adds extra steps in the manufacturing process compared to hand layups, increasing the time required to create a single part. This process also requires a skilled composite technician, as an entire part can be scrapped due to a single vacuum leak [45].

2.4.3 Automated Fibre Placement

Automated fibre placement is a process where a multi-axis computer-controlled machine deposits strands of unidirectional fibres in a preset pattern. This process is most commonly used in aerospace for high-quality and complex parts that require high strength-to-weight ratios. These machines work similarly to a 3d printer but have much more complexity and are often very large. Because of the computer-controlled fibre placement, this manufacturing method is ideal for producing parts repeatably and has very precise control of fibre orientation. Automated fibre placement also has relatively quick production times compared to other manufacturing methods. The primary disadvantage of this manufacturing method is its cost. The machines can cost over a million dollars and require highly skilled technicians to operate them [49].

2.4.4 3D Printing

The advent of 3D printing technology for composite materials has unlocked a new field of composite manufacturing. Companies such as Mark Forged and Anisoprint have been at the forefront of this innovation, offering consumer 3D printers capable of incorporating continuous strands of various fibres—such as carbon, glass, and aramid—into thermoplastic prints with materials such as nylon or PEI [50], [51]. This composite manufacturing technique is unique to thermoplastic composites as the matrix material is heated to its molten state in an extruder and then deposited into a 3d shape along with continuous strands of reinforcement material. This technological advancement has significantly enhanced the mechanical properties of 3D printed parts, thereby expanding their applicability into end-use 3D printed parts.

Current literature studying the mechanical properties of these 3d printed composite parts by Hetrick et al. shows that carbon fibre samples printed according to ASTM D3039 achieved tensile strengths ranging from 179 to 484 MPa with fibre volume fractions of 15.3 and 56.5 percent, respectively [52]. This research demonstrates that the fibre volume in these composites can be tailored to achieve a specific ultimate strength of the material. This customization allows for a wide range of applications, from lightweight structures to high-strength engineering components [53].

Furthermore, predictive analytical models have been developed to facilitate the estimation of the elastic properties of 3D printed parts. Melenka et al. [54] developed an average stiffness method in order to predict the tensile properties of continuous fibre-reinforced samples that demonstrated agreement with experimental results.

2.5 Repair of Thermoset Composites

The repair of thermoset composite structures presents significant challenges for engineers, particularly in terms of accurately predicting the strength of repairs due to environmental factors such as humidity, temperature, and fatigue [55], [56]. Currently, the industry predominantly employs two methods for repair: mechanically fastened repair and adhesive repair [57]. The mechanically fastened repair method is the only approach that is currently accepted for use on aircraft load-bearing structures, and a diagram of the process of performing a bolted repair can be seen below in Figure 2-5 [13], [58]. The first step, seen in Figure 2-5 (a), involves identifying the damaged area and then cutting away the damaged section from the laminate. Next, holes are drilled around the damaged location, and a separate repair patch is manufactured to conform to the top of the panel's original geometry. The new repair patch is then bolted in place, as seen in Figure 2-5 (b). However, this approach introduces new complications, such as a significant amount of added weight to the structure, the potential for bolt corrosion, and the creation of new stress concentrations due to the drilled holes, which can significantly weaken the ultimate strength of the laminate [13]. Additionally, this method is often impractical or unfeasible for complex geometries and fails to replicate the net shape of the original laminate.

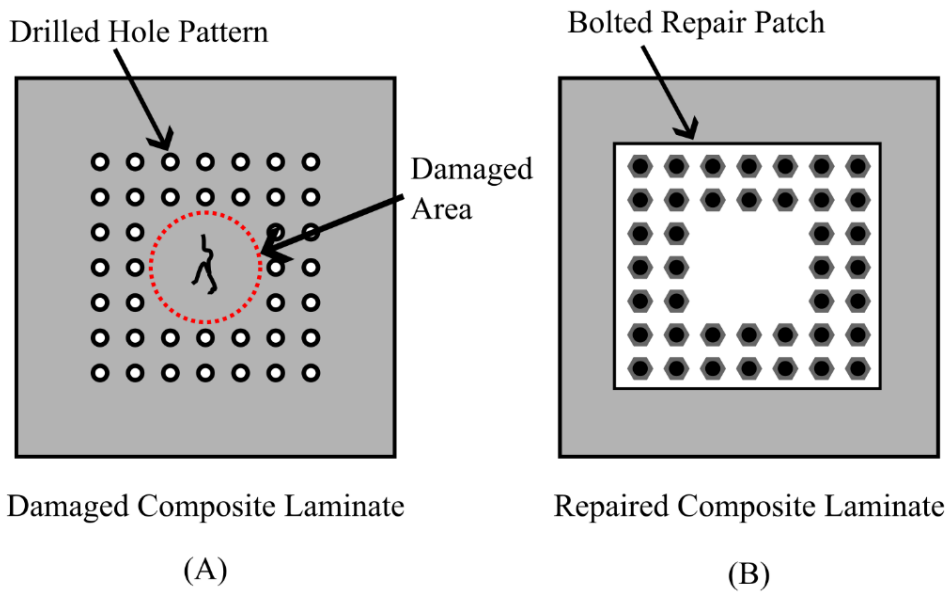

Figure 2-5: Bolted repair process for composite laminates. (a) The damaged composite laminate with a drilled hole pattern around the damaged area to prepare for repair. (b) The composite laminate after repair, showing a bolted repair patch secured over the damaged region to restore strength to the original laminate.

Adhesive bonded repairs are performed by bonding a premade repair patch over the surface of the part, held in place with high strength adhesives. There are multiple strategies employed when performing adhesive repairs and they can be seen below in Figure 2-6, depicting (a) scarf repairs, (b) stepped repairs, or (c) patch repairs.

Scarfed and stepped repairs, seen in Figure 6 (a) and (b), respectively, are performed in a similar way by grinding away the material around the damaged location in the original laminate and a pre-manufactured repair patch is bonded in place with adhesives. They differ in the removal of the damaged laminate because the original laminate is removed at a constant angle in a scarfed repair. This results in a single pre-manufactured repair piece that can be inserted into the removed area and bonded in place. Alternatively, a stepped repair involves cutting out the damaged area in steps,

creating many layers that will each be repaired individually. Scarfed and stepped repairs have shown significant levels of strength recovery between 70 – 95 percent in the literature [59][59]. Another primary advantage of the scarf and stepped repair methods is its ability to take the original net shape of the laminate, which is desirable in specific applications such as aircraft where maintaining smooth surfaces are critical for aerodynamics.

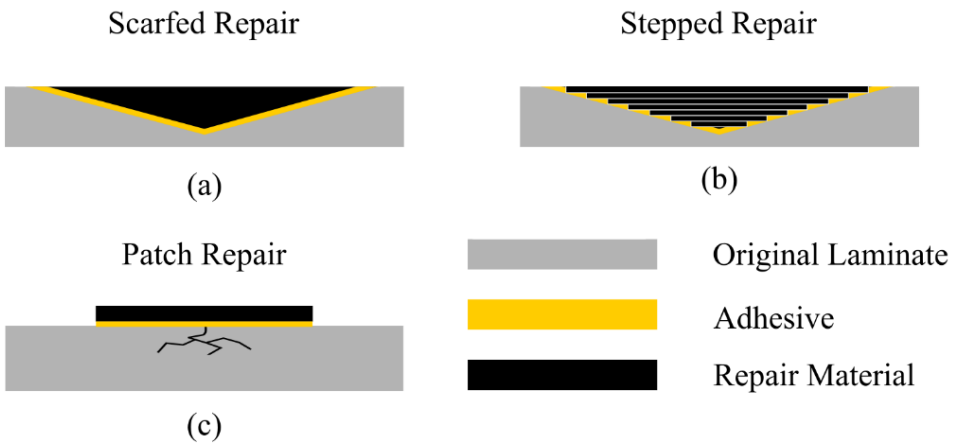

Figure 2-6: Adhesive bonded repair processes. (a) Shows a scarfed repair where a tapered area is ground away from the damaged area in the laminate and a preformed repair patch is adhesively bonded in place. (b) Stepped repair, illustrating a tiered approach with multiple layers of adhesive and repair material. (c) Patch repair, depicting a simple overlay of repair material on a damaged laminate area.

Patch repairs seen in Figure 2-6 (c) are performed by applying a layer of adhesive, and then a repair patch is placed directly on top of the damaged area. This repair method is simpler and faster to apply as it does not require grinding away the damaged area. It also can be performed in the field without the need for costly tooling. Patch shape optimization has been investigated in the literature to increase the strength of the repairs [55]. Mhamdia et al. [60] performed a study investigating the optimal shape of repair patches on aircraft structures. They concluded that patches

in the shape of an H with arrows pointing away from the damaged location as seen below in Figure 2-7, reduced the stress intensify factor by 65%. Ultimately increasing the strength of the repair.

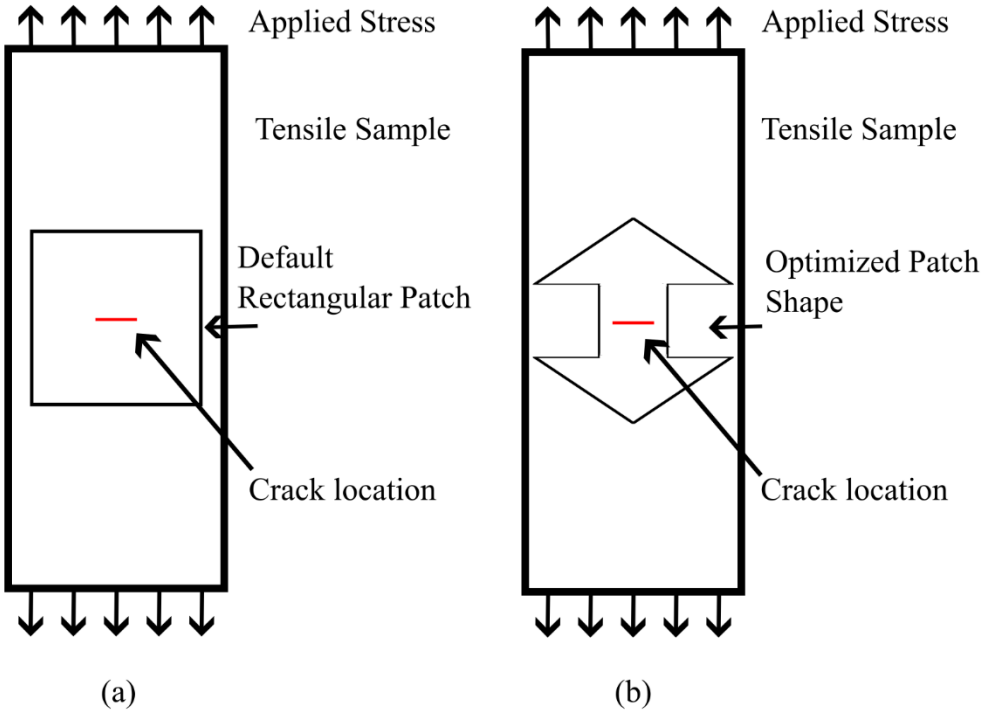

Figure 2-7: Comparison of repair patch shapes for crack reinforcement of composite tensile samples by Mhamdia et al. [60]. (a) Depicts a tensile sample with a default rectangular patch. (b) Shows a tensile sample with the optimized patch shape, designed to distribute stress evenly and enhance the repair effectiveness.

All types of bonded repairs on thermoset composites come with their own challenges, such as an arduous surface preparation process that is critical to ensuring adhesive strength. Other challenges with this repair method include difficulty in predicting the long-term performance of the adhesives, and a lack of reliable non-destructive inspection (NDI) techniques to assess the integrity of the bonded joint [37], [39], [61], [62]. Because of this, adhesive repairs are not approved for use in load-bearing structures due to difficulties characterizing long-term fatigue performance. However, for use in non-loadbearing structures, they offer some advantages, such as reduced weight added

to the structure. Aerodynamically, they also provide a smoother surface finish compared to bolted repairs and can be applied to more complex geometry [58].

Thermoplastic composites are also able to be repaired using both the bolted and adhesive repair method. However, unique to thermoplastic materials, the remeltability of the matrix eliminates the need for adhesives to be used in the adhesive repair process. By heating the bonding interface of the material, the polymer melts and can be joined together to form a cohesive polymer matrix. This elimination of adhesives can drastically reduce the processing time for applying repairs and simplify the repair process [63]. This process, known as plastic welding or fusion bonding, is being studied heavily in the literature and will be discussed in depth in the next section.

2.6 Fusion Bonding

Thermoplastic composites open new avenues for repair methods, owing to the remeltable nature of thermoplastic matrix materials. Fusion bonding, as referenced in the literature, is a broad term used to indicate these new methods of plastic welding [63], [64], [65], [66]. The most promising research areas in fusion bonding techniques are induction, resistance, and ultrasonic welding[67], [68], [69], [70]. These fusion bonding techniques aim to apply heat to the bonding interface of thermoplastic composite structures to raise the temperature of the polymer above their glass transition point for amorphous polymers and melting point for semi-crystalline polymers. During heating, the polymer melts, and its viscosity lowers, allowing for polymer chains to flow across the bonding interface, and pressure is applied. This allows the polymer along the bonding interface to form a cohesive structure. Heat is then removed, and the polymer chains solidify, forming a weld in the structure.

2.6.1 Induction Welding

Induction welding emerges as one of the primary fusion bonding techniques under investigation for the joining or repair of thermoplastic composite materials, and a diagram of the induction welding process to create a lap shear joint can be seen below in Figure 2-8. The fundamental mechanism of induction welding involves passing an alternating current through a coil to induce a variable magnetic field, operating within a frequency range of 200 to 500 kHz [63], [71]. When an electrically conductive material is present within this variable magnetic field, it begins to heat up due to a phenomenon called the Joule heating effect [63]. This phenomenon is caused by the electrical resistance of the conductive material and releases heat to its surroundings. Typically, carbon fibres, metallic meshes, or magnetic particles are employed to induce the necessary heating [72], [73]. When these magnetic field susceptors are in the presence of an alternating magnetic field, eddy currents are induced within them. The power applied to the material, as governed by the Joule effect as seen in Equation 2-1 where f is the frequency of the magnetic field, μ is the magnetic permeability of the material, $H(I)$ is the magnetic field intensity, A is the surface area of the susceptor, and R is the electrical resistance of the susceptor [13], [72]. During the heating phase, pressure is simultaneously applied to the thermoplastic composite, joining the materials. Following this, the magnetic field is removed, and the polymer is allowed to cool, resulting in a solidified composite joint.

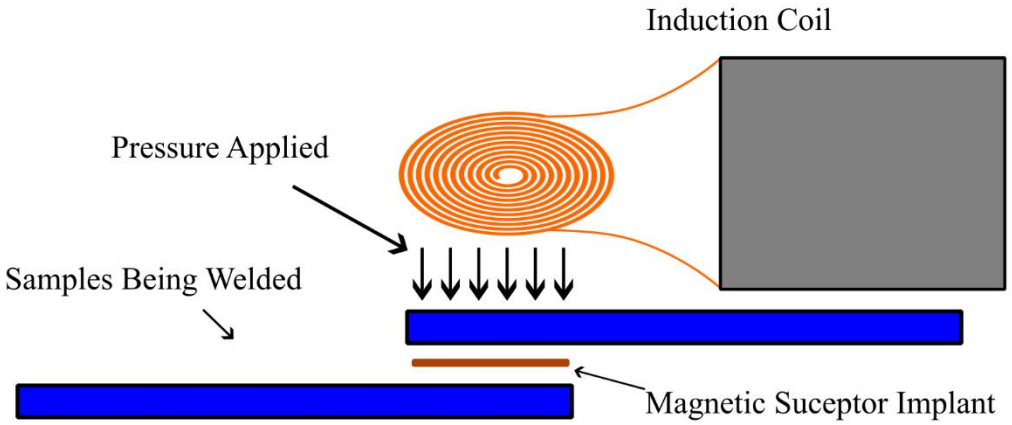

Figure 2-8: Diagram of the induction welding process to create a lap shear joint in two thermoplastic composite samples.

$$P = \frac{(2\pi f \mu H(I)A)^2}{R} \qquad \textit{Equation 2-1}$$

This technique harbors several advantages. Firstly, it does not need to come into contact with the material to apply heating, which is especially beneficial in high-precision or sensitive applications. Secondly, it can induce currents in conductive materials such as carbon fibres without additional susceptor materials. This characteristic is particularly advantageous as it simplifies the process and reduces the requirement for additional materials. Induction welding also demonstrates a remarkable ability to operate efficiently in areas with complex geometries, further broadening its applicability.

However, induction welding also has its share of disadvantages. In cases where the fibres within the composite are not conductive, such as with glass fibres, the technique necessitates using metallic susceptor material to facilitate the induction heating. This requirement could potentially complicate the process and increase the costs involved. Additionally, the method can encounter

issues with non-uniform heat distribution, which is a significant concern as it could lead to inadequate bonding in some areas. Directing the heat to the desired bonding interface also poses a challenge, which could further impede the joint's effectiveness and quality. These challenges underline the critical areas where further research and development could significantly enhance the efficiency and utility of induction welding in thermoplastic composite materials.

Various researchers have investigated this fusion bonding method and reported on key parameters to optimize the use of induction welding in thermoplastic composites. In one such study by Rudolf et al. [74], the influence of the electromagnetic frequency, generator power, distance of the coil to the laminate, and the coil and laminate geometry on the heating rate and heat distribution were investigated. It was found that heat was only generated in closed fibre loops, meaning that it was not possible to heat unidirectional fibres as there were no junctions. The texture of the reinforcement was also found to be very important in the heating of the laminate. This research assisted in laying the foundation of the induction welding process and has been expanded on in recent years to further the induction welding process.

In a study by Becker et al. [75] various parameters affecting the heating and cooling rate of the thermoplastic structure are investigated. From this study, the authors developed an adapted laminate that results in an increased heating rate of 16 K/s compared to a traditional laminate, ultimately increasing the speed of the induction welding process. A novel spray cooling system was also developed to increase the heat removal rate from the surface of the laminate, again reducing the overall processing time. This work offers potential improvements in the continuous induction welding of thermoplastic composite materials, allowing for further adoption of the materials in the industry.

2.6.2 Resistance Welding

Resistance welding is a fusion bonding technique in which an electrical current is passed through a heating element that is placed between two thermoplastic composite laminates. A diagram showing the fabrication of a lap shear joint using this fusion bonding method can be seen below in Figure 2-9. The joule effect generates heat, and an equation for this phenomenon is shown below in Equation 2, where P is the power generated in the heating element, R is the resistance of the heating element, and I is the applied current [76]. In this fusion bonding technique, the heating element is used to apply heat to the thermoplastic polymer, which is then compressed and allowed to cool, solidifying into a single part. Various heating elements can be used in this fusion bonding method, such as carbon fibre or a stainless-steel mesh [77], [78]. This heating element is bonded inside the joint and becomes a permanent part of the structure.

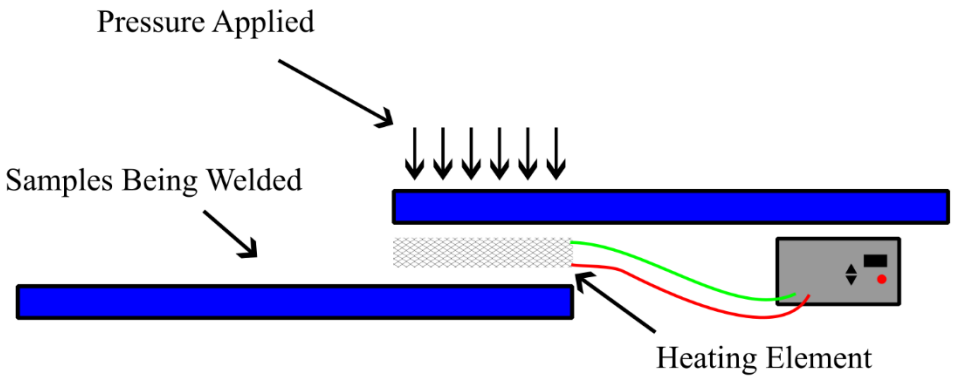

Figure 2-9: Resistance welding diagram of a lap shear joint being created where heat is applied to the bonding interface via a heating element sandwiched between the thermoplastic composite samples.

$$P = RI^2 \qquad \textit{Equation 2-2}$$

The primary advantage of this process is that heat is only generated at the interface of the laminates being bonded. This process can be used even on relatively thick laminates without impacting the overall structure. Another advantage of this process is that very little surface preparation work is required before bonding to create high-strength welds[79], [80].

Seneviratne et al. [64] investigated the lap shear strength of resistance-bonded joints in thermoplastic composites made of low-melt poly-aryl-ether-ketone (LM-PAEK) and unidirectional carbon fibre. This study compared the shear strength of resistance-welded joints to adhesive-bonded joints using various surface preparation methods. They concluded that while adhesive bonding strength varies greatly (up to a 58% change in strength), resistance welded joints only varied by 7.2% with a maximum shear strength of 45 MPa.

Dubé et al. [61] studied the optimal size of a stainless-steel mesh heating element when welding three different thermoplastic composite materials together. This study tested glass fibres and PEI, Carbon fibres and PEI, and Carbon fibres and PEKK, and the best resulting lap shear strengths of 33, 47, and 52 MPa were obtained, respectively. Their study tested four different mesh sizes and determined that the optimal mesh size is a 0.04mm wire diameter and a 0.09mm width between wires. They also state that the fraction of open area to wire diameter is the most important parameter when selecting a mesh heating element.

Ageorges et al. [78] Conducted a study on the optimal processing parameters of resistance welding. One key parameter focused on was the applied pressure during consolidation, and a range of 0.1 to 2.4 MPa was studied. They concluded that the optimal pressure was 0.5 MPa, but an extensive range of pressures from 0.2 to 1.6 MPa produced acceptable results.

2.6.3 Ultrasonic Welding

Ultrasonic welding is performed by applying pressure to the material being welded and then using high-frequency oscillations in the vertical direction, generating heat at the bonding interface. This heat then begins melting the material, and a weld is created. A diagram showing the ultrasonic welding process to create a lap shear joint can be seen below in Figure 2-10. The frequencies used in this bonding process are in the range of 20 – 40 kHz at amplitudes of 10 – 250 microns [63], [76]. Heat in the material is generated by a combination of viscoelastic effects and surface friction between the two materials [81]. Frictional forces are the dominant form of heat generation before the material reaches the glass transition temperature. Above this temperature, viscoelastic heating becomes the dominant heating mechanism [82], [83]. Heat generated by the viscoelastic effects in this process can be described by Equation 2-3 as seen below, where Q is the heat generated, ω is the frequency of the oscillations, E is the elastic modulus of the material, and ϵ is the cyclic strain on the materials[81].

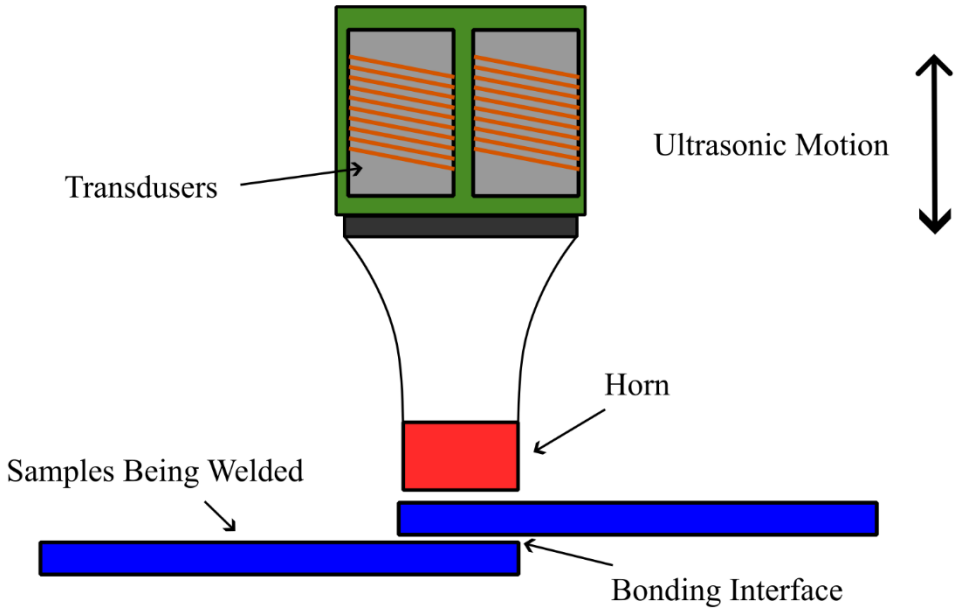

Figure 2-10: Diagram showing the ultrasonic welding process being used to weld two samples together for lap shear testing

$$Q = \frac{\omega * E * \epsilon^2}{2} \qquad \textit{Equation 2-3}$$

One of the primary advantages of this technology is the time required to bond materials compared to other fusion bonding techniques, such as resistance welding or induction welding. Ultrasonic welding of thermoplastic composites can be performed in seconds, reducing cycle time and improving the overall efficiency of the process [84]. There is also no need for resistive wires or inductive susceptors to be used like with resistance welding or inductive welding. Researchers have also been investigating the use of accelerometers mounted to the part to measure the weld quality [85]. This allows users to monitor the weld quality without instrumenting the bonding interface, which could cause adverse effects.

Some of the disadvantages of this process are seen when trying to weld semicrystalline polymers such as PEEK, PEKK or PPS. These polymers absorb more energy and require higher temperatures to transition into their liquid phase [84]. Another issue with this process is its difficulty in welding thicker laminates. Thick laminates tend to absorb more ultrasonic vibrations, reducing the total heat generated at the bonding interface [84].

The heat generated in this fusion bonding method typically concentrates around high points in the laminate, which can be purposely manufactured. These high points are called energy directors and are usually shaped as protrusions meant to direct heat to the bonding interface [79], [81], [82]. Energy directors are not always necessary, and neat polymer films have been shown to work, as seen in research by Bhudolia et al. [86] where lap shear strength tests were performed on liquid thermoplastic/carbon samples. Samples were ultrasonically welded with integrated energy directors as well as flat films of resin and tested according to ASTM D5868-01 to evaluate the lap shear strength of the fusion bonds. In this study, the researchers concluded that while flat film ultrasonic welding was possible, energy directors improved the strength of the bond, resulting in an increase in lap shear strength by 35%.

Various researchers have investigated the use of energy directors and their optimal shape. A study by Chuah et al. [87] studied the optimal shape of energy directors in thermoplastics to determine the shape that provides the optimal welding efficiency. This study compares three energy director shapes: triangular, rectangular and semi-circle. The authors concluded that the semicircular energy directors had the best welding efficiency, followed by the rectangle and then the triangular energy directors.

2.6.4 Conduction Welding

Conduction welding is a process used to join two or more thermoplastic materials together by heating and compressing them together above the glass transition temperature in amorphous polymers or above the melt temperature in semi-crystalline polymers [88]. Heat is transferred from the hot plate, also called a platen, into the parts being welded by conduction heating. This method of welding has been used in literature as a simple and low-cost alternative to more expensive fusion bonding techniques [13], [63], [89], [90]. A diagram of this process can be seen below in Figure 2-11.

This technique has several advantages that should be considered when comparing fusion bonding methods. One of the main advantages is its low cost compared to other fusion bonding methods, which require expensive equipment such as ultrasonic welding. Another advantage is the ability to machine the heated platens to conform to complex geometries. The heated platens can also be made to accommodate large sizes to weld parts in a single operation [91].

However, one of the key disadvantages of this process is the difficulty of welding thick laminates together. Because heat is not generated at the bonding interface but at the laminates' outer surface, the laminate's thickness dictates the heat transfer to the bonding surface. In the case of thick laminates, heat conduction to the bonding interface is limited and increasing the surface temperature of the heated press to accommodate this can go above the operational temperature of the thermoplastic matrix. Another potential disadvantage is the need for the structure to be supported during the compression of the heated platen which can be difficult on complex geometries.

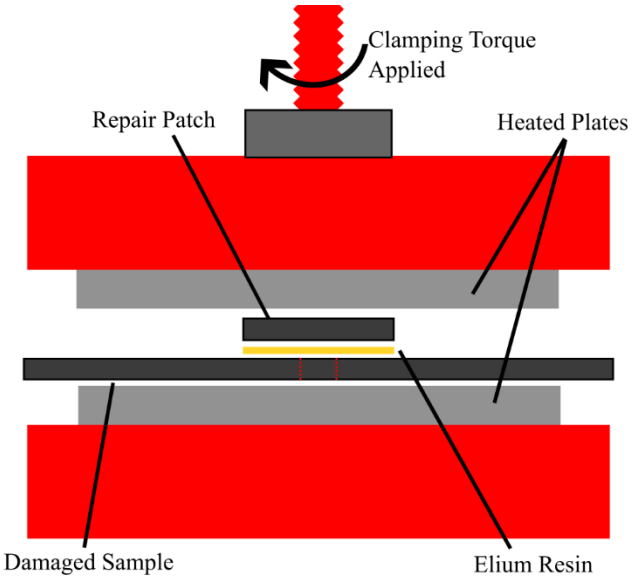

Figure 2-11: Conduction welding process showing a repair patch being applied to a damaged thermoplastic composite sample

Perrin et al. [89] investigated hot plate welding to weld Elium® glass fibre composites to polyamide (PA12), studying the use of a compatibilizer to weld dissimilar polymers together. Sheets of glass fibres were vacuum infused with Elium® resin mixed with a compatibilizer agent of glycidyl methacrylate (GMA), and thin sheets of PA12 were formed by stamping pellets in a heated compression mold. Two glass fibre composite plates were then stacked with a sheet of PA12 in between and placed in a heated press at varying temperatures ranging from 160°C to 240°C for 10 minutes at 0.5 MPa. The welded sheets were tested in a universal testing machine according to ASTM C297 and pulled in tension till failure. The study concluded that welding temperatures of 200°C resulted in the best weld quality and that GMA was a pivotal addition to Elium® resin when attempting to weld with PA12.

Erland et al. [92] utilized the ability of thermoplastics to be remelted to study the repairability of PEEK and chopped carbon fibre composites. In this study, samples are manufactured using a

compression molding process to create samples according to the ASTM D790-03 three-point bending test, and then samples were then tested till failure. The fractured samples were then placed in a heated mold to enable the resin to melt, and repair cracked areas of the samples. This process was repeated up to five times, and re-tested samples showed mechanical properties near identical to the original samples.

In another paper about conduction welding, Tijs et al. [91] worked with aerospace company GKN/Fokker to develop a conduction welding robot capable of welding PEKK/CF composites. Lap shear joints were fabricated from two large sheets of premade composite panels, and static tensile tests were performed according to ASTM D3165. The authors achieved an average fracture stress of 41.9 MPa from their lap shear testing. The study finds that the joint strength is significantly influenced by both the weld quality and the surrounding plies in the laminate, as several delaminations in the original laminates were found after testing. The influence of the interaction of surrounding plies on the conduction of welded joints is crucial for optimizing the welding process and warrants further investigation into this topic in future research.

2.6.5 Comparison of Fusion Bonding Methods

Fusion bonding as a method for joining or repairing thermoplastic composites offers several benefits over traditional approaches like adhesive bonding or mechanical fastening with bolts. While this new method of bonding stands out for its specific advantages, it is important to recognize the various disadvantages that each method possesses when determining its applicability. Below in Table 2-4 a comparison of the four fusion bonding methods discussed in this section is presented. This table aims to highlight their respective strengths and weaknesses and guide a selection of which fusion bonding method to utilize for a given context.

Table 2-4: Strengths and weaknesses of various fusion bonding methods.[13], [63]

Welding Type	**Strengths**	**Weaknesses**
Induction	• No contact with surface • Works on carbon fibers with no susceptor (depending on angle of fibers) • Fast cycle times (30 seconds approx.) • Can work continuously	• Expensive equipment cost • Does not work on thick parts • Requires precise control of power and time settings
Resistance	• Lower cost • Generates heat directly at the interface. • Works regardless of part thickness • Can weld large areas simultaneously	• Resistance wire is left in the bonded joint. • Slower cycle times
Ultrasonic	• Very quick cycle times • Ideal for small, delicate parts • Minimal thermal stresses developed • Very energy efficient	• Expensive equipment cost • Can not weld through thick parts. • Can not weld large areas
Conduction	• Lowest cost • Fast cycle times (30 seconds) • Can weld large areas simultaneously • Can conform to complex geometry while welding	• Can not weld through thick parts • Limited control of weld depth

2.7 Mechanical Testing of Composite Materials

With the growing adoption of thermoplastic composites in critical industries like aerospace and automotive, comprehensive characterization of these materials is imperative. Mechanical testing is a cornerstone in this characterization, providing essential insights into how these composites behave under various load conditions. This section delves into the types of mechanical tests commonly employed, focusing on tensile testing and lap shear joint testing. These tests are also particularly relevant when evaluating composite structure repairs and allows for a comparison to their original undamaged components. Mechanical testing is performed on both undamaged and repaired structures to assess the degree of strength recovery compared to the original strength of the material.

2.7.1 Types of Mechanical Tests

While numerous tests are used to evaluate the mechanical properties of composites, tensile and lap shear joint tests are among the most prevalent. These tests are governed by established standards, such as ASTM D3039, ASTM D5766, ASTM D1002, ASTM D3163 and ASTM D5868, to ensure comparability and reliability of results between studies [93], [94], [95]. A diagram of the primary standards used in this research can be seen below, showing ASTM D3039 tensile testing in Figure 11 (a) and ASTM D5868 lap shear testing in Figure 2-12 (b).

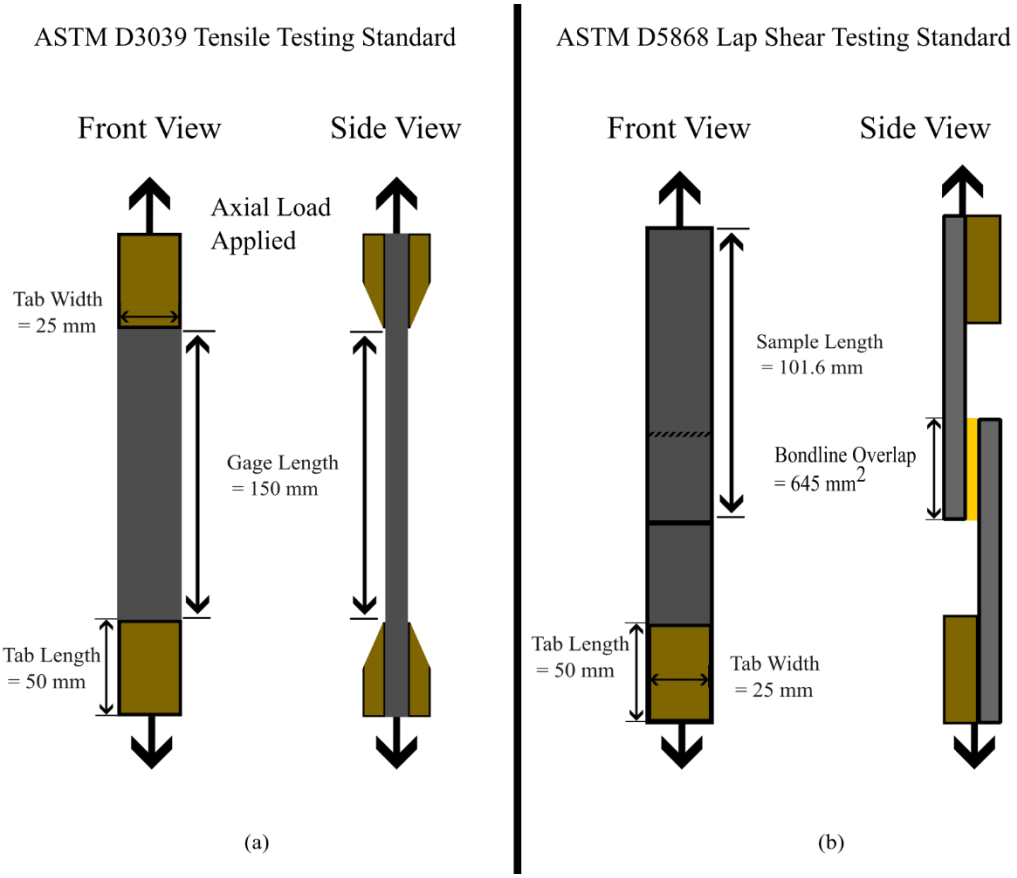

Figure 2-12: Diagram of ASTM sample size for testing standards showing front and side views for (a) tensile testing of composite materials, and (b) lap shear testing of composites.

2.7.2 Tensile Testing

Tensile testing offers fundamental insights into the mechanical behavior of thermoplastic composites by providing critical metrics like ultimate tensile strength, Young's modulus, and overall material toughness. Ultimate Tensile strength is the largest tensile load a sample can withstand before fracture occurs [96]. Young's modulus, also known as the modulus of elasticity, is defined as the ratio of the tensile stress to the tensile strain of the material and is calculated by measuring the slope of the linear section of the stress-strain curve [96]. This property is essential in defining a material's stiffness and how it deforms as a load is applied. Overall material toughness is defined as the area under the stress-strain curve and represents the maximum energy required to fracture the sample. For composite materials, this property is essential for understanding how the

material will respond to impact loading, as a higher toughness will allow for higher impact energy absorption[96].

Notable studies in this area have examined the mechanical properties of various thermoplastic composites and have shown that their mechanical strengths are comparable to thermoset composites [97], [98], [99], [100], [101]. For instance, Kazemi et al. [101] used liquid thermoplastic resin (Elium® 188) to impregnate carbon fibres as well as ultra-high molecular weight polyethylene (UHMWPE) fibres. Their findings suggest that the tensile properties of these thermoplastic composites are comparable to those of thermoset composites while also offering advantages such as improved recyclability and impact resistance.

2.7.3 Real-World Applications and Open Hole Testing

Understanding how thermoplastic composites perform in real-world applications is crucial. In many practical scenarios, such as aerospace applications, composites must accommodate open holes for mechanical fasteners, wire pass-throughs, and other functionalities [102], [103]. Consequently, a growing body of research focuses on assessing the mechanical performance of composites with open holes and research in this area is done in accordance with the standard ASTM D5766 [95].

Guo et al. [102] studied the effects of open hole geometry using woven carbon fibre and epoxy samples with a circular hole, a square hole and an elongated hole they call “racetrack-shaped.” In this study, the open-hole samples and an undamaged control sample were subjected to tensile loading until failure, and digital image correlation was performed during testing to provide full field strain maps of the samples. The authors found that the shape of the holes impacted the stress concentration factor (SCF), and the circular hole had a 36% higher SCF than the square or

racetrack hole. While there was a notable change in SCF depending on the hole shape, there was a negligible effect on the ultimate tensile strength of the different samples.

Kahn et al. [104] investigated the interaction between open holes in a woven carbon fibre laminate sample. This study tested four configurations of open hole samples: one single hole and the other three had two interacting holes at three different angles (0, 45, and 90 degrees). One undamaged sample was also tested as a control. Finite Element Method (FEM), Digital Image Correlation (DIC) and Infrared Thermography (IRT) were used to evaluate the SCF of the specimens. This three-way comparison of FEM, DIC, and IRT was the first of its kind and aimed to understand the failure dynamics of these woven composites and their interacting holes. It was found that adding a second hole in the longitudinal direction led to an enhanced final failure load and a reduced SCF, even compared to the single-hole specimen. The DIC technique identified the critical regions in two-hole specimens. Infrared thermography revealed insights into the failure progression, with differences in the damage between specimens with different hole orientations. An analysis of the fracture surfaces provided further understanding of damage progression in these composites.

2.7.4 Lap Shear Testing

Lap shear testing is commonly used to assess the shear strength of bonded joints. Because of the remeltable nature of thermoplastic composites, this test has gained prevalence in literature when investigating various fusion bonding techniques. The lap shear test for thermoplastic composites is defined by ASTM D5868 and a diagram of the samples used in this test can be seen above in Figure 2-12 (b) [94]. Researchers investigating fusion bonding techniques have used this test method extensively in the literature to evaluate the shear strength of the bond created [64], [69], [70], [77], [78], [79], [89], [105]. There is still not a consensus among researchers on which fusion

bonding method or processing parameters are best as many processes are still in their infancy. A summarized table of recent fusion bonding lap shear testing can be seen below in Table 2-5.

Table 2-5: Summarization of lap shear testing results for various fusion bonded thermoplastic composite materials

Author	Materials Used	Fusion Bonding Technique	Lap Shear Strength
Murray et al. [64]	CF/PMMA	Resistance	20.5 MPa
Dube et al. [70]	CF/PEEK, CF/PEKK, CF/PEI, GF/PEI	Resistance	49 MPa, 52 MPa, 47 MPa, 33 MPa
Xiong et al. [106]	GF/PEI	Resistance	36.8 MPa
Panneerselvam et al. [107]	GF/PP	Resistance	8.62 MPa
Koutras et al. [108]	GF/PPS	Resistance	13.1 ± 0.4 MPa
Bhudolia et al.[86]	CF/PMMA	Ultrasonic	18.68 MPa
Villegas et al. [109]	CF/PEI	Ultrasonic	37 ± 1.6 MPa
Kwon et al. [110]	CF/PEKK	Induction	33.2 ± 0.5 MPa
O'Shaughnessey et al. [111]	CF/PPS	Induction	31.3 ± 3.5 MPa
Lionetto et al. [112]	CF/PEEK	Induction	30.1 ± 0.6 MPa
Tijs et al. [91]	CF/PEKK	Conduction	41.7 MPa

2.8 Digital Image Correlation

Digital Image Correlation (DIC) is an optical method of measuring surface deformation and strain without contacting the sample's surface. Over the past few decades, DIC has gained tremendous popularity in experimental mechanics and materials science, given its ability to provide detailed insights into material behaviour under various loading conditions without contacting the sample [113]. The foundation of this analysis technique revolves around collecting images of a specimen as it undergoes loading and using computer analysis to track the displacement of the sample over time. DIC can be performed in two and three dimensions depending on the number of cameras used, and a diagram of the two most common setups can be seen below in Figure 2-14. 2D DIC (a) uses a single camera and is limited to recording the in-plane deformation of a sample. In contrast, 3D DIC (b), also called stereo DIC, uses two or more cameras to record in-plane and out-of-plane deformation. DIC has been used extensively in the study of composite materials because of its ability to measure strain over an inhomogeneous area, such as a woven fabric or braid, as well as samples with complex three-dimensional geometry [90], [114], [115].

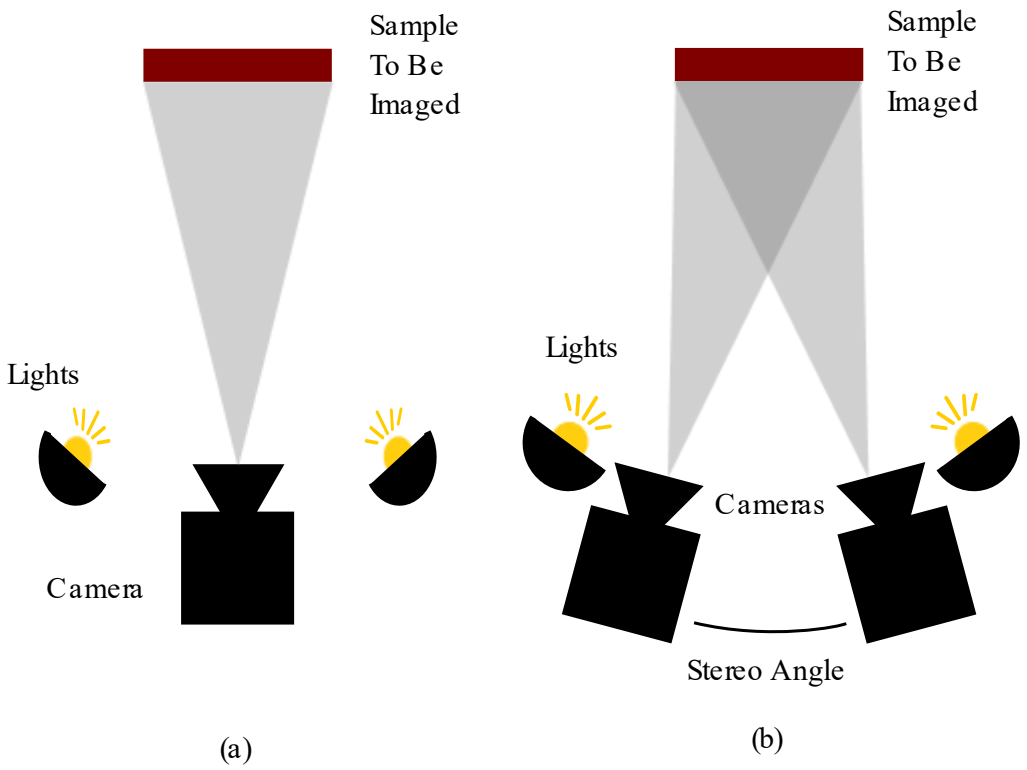

Figure 2-13: Diagram of two different DIC setups. (a) 2D DIC uses a single camera to measure in plane deformation of a sample. (b) shows 3D DIC where two cameras at an angle to each other are calibrated to measure in plane and out of plane deformation.

To perform DIC, the surface of the test sample is painted with a speckle pattern that allows the camera to track movement as the sample is loaded. A high-quality speckle pattern is defined as having a high contrast, random pattern with no isentropic directionality [116]. An example of a high-quality speckle pattern can be seen below in Figure 2-14 (a), showing a composite sample with high-contrast speckles painted onto the sample's surface. As a load is applied to the sample, it undergoes deformation; cameras focused on the sample capture this physical change in real time. The core of the DIC technique involves a cross-correlation algorithm, which tracks the movement of the speckle patterns during the deformation phase. Once captured and analyzed by the algorithm,

these movements are transformed into a detailed strain map, providing an intricate visualization of the strain distribution across the surface of the sample seen in Figure 2-14 (b).

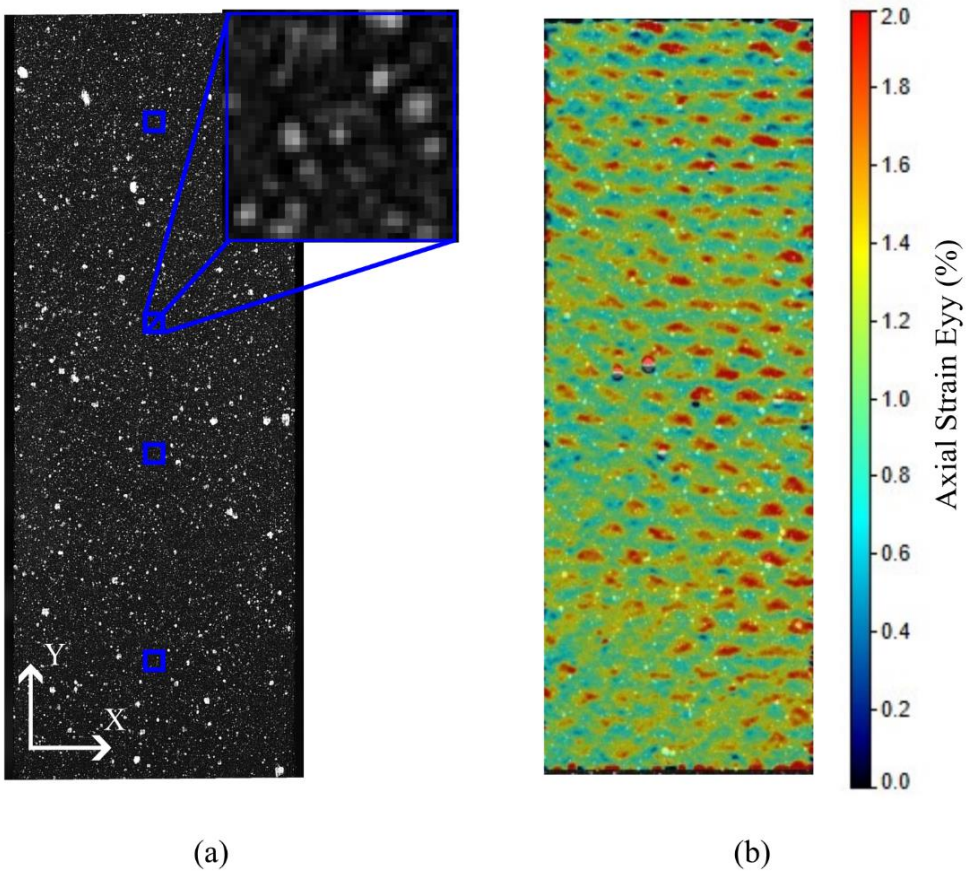

Figure 2-14: (a) Example image of a composite sample pained with high contrast speckles and a zoomed in subset that is used to track deformation of the sample during loading. (b) A computed strain map of a composite sample showing the distribution of strain across a sample undergoing loading.

The strengths of DIC include its non-contact nature, which allows for measurements without influencing the test sample's behaviour. This method is also highly versatile and can be applied to a wide range of materials and geometric configurations [113]. Moreover, DIC offers high-resolution data and can cover both small and large areas, depending on the setup. However, there are also weaknesses to consider. The accuracy of DIC can be affected by lighting conditions, and the setup can be sensitive to environmental factors such as vibrations. Additionally, the technique's

success is highly dependent on the quality of the speckle pattern and the calibration of the cameras, requiring careful preparation and setup [116]. Despite these challenges, DIC remains a powerful tool for engineers and researchers, providing valuable insights into material behaviour under various loading conditions.

In the field of composite materials, DIC offers insights into material deformation at a resolution that simply cannot be offered using strain gauges. Because of these benefits, many researchers have used DIC to aid in their analysis of composite materials when performing mechanical testing.

In a study by Guo et al. [102] the failure mechanisms of woven composite samples with various shapes (Circular, Racetrack, and Square) of open holes were studied using DIC. By using DIC, the researchers were able to compare the strain fields against their finite element model for further validation. From this study, the researchers concluded that the strain distributions visualized by DIC were significantly affected by the open hole shape, and all samples failed in specific locations determined by the stress concentrations formed from each of the various hole shapes. They also concluded that the stress concentrations were mainly distributed on the woven textile's warp yarns and that the circular specimen's stress concentration factor was 36% higher than that of the racetrack and square hole specimens. This study highlights some of the advantages of DIC's use in analyzing composite materials, as the strain analysis performed in this study would not have been possible by using conventional strain measurement techniques.

Caminero et al. [117] utilized DIC to assess the damage and repair of thermoset composite structures repaired with a scarfed repair patch. This study successfully applied both 2D and 3D DIC techniques to measure the localized strains occurring in various laminate stacking sequences as well as adhesively bonded repair patches. Areas that showed highly localized strains from the DIC assessment were further examined with X-ray radiography to reveal matrix cracking and

delamination that had occurred during testing. Through the use of DIC, the authors were able to identify damage that occurred during testing that was not plainly visible, highlighting another advantage of this evaluation technique.

A comprehensive review of DIC analysis of composite structures was conducted by Holmes et al. [118] to provide recommendations to researchers utilizing DIC in order to aid in achieving high-quality deformation measurements. The authors investigate the number of publications utilizing DIC in composite material analysis from the year 2000 until 2023 and find a significant increase in publications starting in the year 2010 and reaching the current level of approximately 8000 publications in 2023. A high-level analysis of DIC use in various loading conditions is presented. The resulting strain fields from many publications are analyzed to show how different failure modes present themselves in the strain fields. The authors conclude with recommendations for avenues that future researchers should work to address to fill in current gaps in the literature. Key gaps are identified to be improvements in camera frame rate and resolution, multi-technique characterization such as micro-CT and thermography analysis to further support the DIC analysis performed, and further analysis on novel materials such as thermoplastic composites and hybrid composites.

2.9 Gaps in literature

Thermoplastic composites offer a sustainable avenue for the composite material industry and open the door for many new manufacturing processes. Specifically, the advent of liquid thermoplastic composites that provide the ability to manufacture composites through traditional methods could dramatically reduce the life cycle impact of composite materials. Further reducing the environmental impact of these materials, their repairability must be studied to enable longer part lifespan and, ultimately, waste reduction. To date, limited research has focused on repairing damaged composite structures using simplistic patch repairs enabled by the properties of thermoplastic composites. Significant gaps exist in several key areas. These include defining the optimal size of the repair patch, quantifying what types of damage can be repaired, how these repair patches can be applied, and evaluating the overall impact on the mechanical properties of the thermoplastic composite material.

In the field of fusion bonding, available research in the area focuses almost exclusively on other methods, such as induction welding [71], [75], [110], [111], resistance welding [62], [77], [78], [108], and ultrasonic welding [68], [69], [84], [86]. Conduction welding emerges as an invaluable tool for manufacturing and repair of thermoplastic composite materials. Despite its potential benefits, such as cost-effective equipment setups, quick cycle times, and its ability to be adapted to many shapes and sizes, current research in this area is limited. The existing research in this area was done by Tijs et al. [91]. Focuses exclusively on the application of welding CF/PEEK composites. This study does not explicitly detail their welding methodology, omitting the processing parameters such as temperature and compaction pressure used to perform the conduction welding described in the study. Therefore, a gap exists in the literature to detail processing parameters such as the welding temperature, compaction pressure, and cycle time. By

optimizing these parameters, an increase in shear strength can be achieved, further improving the effectiveness of patch repairs.

From the review of the current literature presented, there remains significant room for the investigation of the material properties of liquid thermoplastic composites and the repair of said materials through lower-cost fusion bonding methods such as conduction welding. By filling these gaps in the literature, further thermoplastic composites could be adopted, ultimately allowing for more sustainable materials to be used in a wide range of industries.

2.10 Proposed Study

To address the gaps in the current literature, the following chapters detail studies with the aim of filling these gaps. Chapter three focuses on the repair of liquid thermoplastic composites by applying patch repairs using conduction welding. First, the fabrication of composite specimens using novel liquid thermoplastic is explored, and specimens are fabricated for testing. Next, various repair patch sizes are applied to damaged samples and their tensile strength is tested. During testing, DIC is utilized to assist in the analysis of the repair patches and provides strain mapping of the samples and repair patches. The failure modes are analyzed, and finally, a statistical analysis of the ultimate tensile strength is performed, determining the effectiveness of the various repair patch sizes. In a follow-up study presented in chapter four, the shear strength of liquid thermoplastic composites is analyzed in detail. This study aims to determine the optimal processing parameters to increase the conduction weld's lap shear strength, ultimately enabling stronger repairs. This is done by varying key parameters of temperature and compaction pressure and presents guidelines for future research in the field of conduction welding. Through these studies, the author aims to fill some of the current gaps in the literature and further advance the adoption of liquid thermoplastic composites.

2.11 References

[1] Composites World, “Boeing sets pace for composite usage in large civil aircraft.” Accessed: Nov. 02, 2023. [Online]. Available: https://www.compositesworld.com/articles/boeing-sets-pace-for-composite-usage-in-large-civil-aircraft

[2] Rocket Lab, “Electron Rocket.” Accessed: Nov. 02, 2023. [Online]. Available: https://www.rocketlabusa.com/launch/electron/

[3] “Global Thermoset Composites Industry,” Dec. 2023. Accessed,” Mar. 2023.

[4] “Global Thermoset Composites Industry,” Dec. 2023. Accessed: Dec. 04, 2023. [Online]. Available: https://www.reportlinker.com/p06033124/Global-Thermoset-Composites-Industry.html

[5] Y. Yang, R. Boom, B. Irion, D. J. van Heerden, P. Kuiper, and H. de Wit, “Recycling of composite materials,” *Chemical Engineering and Processing: Process Intensification*, vol. 51, pp. 53–68, Jan. 2012, doi: 10.1016/j.cep.2011.09.007.

[6] Painter Paul C. and Coleman Michael M., *Essentials of Polymer Science and Engineering*. 2009.

[7] R. Stewart, “Thermoplastic composites-recyclable and fast to process,” 2011. [Online]. Available: www.reinforcedplastics.com

[8] M. Kayaaslan, T. Coskun, U. M. Unlu, and O. S. Sahin, “Effects of thickness, fibre orientation and fabric textile on the low-velocity impact performances of thermoset and thermoplastic composites,” *Journal of Thermoplastic Composite Materials*, vol. 36, no. 11, pp. 4408–4429, Nov. 2023, doi: 10.1177/08927057231158536.

[9] P. Bajurko, “Comparison of damage resistance of thermoplastic and thermoset carbon fibre-reinforced composites,” *Journal of Thermoplastic Composite Materials*, vol. 34, no. 3, pp. 303–315, Mar. 2021, doi: 10.1177/0892705719844550.

[10] A. J. ; Ogugua, C. J. Sinke, and J. A. Dransfeld, “Comparative life cycle assessment of thermoplastic and thermosetting CFRP in aerospace applications,” 2022.

[11] A. D. La Rosa, D. R. Banatao, S. J. Pastine, A. Latteri, and G. Cicala, “Recycling treatment of carbon fibre/epoxy composites: Materials recovery and characterization and environmental impacts through life cycle assessment,” *Compos B Eng*, vol. 104, pp. 17–25, Nov. 2016, doi: 10.1016/j.compositesb.2016.08.015.

[12] D. S. Cousins, Y. Suzuki, R. E. Murray, J. R. Samaniuk, and A. P. Stebner, “Recycling glass fiber thermoplastic composites from wind turbine blades,” *J Clean Prod*, vol. 209, pp. 1252–1263, Feb. 2019, doi: 10.1016/j.jclepro.2018.10.286.

[13] J. Barroeta Robles, M. Dubé, P. Hubert, and A. Yousefpour, “Repair of thermoplastic composites: an overview,” *Advanced Manufacturing: Polymer and Composites Science*, vol. 8, no. 2. Taylor and Francis Ltd., pp. 68–96, 2022. doi: 10.1080/20550340.2022.2057137.

[14] “International Forecast: Thermoplastic Composite Industry 2023,” Dec. 2023. Accessed: Dec. 04, 2023. [Online]. Available: https://www.reportlinker.com/p06284374/Thermoplastic-Composite-Global-Market-Report.html

[15] P. Dumont, F. Martoïa, and L. Orgéas, “Compression moulding,” *Design and Manufacture of Structural Composites*, pp. 273–300, Jan. 2023, doi: 10.1016/B978-0-12-819160-6.00018-4.

[16] J. L. Thomason, “The influence of fibre length, diameter and concentration on the impact performance of long glass-fibre reinforced polyamide 6,6,” *Compos Part A Appl Sci Manuf*, vol. 40, no. 2, pp. 114–124, Feb. 2009, doi: 10.1016/j.compositesa.2008.10.013.

[17] G. Gardiner, “The making of glass fiber,” Composites World. Accessed: Nov. 03, 2023. [Online]. Available: https://www.compositesworld.com/articles/the-making-of-glass-fiber

[18] S. M. Aldosari, M. Khan, and S. Rahatekar, “Manufacturing carbon fibres from pitch and polyethylene blend precursors: a review,” *Journal of Materials Research and Technology*, vol. 9, no. 4, pp. 7786–7806, Jul. 2020, doi: 10.1016/j.jmrt.2020.05.037.

[19] “The making of carbon fiber,” Composites World. Accessed: Nov. 03, 2023. [Online]. Available: https://www.compositesworld.com/articles/the-making-of-carbon-fiber

[20] K. Shirasu, C. Nagai, and K. Naito, “Mechanical anisotropy of PAN-based and pitch-based carbon fibers,” *Mechanical Engineering Journal*, vol. 7, no. 4, pp. 19-00599-19–00599, 2020, doi: 10.1299/mej.19-00599.

[21] K. K. Chawla and N. Chawla, “Fibrous reinforcements for composites,” *Comprehensive Composite Materials II*, pp. 1–12, Jan. 2017, doi: 10.1016/B978-0-12-803581-8.09874-X.

[22] R. Tonk, “Natural fibers for sustainable additive manufacturing: A state of the art review,” *Mater Today Proc*, vol. 37, pp. 3087–3090, 2021, doi: 10.1016/j.matpr.2020.09.017.

[23] V. V Vasiliev, R. M. Jones, and L. I. Man, “Mechanics of composite structures,” Boca Raton, 1993. doi: https://doi.org/10.1201/9780203747858.

[24] FibreGlast, “Polyester Resins & Gel Coats.” Accessed: Nov. 03, 2023. [Online]. Available: https://www.fibreglast.com/category/Polyester_Resins.

[25] Omnexus, “Key Applications of Polymethyl Methacrylate,” Special Chem. Accessed: Nov. 03, 2023. [Online]. Available: https://omnexus.specialchem.com/selection-guide/polymethyl-methacrylate-pmma-acrylic-plastic/key

[26] Omnexus, “Polyamide (PA) or Nylon: Complete Guide,” SpecialChem. Accessed: Nov. 03, 2023. [Online]. Available: https://omnexus.specialchem.com/selection-guide/polyamide-pa-nylon.

[27] S. M. Zol *et al.*, “Description of Poly(aryl-ether-ketone) Materials (PAEKs), Polyetheretherketone (PEEK) and Polyetherketoneketone (PEKK) for Application as a Dental Material: A Materials Science Review,” *Polymers*, vol. 15, no. 9. MDPI, May 01, 2023. doi: 10.3390/polym15092170.

[28] K. K. Chawla, *Composite materials: Science and engineering, third edition*. Springer New York, 2012. doi: 10.1007/978-0-387-74365-3.

[29] L. BOOGH and R. MEZZENGA, “Processing Principles for Thermoset Composites,” in *Comprehensive Composite Materials*, Elsevier, 2000, pp. 671–699. doi: 10.1016/B0-08-042993-9/00221-7.

[30] I. O. Oladele *et al.*, “Modern Trends in Recycling Waste Thermoplastics and Their Prospective Applications: A Review,” *Journal of Composites Science*, vol. 7, no. 5. MDPI, May 01, 2023. doi: 10.3390/jcs7050198.

[31] JEC Group, “Market volume of polymer composite materials worldwide from 2010 to 2021, with a forecast until 2026, by application sector,” Dec. 2023.

[32] Arkema, “Thermoplastic resin Elium® for recyclable composites.” Accessed: Sep. 05, 2023. [Online]. Available: Thermoplastic resin Elium® for recyclable composites

[33] S. K. Bhudolia, S. C. Joshi, A. Bert, B. Yi Di, R. Makam, and G. Gohel, “Flexural characteristics of novel carbon methylmethacrylate composites,” *Composites Communications*, vol. 13, pp. 129–133, Jun. 2019, doi: 10.1016/j.coco.2019.04.007.

[34] “Elium® Technical Data Sheets,” MatWeb.

[35] “FiberGlast 4500 Infusion Epoxy Resin Technical Data Sheet”.

[36] “SikaBiresin® CR72 Infusion Epoxy Technical Data Sheet”.

[37] “Pro Set INF-114 Technical Data Sheet,” 2014.

[38] “IN2 epoxy infusion resin-Technical Datasheet.” [Online]. Available: www.easycomposites.co.uk|sales@easycomposites.co.uk

[39] S. K. Bhudolia and S. C. Joshi, “Low-velocity impact response of carbon fibre composites with novel liquid Methylmethacrylate thermoplastic matrix,” *Compos Struct*, vol. 203, pp. 696–708, Nov. 2018, doi: 10.1016/j.compstruct.2018.07.066.

[40] M. E. Kazemi, L. Shanmugam, D. Lu, X. Wang, B. Wang, and J. Yang, “Mechanical properties and failure modes of hybrid fiber reinforced polymer composites with a novel liquid thermoplastic resin, Elium®®,” *Compos Part A Appl Sci Manuf*, vol. 125, Oct. 2019, doi: 10.1016/j.compositesa.2019.105523.

[41] T. Pini, F. Caimmi, F. Briatico-Vangosa, R. Frassine, and M. Rink, “Fracture initiation and propagation in unidirectional CF composites based on thermoplastic acrylic resins,” *Eng Fracture Mech*, vol. 184, pp. 51–58, Oct. 2017, doi: 10.1016/j.engfracmech.2017.08.023.

[42] S. K. Bhudolia, P. Perrotey, and S. C. Joshi, “Enhanced vibration damping and dynamic mechanical characteristics of composites with novel pseudo-thermoset matrix system,” *Compos Struct*, vol. 179, pp. 502–513, Nov. 2017, doi: 10.1016/j.compstruct.2017.07.093.

[43] G. Gohel, S. K. Bhudolia, K. F. Leong, and P. Gerard, “On the structural damping response of hollow carbon composite shafts with room temperature curable novel acrylic liquid thermoplastic resin,” *Composites Communications*, vol. 29, Jan. 2022, doi: 10.1016/j.coco.2021.100990.

[44] O. A. Ekuase, N. Anjum, V. O. Eze, and O. I. Okoli, “A Review on the Out-of-Autoclave Process for Composite Manufacturing,” *Journal of Composites Science*, vol. 6, no. 6. MDPI, Jun. 01, 2022. doi: 10.3390/jcs6060172.

[45] G. Sumithra, R. N. Reddy, G. Dheeraj Kumar, S. Ojha, G. Jayachandra, and G. Raghavendra, “Review on composite classification, manufacturing, and applications,” *Mater Today Proc*, May 2023, doi: 10.1016/j.matpr.2023.04.637.

[46] E. A. Birt and R. A. Smith, “A review of NDE methods for porosity measurement in fibre-reinforced polymer composites,” *Insight - Non-Destructive Testing and Condition Monitoring*, vol. 46, no. 11, pp. 681–686, Nov. 2004, doi: 10.1784/insi.46.11.681.52280.

[47] M. Elkolali, L. P. Nogueira, P. O. Rønning, and A. Alcocer, “Void Content Determination of Carbon Fiber Reinforced Polymers: A Comparison between Destructive and Non-Destructive Methods,” *Polymers (Basel)*, vol. 14, no. 6, Mar. 2022, doi: 10.3390/polym14061212.

[48] L. Liu, B. M. Zhang, D. F. Wang, and Z. J. Wu, “Effects of cure cycles on void content and mechanical properties of composite laminates,” *Compos Struct*, vol. 73, no. 3, pp. 303–309, Jun. 2006, doi: 10.1016/j.compstruct.2005.02.001.

[49] A. Brasington, C. Sacco, J. Halbritter, R. Wehbe, and R. Harik, “Automated fiber placement: A review of history, current technologies, and future paths forward,” *Composites Part C: Open Access*, vol. 6. Elsevier B.V., Oct. 01, 2021. doi: 10.1016/j.jcomc.2021.100182.

[50] “Markforged.” Accessed: Oct. 21, 2023. [Online]. Available: https://markforged.com/

[51] “Anisoprint,” Stop metal thinking, start anisoprinting. Accessed: Oct. 21, 2023. [Online]. Available: https://anisoprint.com/solutions/

[52] D. R. Hetrick, S. H. R. Sanei, C. E. Bakis, and O. Ashour, “Evaluating the effect of variable fiber content on mechanical properties of additively manufactured continuous carbon fiber composites,” *Journal of Reinforced Plastics and Composites*, vol. 40, no. 9–10, pp. 365–377, May 2021, doi: 10.1177/0731684420963217.

[53] M. Khosroupour Arabi and N. Kordani, “3D-printing of Continuous Fiber: A review of processes, materials and properties,” *Polymer-Plastics Technology and Materials*, vol. 62, no. 12. Taylor and Francis Ltd., pp. 1525–1559, 2023. doi: 10.1080/25740881.2023.2222793.

[54] G. W. Melenka, B. K. O. Cheung, J. S. Schofield, M. R. Dawson, and J. P. Carey, “Evaluation and prediction of the tensile properties of continuous fiber-reinforced 3D printed structures,” *Compos Struct*, vol. 153, pp. 866–875, Oct. 2016, doi: 10.1016/j.compstruct.2016.07.018.

[55] S. Mohammadi, M. Yousefi, and M. Khazaei, “A review on composite patch repairs and the most important parameters affecting its efficiency and durability,” *Journal of Reinforced Plastics and Composites*, vol. 40, no. 1–2, pp. 3–15, Jan. 2021, doi: 10.1177/0731684420941602.

[56] S. Budhe, M. D. Banea, and S. de Barros, “Bonded repair of composite structures in aerospace application: a review on environmental issues,” *Applied Adhesion Science*, vol. 6, no. 1. Springer International Publishing, Dec. 01, 2018. doi: 10.1186/s40563-018-0104-5.

[57] J. P. Reis, M. de Moura, and S. Samborski, “Thermoplastic composites and their promising applications in joining and repair composites structures: A review,” *Materials*, vol. 13, no. 24. MDPI AG, pp. 1–33, Dec. 02, 2020. doi: 10.3390/ma13245832.

[58] M. Préau, “Defect Management in Vacuum Bag Only Semipreg Processing of Co-bonded Composite Repairs,” 2016.

[59] C. N. D. Chun Hui Wang, Bonded Joints and Repairs to Composite Airframe Structures, 1st ed. 2015.

[60] M. Rachid, B. Serier, B. Bachir Bouiadjra, and M. Belhouari, “Numerical analysis of the patch shape effects on the performances of bonded composite repair in aircraft structures,” *Compos B Eng*, vol. 43, no. 2, pp. 391–397, Mar. 2012, doi: 10.1016/j.compositesb.2011.08.047.

[61] L. S. M. B. and B. S. John S. Tomblin, “Effects of Repair Procedures on Bonded Repairs of Airframe Structures,” 2017.

[62] W. P. Seneviratne, J. S. Tomblin, and B. L. Saathoff, “Influence of various surface preparation techniques on resistance welded and adhesively bonded unidirectional thermoplastic composite joints,” 2021.

[63] A. Yousefpour, M. Hojjati, and J. P. Immarigeon, “Fusion bonding/welding of thermoplastic composites,” *Journal of Thermoplastic Composite Materials*, vol. 17, no. 4, pp. 303–341, Jul. 2004, doi: 10.1177/0892705704045187.

[64] R. E. Murray, J. Roadman, and R. Beach, “Fusion joining of thermoplastic composite wind turbine blades: Lap-shear bond characterization,” *Renew Energy*, vol. 140, pp. 501–512, Sep. 2019, doi: 10.1016/j.renene.2019.03.085.

[65] C. Ageorges, L. Ye, and M. Hou, “Advances in fusion bonding techniques for joining thermoplastic matrix composites: a review,” *Compos Part A Appl Sci Manuf*, vol. 32, no. 6, pp. 839–857, Jun. 2001, doi: 10.1016/S1359-835X(00)00166-4.

[66] A. Yousefpour, M. Hojjati, and J. P. Immarigeon, “Fusion bonding/welding of thermoplastic composites,” *Journal of Thermoplastic Composite Materials*, vol. 17, no. 4. pp. 303–341, Jul. 2004. doi: 10.1177/0892705704045187.

[67] W. Suwanwatana, S. Yarlagadda, and J. W. Gillespie, “Hysteresis heating based induction bonding of thermoplastic composites,” *Compos Sci Technol*, vol. 66, no. 11–12, pp. 1713–1723, Sep. 2006, doi: 10.1016/j.compscitech.2005.11.009.

[68] H. Li, C. Chen, R. Yi, Y. Li, and J. Wu, “Ultrasonic welding of fiber-reinforced thermoplastic composites: a review,” *International Journal of Advanced Manufacturing Technology*, vol. 120, no. 1–2. Springer Science and Business Media Deutschland GmbH, pp. 29–57, May 01, 2022. doi: 10.1007/s00170-022-08753-9.

[69] G. P. Zhang, J. C. Li, Z. X. Liu, and P. C. Wang, “Application of ultrasonic welding to repair adhesively bonded short carbon fiber reinforced Nylon 6 composites,” *Int J Adhes Adhes*, vol. 100, p. 102603, Jul. 2020, doi: 10.1016/J.IJADHADH.2020.102603.

[70] M. Dubé, A. Chazerain, P. Hubert, A. Yousefpour, and H. E. Bersee, “Characterization of resistance-welded thermoplastic composite double-lap joints under static and fatigue loading,” *Journal of Thermoplastic Composite Materials*, vol. 28, no. 6, pp. 762–776, Jun. 2015, doi: 10.1177/0892705713490714.

[71] B. K. Choi, C. S. Kang, M. H. Yoo, and M. K. Seo, “Effect of Processing Parameters on Bonding Performance of a Carbon Fiber/Polyetheretherketone Thermoplastic Composite Prepared by Induction Welding,” *Materials*, vol. 16, no. 11, Jun. 2023, doi: 10.3390/ma16113954.

[72] R. Rudolf, P. Mitschang, and M. Neitzel, “Induction heating of continuous carbon-fibre-reinforced thermoplastics.” [Online]. Available: www.elsevier.com/locate/compositesa

[73] B. K. Fink, S. Yarlagadda, and J. W. Gillespie, “Design of a Resistive Susceptor for Uniform Heating During Induction Bonding of Composites,” 2000.

[74] R. Rudolf, P. Mitschang, and M. Neitzel, “Induction heating of continuous carbon-fibre-reinforced thermoplastics.” [Online]. Available: www.elsevier.com/locate/compositesa

[75] S. Becker and P. Mitschang, “Process Improvement of Continuous Induction Welding of Carbon Fiber-Reinforced Polymer Composites,” *J Mater Eng Perform*, vol. 31, no. 9, pp. 7049–7060, Sep. 2022, doi: 10.1007/s11665-022-06842-0.

[76] Christophe Ageorges and Lin Ye, *Fusion Bonding of Polymer Composites: From Basic Mechanisms to Process Optimization*. 2002.

[77] M. Dubé, P. Hubert, J. N. A. H. Gallet, D. Stavrov, H. E. N. Bersee, and A. Yousefpour, "Metal mesh heating element size effect in resistance welding of thermoplastic composites," *J Compos Mater*, vol. 46, no. 8, pp. 911–919, Apr. 2012, doi: 10.1177/0021998311412986.

[78] C. Ageorges, L. Ye, and M. Hou, "Experimental investigation of the resistance welding of thermoplastic-matrix composites. Part II: optimum processing window and mechanical performance," 2000.

[79] I. F. Villegas, L. Moser, A. Yousefpour, P. Mitschang, and H. E. N. Bersee, "Process and performance evaluation of ultrasonic, induction and resistance welding of advanced thermoplastic composites," *Journal of Thermoplastic Composite Materials*, vol. 26, no. 8, pp. 1007–1024, Sep. 2013, doi: 10.1177/0892705712456031.

[80] W. P. Seneviratne, J. S. Tomblin, and B. L. Saathoff, "influence of various surface preparation techniques on resistance welded and adhesively bonded unidirectional thermoplastic composite joints."

[81] G. Palardy and I. F. Villegas, "On the effect of flat energy directors thickness on heat generation during ultrasonic welding of thermoplastic composites," *Compos Interfaces*, vol. 24, no. 2, pp. 203–214, Feb. 2017, doi: 10.1080/09276440.2016.1199149.

[82] Z. Zhang, X. Wang, Y. Luo, Z. Zhang, and L. Wang, "Study on heating process of ultrasonic welding for thermoplastics," *Journal of Thermoplastic Composite Materials*, vol. 23, no. 5, pp. 647–664, Sep. 2010, doi: 10.1177/0892705709356493.

[83] A. Levy, S. Le Corre, and I. Fernandez Villegas, "Modeling of the heating phenomena in ultrasonic welding of thermoplastic composites with flat energy directors," *J Mater Process Technol*, vol. 214, no. 7, pp. 1361–1371, 2014, doi: 10.1016/j.jmatprotec.2014.02.009.

[84] S. K. Bhudolia, G. Gohel, K. F. Leong, and A. Islam, "Advances in ultrasonic welding of thermoplastic composites: A review," *Materials*, vol. 13, no. 6, Mar. 2020, doi: 10.3390/ma13061284.

[85] T. G. G. Avraham Benatar, "Ultrasonic welding of PEEK graphite APC-2 composites," *Polym Eng Sci*, vol. 29, no. 23, pp. 1705–1721, Dec. 1989.

[86] S. K. Bhudolia, G. Gohel, J. Kantipudi, K. F. Leong, and R. J. Barsotti, "Ultrasonic welding of novel carbon/ Elium® thermoplastic composites with flat and integrated energy directors: Lap shear characterisation and fractographic investigation," *Materials*, vol. 13, no. 7, Apr. 2020, doi: 10.3390/ma13071634.

[87] Y. K. Chuah, L. H. Chien, B. C. Chang, and S. J. Liu, “Effects of the shape of the energy director on far-field ultrasonic welding of thermoplastics,” *Polym Eng Sci*, vol. 40, no. 1, pp. 157–167, 2000, doi: 10.1002/pen.11149.

[88] M. J. Troughton, Ed., “Chapter 1 - Heated Tool Welding,” in *Handbook of Plastics Joining (Second Edition)*, Second Edition., Boston: William Andrew Publishing, 2009, pp. 3–13. doi: https://doi.org/10.1016/B978-0-8155-1581-4.50003-2.

[89] H. Perrin, M. Bodaghi, V. Berthé, S. Klein, and R. Vaudemont, “On the Hot-Plate Welding of Reactively Compatibilized Acrylic-Based Composites/Polyamide (PA)-12,” *Materials*, vol. 16, no. 2, Jan. 2023, doi: 10.3390/ma16020691.

[90] L. Li, W. Liu, Y. Wang, and Z. Zhao, “Mechanical performance and damage monitoring of CFRP thermoplastic laminates with an open hole repaired by 3D printed patches,” *Compos Struct*, vol. 303, Jan. 2023, doi: 10.1016/j.compstruct.2022.116308.

[91] B. H. A. H. Tijs, M. H. J. Doldersum, A. Turon, J. E. A. Waleson, and C. Bisagni, “Experimental and numerical evaluation of conduction welded thermoplastic composite joints,” *Compos Struct*, vol. 281, Feb. 2022, doi: 10.1016/j.compstruct.2021.114964.

[92] S. Erland, H. Stevens, and L. Savage, “The re-manufacture and repairability of poly(ether ether ketone) discontinuous carbon fibre composites,” *Polym Int*, vol. 70, no. 8, pp. 1118–1127, Aug. 2021, doi: 10.1002/pi.6220.

[93] ASTM International, “Standard Test Method for Tensile Properties of Polymer Matrix Composite Materials 1,” 2014, doi: 10.1520/D3039_D3039M-14.

[94] ASTM International, “Standard Test Method for Lap Shear Adhesion for Fiber Reinforced Plastic (FRP) Bonding,” 2023, doi: 10.1520/D5868-01R23.

[95] ASTM International, “Standard Test Method for Open-Hole Tensile Strength of Polymer Matrix Composite Laminates.” Accessed: Dec. 10, 2023. [Online]. Available: https://www.astm.org/d5766_d5766m-11r18.html

[96] R. C. Hibbeler, *Mechanics of Materials*, 10th ed. Pearson Education, 2017.

[97] M. Eftekhari and A. Fatemi, “Tensile behavior of thermoplastic composites including temperature, moisture, and hygrothermal effects,” *Polym Test*, vol. 51, pp. 151–164, May 2016, doi: 10.1016/j.polymertesting.2016.03.011.

[98] A. Todoroki *et al.*, “Tensile property evaluations of 3D printed continuous carbon fiber reinforced thermoplastic composites,” *Advanced Composite Materials*, vol. 29, no. 2, pp. 147–162, Mar. 2020, doi: 10.1080/09243046.2019.1650323.

[99] H. M. M. A. Rashed, M. A. Islam, and F. B. Rizvi, “effects of process parameters on tensile strength of jute fiber reinforced thermoplastic composites,” 2006. [Online]. Available: http://jname.8m.net

[100] K. Naito and H. Oguma, “Tensile properties of novel carbon/glass hybrid thermoplastic composite rods,” *Compos Struct*, vol. 161, pp. 23–31, Feb. 2017, doi: 10.1016/j.compstruct.2016.11.042.

[101] M. E. Kazemi, L. Shanmugam, D. Lu, X. Wang, B. Wang, and J. Yang, “Mechanical properties and failure modes of hybrid fiber reinforced polymer composites with a novel liquid thermoplastic resin, Elium®,” *Compos Part A Appl Sci Manuf*, vol. 125, Oct. 2019, doi: 10.1016/j.compositesa.2019.105523.

[102] Q. Guo, Y. Zhang, D. Li, M. Li, X. Sun, and L. Chen, “Tensile properties and failure mechanism of 3D woven composites containing holes of different geometries,” *Thin-Walled Structures*, vol. 166, Sep. 2021, doi: 10.1016/j.tws.2021.108115.

[103] U. A. Khashaba and A. I. Khdair, “Open hole compressive elastic and strength analysis of CFRE composites for aerospace applications,” *Aerosp Sci Technol*, vol. 60, pp. 96–107, Jan. 2017, doi: 10.1016/j.ast.2016.10.026.

[104] R. M. A. Khan, T. Shafighfard, H. Q. Ali, M. Mieloszyk, and M. Yildiz, “Strength prediction and experimental damage investigations of plain woven CFRPs with interacting holes using multi-instrument measurements,” *Polym Compos*, vol. 44, no. 6, pp. 3594–3609, Jun. 2023, doi: 10.1002/pc.27347.

[105] G. Gohel, S. K. Bhudolia, J. Kantipudi, K. F. Leong, and R. J. Barsotti, “Ultrasonic welding of novel Carbon/Elium® with carbon/epoxy composites,” *Composites Communications*, vol. 22, Dec. 2020, doi: 10.1016/j.coco.2020.100463.

[106] X. Xiong, D. Wang, R. Ren, P. Zhao, X. Cui, and S. Ji, “Improved mechanical properties of resistance welded joints of thermoplastic composites by versatile graphene oxide,” *J Adhes Sci Technol*, vol. 35, no. 10, pp. 1099–1113, 2021, doi: 10.1080/01694243.2020.1834288.

[107] K. Panneerselvam, S. Aravindan, and A. Noorul Haq, “Study on resistance welding of glass fiber reinforced thermoplastic composites,” *Mater Des*, vol. 41, pp. 453–459, Oct. 2012, doi: 10.1016/j.matdes.2012.05.025.

[108] N. Koutras, I. F. Villegas, and R. Benedictus, “Influence of temperature on the strength of resistance welded glass fibre reinforced PPS joints,” *Compos Part A Appl Sci Manuf*, vol. 105, pp. 57–67, Feb. 2018, doi: 10.1016/j.compositesa.2017.11.003.

[109] I. F. Villegas and G. Palardy, “Ultrasonic welding of thermoplastic composite coupons for mechanical characterization of welded joints through single lap shear testing,” *Journal of Visualized Experiments*, vol. 2016, no. 108, Feb. 2016, doi: 10.3791/53592.

[110] B. Kwon, H. Choe, J. Jeong, H. Ju, J. H. Kweon, and Y. W. Nam, “Static and fatigue behavior of induction-welded single lap carbon fiber reinforced polyetherketoneketone thermoplastic composite joints,” *J Compos Mater*, vol. 55, no. 28, pp. 4183–4193, Dec. 2021, doi: 10.1177/00219983211033891.

[111] P. Gouin O'Shaughnessey, M. Dubé, and I. Fernandez Villegas, "Modeling and experimental investigation of induction welding of thermoplastic composites and comparison with other welding processes," *J Compos Mater*, vol. 50, no. 21, pp. 2895–2910, Sep. 2016, doi: 10.1177/0021998315614991.

[112] F. Lionetto, S. Pappadà, G. Buccoliero, and A. Maffezzoli, "Finite element modeling of continuous induction welding of thermoplastic matrix composites," *Mater Des*, vol. 120, pp. 212–221, Apr. 2017, doi: 10.1016/j.matdes.2017.02.024.

[113] H. Schreier, J. J. Orteu, and M. A. Sutton, *Image correlation for shape, motion and deformation measurements: Basic concepts, theory and applications*. Springer US, 2009. doi: 10.1007/978-0-387-78747-3.

[114] A. Khudiakova, V. Grasser, C. Blumenthal, M. Wolfahrt, and G. Pinter, "Automated monitoring of the crack propagation in mode 1 testing of thermoplastic composites by means of digital image correlation," *Polym Test*, vol. 82, Feb. 2020, doi: 10.1016/j.polymertesting.2019.106304.

[115] M. Gljušćić, M. Franulović, D. Lanc, and Božić, "Application of digital image correlation in behavior modelling of AM CFRTP composites," *Eng Fail Anal*, vol. 136, Jun. 2022, doi: 10.1016/j.engfailanal.2022.106133.

[116] Y. L. Dong and B. Pan, "A Review of Speckle Pattern Fabrication and Assessment for Digital Image Correlation," *Exp Mech*, vol. 57, no. 8, pp. 1161–1181, Oct. 2017, doi: 10.1007/s11340-017-0283-1.

[117] M. A. Caminero, M. Lopez-Pedrosa, C. Pinna, and C. Soutis, "Damage assessment of composite structures using digital image correlation," *Applied Composite Materials*, vol. 21, no. 1, pp. 91–106, 2014, doi: 10.1007/s10443-013-9352-5.

[118] J. Holmes, S. Sommacal, R. Das, Z. Stachurski, and P. Compston, "Digital image and volume correlation for deformation and damage characterisation of fibre-reinforced composites: A review," *Composite Structures*, vol. 315. Elsevier Ltd, Jul. 01, 2023. doi: 10.1016/j.compstruct.2023.116994.

Chapter 3: Enhancing Composite Material Sustainability: A Study on the Repairability of Liquid Thermoplastic-Based Composites

3.1 Introduction

Over the last decade, composite materials are increasingly used in numerous industries, including aerospace, automotive and energy [1]. The increasing usage is projected to keep growing throughout the 2030's, with an annual growth rate of 7.29% globally [2]. The steady industry growth can be attributed to the ideal mechanical properties of fibre-reinforced polymers concerning their strength-to-weight ratio. The material properties of fibre-reinforced polymers are also tailorable to specific applications by orienting fibres in the direction of loading. By using these strategies, designers and engineers can create materials that are able to resist loads in specific directions and remove material in unnecessary areas, ultimately leading to stronger and lighter end products.

However, one issue that the use of composite materials is creating is the lack of practical and economical ways to recycle the material when it is damaged or has reached its end of life [3], [4]. Traditional composite materials are comprised of a reinforcing fibre material and a matrix material. One of the most common matrix materials in use today is thermoset epoxy resin [5]. The polymer chains that comprise a thermoset epoxy undergo cross-linking during their cure, which results in the polymer chains forming covalent bonds, holding the polymer chains in place [6]. Once cured, the thermoset polymer can no longer be remelted or reshaped and cannot enter a liquid phase again. Furthermore, the irreversible nature of the curing process complicates the repair of thermoset composites, as the material cannot be softened or reformed to correct defects or damage. Because

of this cross-linking process, it is currently difficult to recycle thermoset composites economically and ultimately lead to an accumulation of composite materials building up in landfills [7], [8].

Thermoplastic composite materials have the potential to change this sustainability issue. The production of traditional thermoplastic composites has historically presented formidable manufacturing challenges because of the high temperatures required to infuse fibers with a polymer melt. Common plastics used in thermoplastic composites, such as Polypropylene (PP) or Polyether ether ketone (PEEK), often necessitate complex techniques such as, injection moulding or heated compression moulding because they require high temperatures to transition into a polymer melt [9]. A recent development that holds promise in addressing these challenges is the Polymethyl methacrylate (PMMA) based Elium® resin, a family of liquid thermoplastic resins developed by Arkema [10]. Liquid matrix materials are ideal for creating composite materials because they lend themselves to simple manufacturing techniques such as hand layups and vacuum-assisted resin infusions [11]. These manufacturing methods are much simpler and more cost-effective at lower production quantities, which is one of the reasons traditional thermoset epoxies are typically preferred. Liquid thermoplastic resin presents an intriguing proposition as a drop-in replacement for thermoset epoxy, potentially reshaping the composite materials industry and helping to reduce their sustainability issues.

What distinguishes Elium® liquid thermoplastic resin from other epoxies is its maintenance of intrinsic thermoplastic properties while being a low-viscosity resin before curing, having a viscosity value of 100 centipoise at 25°C [10]. In addition to its manufacturability, its thermoplastic properties allow for reheating and remelting the matrix material, enabling new manufacturing and repair methods that were previously difficult or impossible on epoxy resins. Furthermore, these thermoplastic attributes position liquid thermoplastic resin as a considerably more recyclable

alternative to conventional thermoset materials. Recycling thermoplastics can be achieved through various methods, such as grinding, pyrolysis, or solvent dissolution, with the potential to significantly diminish the carbon footprint associated with composite materials [12].

Another way that liquid thermoplastic resin can help reduce the environmental footprint that composite materials create is by enabling new repair methods. Traditional epoxy-based repair methods for composite materials are relatively rare, primarily due to the challenges associated with effectively repairing thermoset matrix composites. The most common repairs performed on traditional thermoset composites are bolted repairs, which involve drilling holes in the laminate and mechanically fastening a premade repair patch with a grid of bolts [13]. This type of repair patch can have significant downsides, such as creating stress concentrations at bolt holes and can be difficult or impossible to apply depending on the laminate's geometry. It also takes substantial surface preparation, resulting in a lengthy and costly repair. Adhesive repairs have been conducted in several studies and have shown significant improvements in strength recovery, achieving up to 90% of the original undamaged sample [14], [15], [16]. However, these repairs also suffer similar drawbacks when it comes to significant surface preparation and difficulty predicting the long-term performance of the adhesive under cyclic loading scenarios [17]. In contrast, the adoption of thermoplastic matrix materials offers a distinct advantage by allowing the use of fusion bonding techniques, commonly referred to as plastic welding [18], [19]. This innovative approach presents an opportunity for minimal preparation repairs that are both rapid and straightforward to execute [20].

This research paper evaluates the effectiveness of repairing thermoplastic composites with repair patches using a liquid thermoplastic resin. These repair patches are applied using a low-cost method called conduction welding, implemented through a heated press. Conduction welding is a

process where heated platens compress the repair patch and the sample at a temperature above the glass transition point of the thermoplastic matrix. This enables the polymer at the interface to melt and join the repair patch to the sample [21]. Previous research on the use of conduction welding to join thermoplastic composites has been limited, and there have yet to be widely accepted optimized processing parameters for conduction welding. However, some research has been performed to determine critical parameters affecting the strength of welded thermoplastics, such as the tool temperature, welding time, and contact pressure [22], [23], [24].

To assess the efficacy of conduction welded repairs, tensile testing was employed, comparing the repaired samples and their varying patch sizes to both undamaged and damaged samples without any repair. To simulate real-world constraints, a one-sided repair approach was adopted, reflecting scenarios where access is limited to the internal surface of a composite component. Furthermore, this study employed 2D Digital Image Correlation (DIC) techniques to visualize and analyze the strain field on both the front and back sides of the samples. DIC has been used extensively in recent studies to analyze composite structures and repairs due to its ability to map strain fields over the surface of the entire sample instead of taking single-point strain measurements with devices such as a strain gauge [25], [26], [27], [28], [29], [30], [31], [32], [33], [34]. This DIC-based strain analysis provides valuable insights into the performance of the repair patch and its impact on the structural integrity of the composite material.

Further highlighting DIC's use in composite research, a study by Caminero et al. [32] proposes DIC as an effective measurement tool in assessing the performance of repairs to composite structures. This study focused on open hole specimens and adhesively bonded scarf repairs, measuring surface strain, and comparing the results to finite element analysis to validate results. The authors also utilized X-ray radiography to confirm the presence of matrix cracks occurring at

locations that were previously highlighted by DIC that revealed localized strain concentrations. This research demonstrates some of the benefits that DIC can provide to researchers, assisting in the analysis of composite materials.

By examining the repair process and its influence on the mechanical properties of liquid thermoplastic composites, this research aims to contribute essential knowledge to the field of composite material repair, shedding light on the viability and effectiveness of conduction welding as a low-cost, rapid, repair method, ultimately enabling the reduction of the carbon footprint of composite materials.

3.2 Methodology

This study tested five sample types: an undamaged sample as a control, a damaged sample with no repair, and repaired samples with a 12.5mm X 12.5mm patch, a 25mm X 25mm patch, and a 25mm X 50 mm patch. Each sample type had three samples for a total of 15 samples manufactured. A diagram of the sample types can be seen below in Figure 3-1 (a), showing the sample dimensions and repair patch sizes. The fabricated samples before testing can be seen in Figure 3-1 (b). Undamaged samples represent a reference sample with no defects. Damaged samples have a 6.25mm hole in the center of the sample which accounts for one quarter of the load bearing fibers to be removed. The size of the repair patches was chosen to be two times, four times, or eight times larger than the hole diameter. These sizes were chosen with the objective of identifying the optimal size of the repair patch relative to the size of the damage in order to define an optimal patch size and avoid using unnecessarily large patches during repairs. The chosen patch sizes also ensure that the whole repair patch was visible when performing DIC while still offering a wide range of repair patch sizes to evaluate.

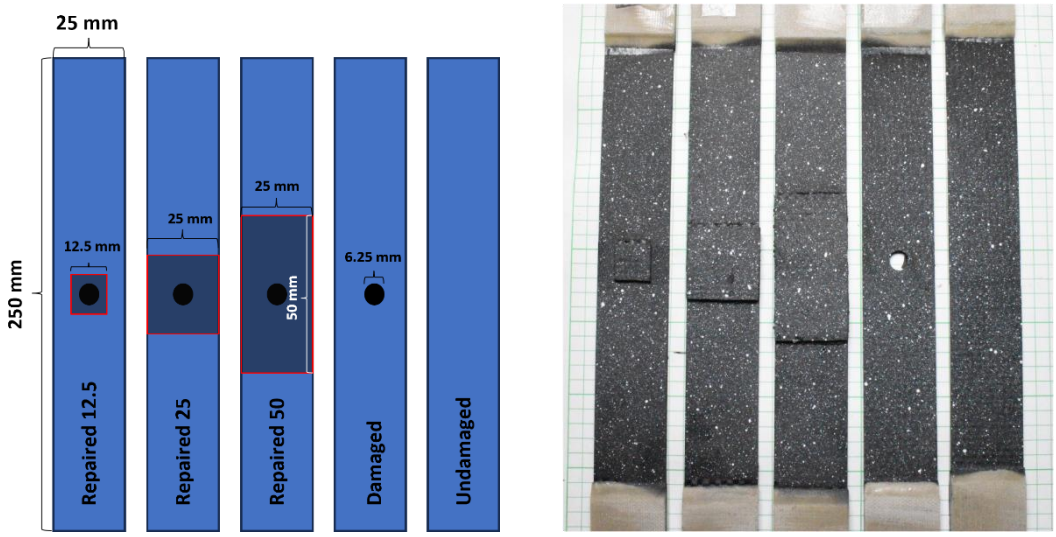

(a) (b)

Figure 3-1: (a) Diagram of the samples used in this study showing dimensions of the samples and repair patches. (b) Manufactured samples with repair patches and speckling applied before tensile testing.

3.2.1 Sample Preparation

3.2.1.1 Composite Pannel Fabrication

A panel of 5.7oz, 3k, plain woven carbon fibre and Elium® 188 O liquid thermoplastic resin was created via a resin infusion process, as seen below in Figure 3-2. First, a steel plate was coated with six layers of release agent (Frekote 700-NC Release, Henkel, Düsseldorf, Germany). Next, Sealant tape (AT-200Y, Airtech, Huntington Beach, California, USA) was placed around the edge of the plate. The carbon fibre plies were cut from a roll to a size of 300 x 635 mm and placed manually on the steel plate. The layup schedule for the fibres was six carbon fibre layers at an angle of $[0, 90]_6$.Which resulted in a final laminate thickness of 1.5 mm. A layer of peel ply (Bleeder Lease-B Airtech, Huntington Beach, California, USA) and flow mesh (Greenflow 75, Airtech, Huntington Beach, California, USA) were placed over the fibres. Finally, a nylon vacuum bag film (Wrightlon 7400, Airtech, Huntington Beach, California, USA) was set on top, and a vacuum was drawn using custom thermoplastic polyurethane (TPU) through bag connectors. Leak checks were performed on the vacuum bag, and after all leaks were eliminated, the two parts of

the Elium® thermoplastic resin were mixed. The resin was mixed at a ratio of 100 parts Elium® 188 O resin to 3 parts Luperox AFR40 hardener by weight for 3 minutes and it was then placed in a degassing chamber for 10 minutes. Next, the resin was removed from the degassing chamber and allowed to flow into the vacuum bag, infusing the carbon fibre. Once completely infused, the resin feed line was clamped off, the panel was left to cure overnight, and then the panel was removed from the vacuum bag. The final dimensions of the panel were 300 X 635 mm.

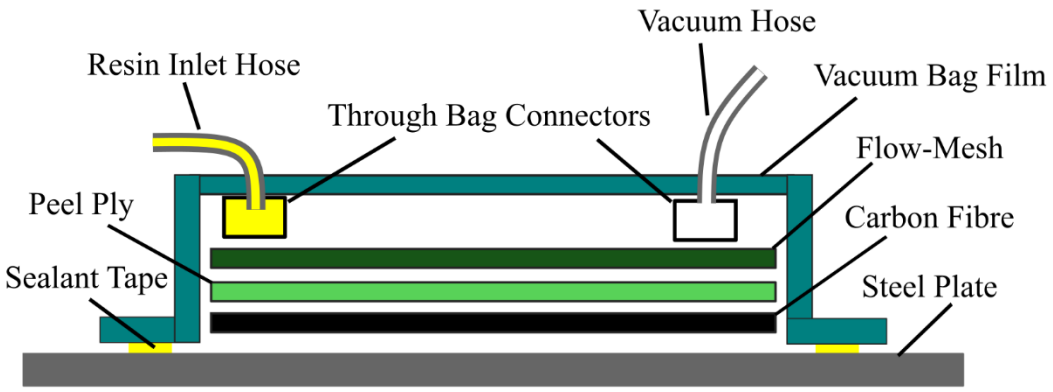

Figure 3-2: Diagram of the resin infusion process showing key components of the manufacturing process.

3.2.1.2 Sample and Patch Fabrication

After the composite panel was manufactured, a total of 15 tensile samples and nine repair patches were cut out using a waterjet (Flow Mach 2 4020B, Flow International, Washington, USA). The tensile samples were cut to 250 mm X 25 mm, as stated in ASTM D3039 [35]. The three repair patch sizes evaluated in this study were 12.5 X 12.5 mm, 25 X 25 mm, and 25 X 50 mm. After water jet cutting, all samples and repair patches were measured with five measurements using a micrometer (Starrett 3732, Starrett, North Carolina, USA) to calculate the cross-sectional area of each sample.

3.2.1.3 Drilling of Holes for Damaged and Repaired Samples

The samples were damaged by drilling a hole in the center of the sample using a 3d printed jig and a drill press (Skil 3320, Illinois, USA) with a 6.25mm drill bit. This was chosen to have a repeatable form of fiber fracture that affected all samples similarly.

3.2.1.4 End Tab Bonding

End tabs made of 1.6 mm thick G-10 Fibreglass (Garolite G-10, Accurate Plastics, New York, USA) were bonded to the ends of the samples to provide a surface for the hydraulic grips to hold. This surface provided a means of protecting the sample from the compressive forces of the grips during testing. The end tab ends were sanded to a taper angle of 12 degrees using a 3d printed jig fixed to a belt sander, (SKIL 3376, SKIL, Illinoi, USA) as recommended by the Washington Office of Aviation Research [36]. This is done to reduce the stress concentrations that could form from sharp edges at the end of the tab. End tabs also ensure a uniform longitudinal load throughout the sample during testing. The end tabs were adhered to the samples with epoxy (FIBREGLAST 2000, Fibre Glast Developments, Ohio, USA) and hardener (FIBREGLAST, Fibre Glast Developments, Ohio, USA 2020) at a ratio of 100:23 by weight. A diagram of the end tabs can be seen below in Figure 3-3 showing the length, thickness, and taper angle of the end tabs and the gage length of the sample, representing the area the sample will fracture in during testing.

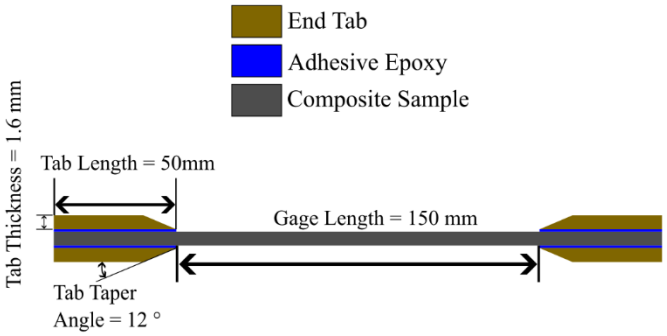

Figure 3-3: End tab bonding diagram showing the composite sample, the adhesive, and the end tabs

3.2.1.5 Differential Scanning Calorimetry (DSC) of Elium® Resin

Differential scanning calorimetry (DSC) (Q250 Discover DSC, TA Instruments, New Castle, DE, USA) was performed on cured samples of liquid thermoplastic resin (Elium® 188 O, Arkema, Colombes, France). The test was set to ramp from 40 °C to 220 °C at a rate of 10 °C/min in a nitrogen atmosphere, and the heat flow from the material was measured during the first heating run. All samples were approximately 10 mg $\pm$ 1 mg. This test was performed to determine the glass transition (T_g) point of the Elium® resin, which indicates the minimum temperature needed to bond the repair patches to the samples.

The results of the DSC measurement can be seen below in Figure 3-4. The glass transition point can be identified on a DSC curve as the midpoint of the rise in the heat flow, indicating an exothermic reaction [6]. From this test, the glass transition point of Elium® 188 O resin is 76 °C, which also aligns with the manufacturer's datasheet. The DSC curve in Figure 3-4 also shows that the polymer is amorphous, indicated by the lack of an identifiable melting point in the curve [37].

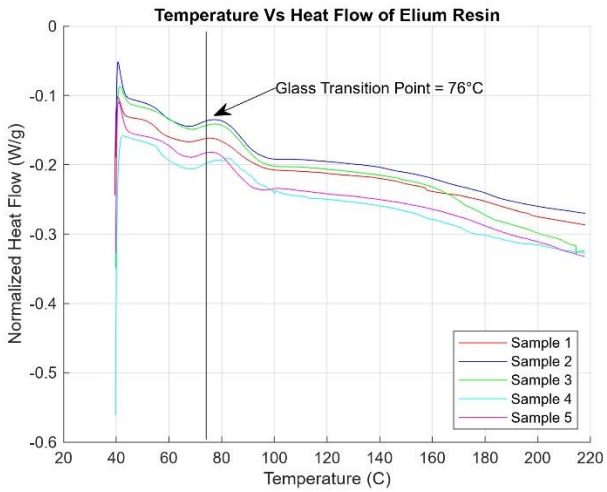

Figure 3-4: DSC curve for Elium® resin measuring heat flow vs temperature showing the glass transition point of Elium® 188 O resin at 76 °C

3.2.1.6 Repair Patch Application

The repair patches in this study were applied to the damaged samples using a conduction welding process. Conduction welding is a simple, low-cost method of plastic welding thermoplastic composites together [21]. By compressing the repair patch and the sample together utilizing a heated press, heat is conducted through the sample and the Elium resin in the sample transitions to a polymer melt. The thermoplastic matrix begins to flow across the bonding interface and the two samples bond together. Conduction welding in this study was performed using a heated press (Heat Press CK220, YaeTek, China) and a diagram can be seen below in Figure 3-5 showing how the repair patches were applied.

First, the bonding areas were cleaned with isopropyl alcohol. Next, the repair patch was brushed with approximately one gram of uncured Elium® resin to ensure that no dry spots would be present in the bonding interface. The repair patch was centered on the hole in the damaged sample and then placed into the heated press. To determine an acceptable temperature for the heated press, the data from Figure 3-4 was used, and the press was set to a temperature of 150 °C. This temperature,

being double that of the glass transition point was chosen to ensure that the resin becomes sufficiently fluid allowing it to properly flow and ultimately minimize voids or dry spots. A clamping pressure of 12 Bar was then applied to the repair patch to ensure intimate contact between the sample and the repair patch, again minimizing the potential for voids to form. The pressure and heat were applied for 45 seconds ensuring a uniform heat distribution and allowing time for the resin to flow. The samples were then removed and cooled at room temperature, resulting in a resolidified matrix.

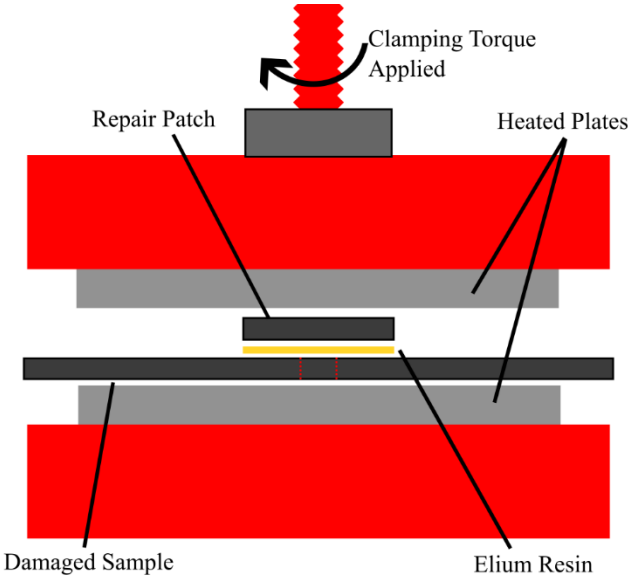

Figure 3-5: Heated press used to bond repair patches to damaged samples.

3.2.2 Lap Shear Testing

Lap shear tests were performed using an MTS 809 Axial/Torsional universal testing frame. This test was done to determine the shear strength of the conduction welded repair patches used in the repaired samples of this study. Seven lap shear joints were fabricated for testing following ASTM D5868, and a diagram of the sample configuration can be seen below in Figure 3-6 [38]. The bonding methodology was identical to the repair patch application, as stated in section 3.2.1.6. The

lap shear joints had an overlap of 25mm by 25mm, resulting in an area of 6.25 cm^2. The samples were placed in the hydraulic grips of the MTS testing frame at a clamping pressure of 2000 Psi and pulled in tension at a rate of 2mm/min until failure.

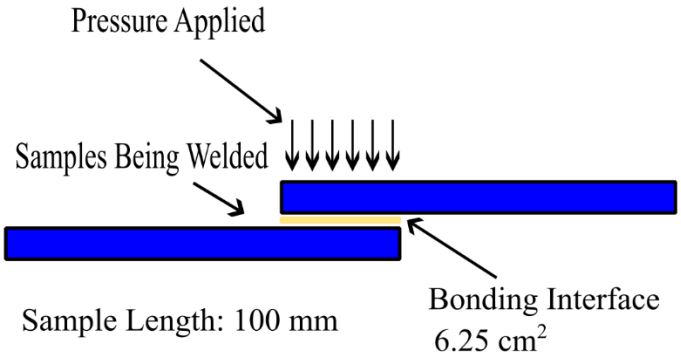

Figure 3-6: Diagram of lap shear samples according to ASTM D5868

3.2.3 Tensile Testing of Composite Samples

Tensile Testing for the samples was performed using a universal testing frame (MTS 809 Axial/Torsional, MTS Systems, Minnesota, USA) as seen below in Figure 3-7, along with the DIC and lighting setup. The samples were placed in the hydraulic grips at a clamping pressure of 2000 Psi and pulled in tension at a rate of 2mm/min until failure, according to ASTM D3039 [35]. Two-sided 2D DIC was performed during tensile testing to evaluate the axial strain throughout the material as it undergoes deformation. Images of the front and back side of the samples were then used to compare the results from the patched and unpatched sides of the sample.

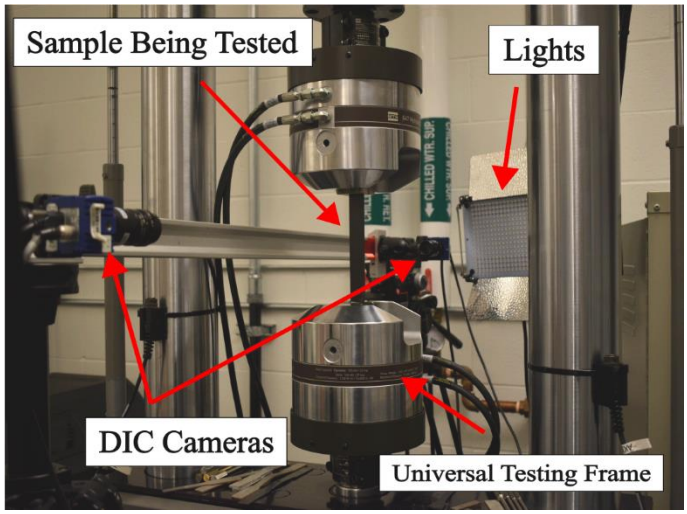

Figure 3-7: Annotated Image of universal testing frame showing the sample testing and DIC camera setup

3.2.4 Digital Image Correlation

DIC is a non-contacting surface deformation measurement technique that allows for full-field strain mapping of a sample as it undergoes loading [39]. In this study DIC is used to visualize the strain fields around the repair patches and the holes during tensile testing. The process works by analyzing the movement of an object frame by frame and calculates the strain as the object's surface undergoes deformation [39]. Deformation tracking is enabled by a speckle pattern painted onto the sample's surface before testing. Panel lights illuminate the sample, and cameras capture the motion of the speckles as the sample undergoes loading. Single camera, 2D DIC was performed on both sides of the samples to evaluate the stress on the front and back of the samples. These measurements were performed as samples underwent tensile testing to analyze the stress throughout the entire field of view. All DIC parameters can be seen below in Table 3-1.

3.2.4.1 Sample Painting and Speckling for DIC Analysis

Speckling is an essential part of the DIC process, as the high-contrast speckles are what the cross-correlation algorithm uses to track the deformation in the sample [40]. First, the samples were coated with matte black primer (Flat Black Primer, Rust-oleum, Illinois, USA). Matte paint with minimal light reflection is ideal as it provides a good base colour for high-contrast white speckles to be applied on the surface. An airbrush (H1017, Paasche, Wisconsin, USA) filled with water-based white paint (Opaque White, CreateX Colors, Connecticut, USA) was used to randomly apply small white dots on the sample, which were tracked in the DIC software. An example of the speckling pattern on an undamaged sample can be seen below in Figure 3-8 (a) along with a pixel intensity plot of the image, showing the high contrast speckling.

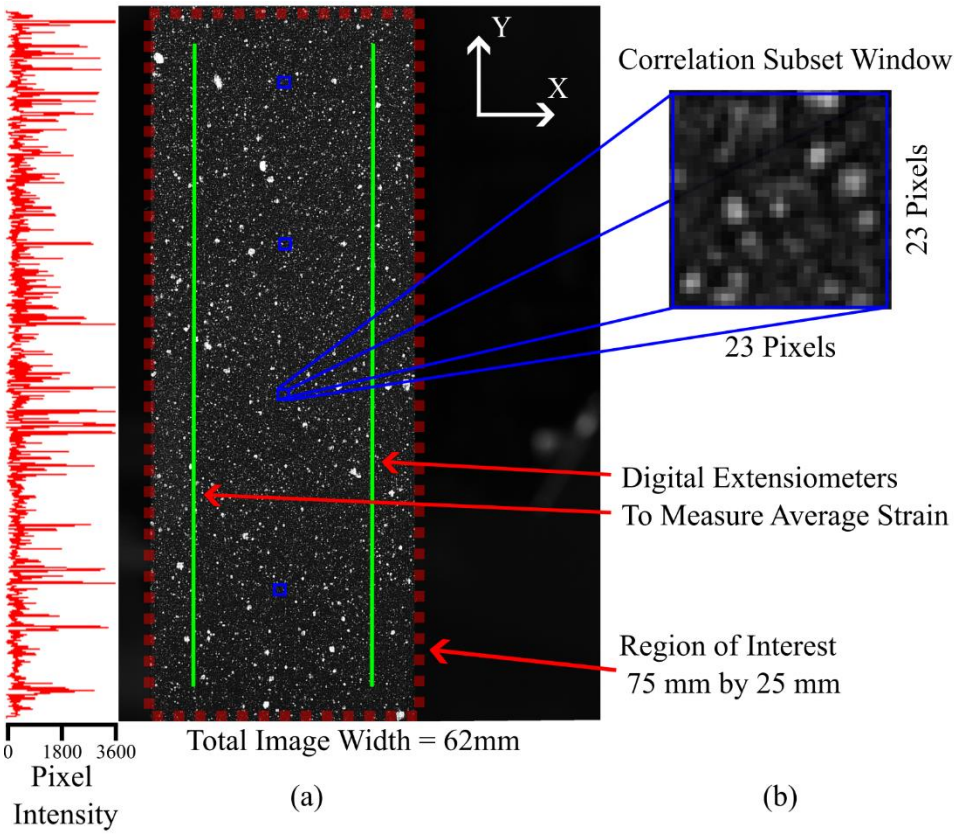

Figure 3-8: Speckle pattern of an undamaged sample used in DIC analysis highlighting the region of interest of 75 mm by 25 mm and the total image width of 75 mm by 62 mm. (a) Digital extensometers were added to measure the average strain over the total surface of the sample. (b) A magnified correlation subset window measuring 23 by 23 pixels which is used to compute displacement and strain by tracking speckle movement during deformation.

3.2.4.2 DIC Setup

In this research, two LaVision Imager cameras (M-Lite 5M, LaVision, Göttingen, Germany), equipped with a 50 mm focal length lens were used to capture high-resolution images of the samples. All strain fields were generated using LaVision's Davis 10.2 software. The lens's 50 mm focal length necessitated a working distance of 490 mm for the cameras, which resulted in a total field of view of 75mm by 62mm as seen in Figure 3-8 (a). This specific field of view was crucial as it allowed for capturing the entire 50mm repair patch while maintaining sufficient resolution to observe the smaller 12.5mm repair patch. To adapt to the rectangular nature of the field of view,

the cameras were mounted horizontally, maximizing the coverage of the sample within the frame. A frame rate of 15 frames per second was chosen for data collection, as this relatively rapid rate is particularly beneficial when analyzing samples that fracture in a brittle manner, allowing for more detailed observation of crack formation in the moments before fracture. During the processing phase, the correlation subset size was set to 23 pixels by 23 pixels with a step size of 8 pixels and an example of this subset size can be seen above in Figure 3-8 (b). This configuration was selected to enhance the resolution of the strain data, enabling more accurate and detailed results, which is essential for a comprehensive understanding of the material behaviour under stress.

Table 3-1: Digital image correlation parameters and settings used.

DIC Parameter	Settings
Cameras Used	LaVision Imager M-Lite 5M
Focal Length of Lens	50 mm
Working Distance of Cameras	490 mm
Region of Interest (ROI)	75 x 25 mm
Correlation Subset Window Size	23 x 23 pixels
Correlation Step Size	8 pixels
Frame Rate	15 Frames Per Second
Image Scale Factor	36 pixels/mm

3.3 Results and Discussion

3.3.1 Lap Shear Testing

Testing the lap shear strength of the conduction welding process in this study yielded an average shear strength of 8.58 ± 0.87 MPa and results can be seen below in Figure 3-9. To evaluate the effectiveness of this conduction welding process, it is beneficial to compare these results with other fusion bonding techniques that used the same liquid thermoplastic resin. For instance, Bhudolia et al. [41] achieved a maximum shear strength of 18.68 MPa using Elium® resin and carbon fiber

composites. Similarly, Murray et al. [42] reported even higher lap shear strengths, up to 22.5 MPa, with resistance and induction welding. These disparities in shear strength suggest that while liquid thermoplastic resin inherently possesses high shear strength capabilities, the specific conduction welding technique used here may not create an optimal bond, leading to reduced repair effectiveness. This could be attributed to potential issues in the conduction welding process, such as excessively high temperatures that may degrade the polymer, or overly high compaction pressures leading to resin squeeze-out and dry spots in the bonding area. Another critical factor could be the optimization of the cooldown process; proper control could enhance crystallization in the PMMA liquid thermoplastic, thereby improving mechanical properties [6].

Further work is warranted to refine the conduction welding process, considering its numerous practical applications in manufacturing thermoplastic composites. This process holds distinct advantages over other fusion bonding methods, such as resistance welding, where the embedded heating element can compromise structural integrity and pose challenges in simulating joint strength due to complex interactions with the melted polymer. Ultrasonic welding, while promising, is limited to smaller areas due to equipment constraints, restricting its applicability to larger composite structures welds [43]. Conduction welding, conversely, offers the flexibility of shaping the heated platen to accommodate various component sizes and shapes, resulting in a cohesive polymer structure without the limitations seen in other techniques [44].

One example of the application of conduction welding is the work done by Willem et al. [45] to weld stringers to an aircraft fuselage. This work was done as a technology demonstration to investigate the manufacturing of an aircraft fuselage without fasteners and aims to showcase conduction welding's potential in large-scale manufacturing. Expanding on this work, a theoretical application of the conduction welding process could be further innovated to produce continuous

welding which could be performed by using a heated roller. Welding parts together on an assembly line in an uninterrupted process has the potential to significantly enhance efficiency and consistency in production.

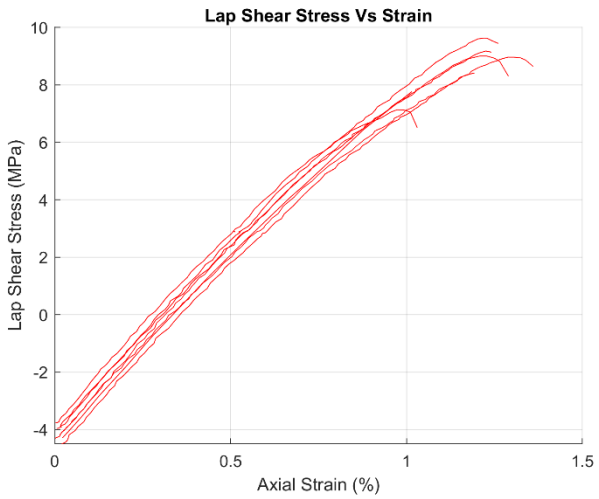

Figure 3-9: Lap shear strength of convection welded samples

3.3.2 Tensile Stiffness Results

As stated above in section 3.2.1.2, the cross-sectional area of each sample was calculated from multiple micrometer measurements and the average sample size was 25.03 ± 0.02 mm wide and 1.50 ± 0.02 mm thick. This resulted in an average cross-sectional area of 37.74 ± 0.44 mm^2. The average stress was then calculated for each sample, and a stress-strain curve was generated, which can be seen below in Figure 3-10.

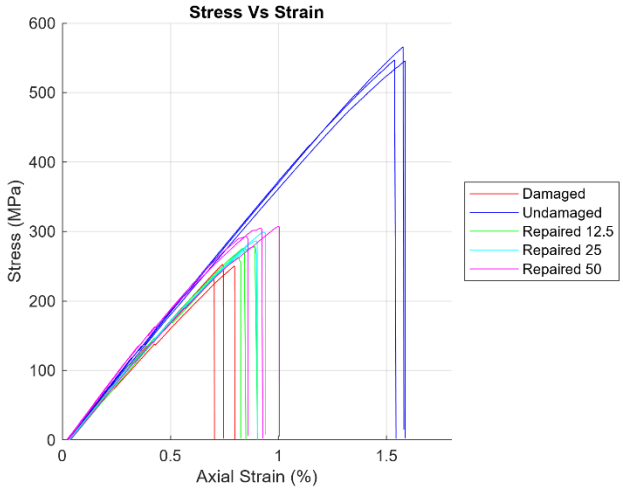

Figure 3-10: Stress-strain curve for each sample. In this plot, the damaged, undamaged, and repair patches of 12.5mm, 25mm, and 50 mm are compared.

The strain of each sample was obtained using a digital extensometer in the Davis 10.2 software. Two extensometers were placed on the sample at a gauge length of 70 mm and were located 5 mm from each edge of the sample as seen in Figure 3-8 (a). This method of strain analysis allows for an accurate average strain measurement over the region of interest and reduces sources of error from the universal testing frame such as crosshead compliance or grip movement [46]. The average stress in each sample is determined using Equation 3-1 [47]. Where σ is the average stress, F is the applied force in tension and A_c is the cross-sectional area of the sample.

$$\sigma = \frac{F}{A_c} \qquad \textit{Equation 3-1}$$

The goal of this study is to compare the efficacy of the repairs to the undamaged samples; therefore, the original undamaged cross-sectional area of each sample is used in this equation. This standardizes the comparison of ultimate tensile strength between samples and ensures that variations in the strength of the samples are attributed to the material properties of the repair

patches rather than the differences in the geometry of the samples. This also allows us to evaluate the percentage of recovered strength with respect to the undamaged samples. It is important to note that while this method provides a standard baseline for comparison it does not account for the true cross-sectional area of the samples. The average actual cross-sectional areas of each sample type are illustrated in Figure 3-11, where the damaged samples are smaller, and the repaired samples are significantly larger.

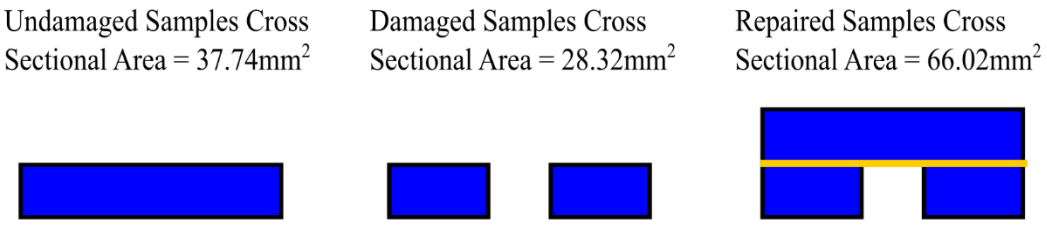

Figure 3-11: Representation of the true cross-sectional area of each sample type (Undamaged, Damaged, Repaired) along the centerline

From the stress-strain plot in Figure 3-10, Young's modulus (E) was obtained by calculating the slope of each sample's stress-strain curve, and the equation can be seen below in Equation 2 [47]. The average Young's modulus for all samples was fairly consistent and found to be 38.66 ± 1.74 GPa and a table of the average Young's modulus for each sample type can be seen below in

Table 3-2. The table shows that the calculated Young's modulus had no significant changes between sample types, meaning that the stiffness is unaffected by the induced damage or repair.

$$E = \frac{\sigma}{\varepsilon} \qquad \textit{Equation 3-2}$$

Table 3-2: Average Young's modulus and standard deviation for each sample type

Sample Type	Average Young's Modulus (GPa)
Undamaged	39.82 ± 0.70
Damaged	36.61 ± 1.10
Repaired 12.5	38.14 ± 0.50
Repaired 25	38.11 ± 0.33
Repaired 50	40.62 ± 1.75

The toughness of each sample was calculated using Equation 3, where the integral from 0 to the maximum strain (ε) for each stress curve (σ) from Figure 3-10 gives us the toughness of the sample [47]. The toughness changed significantly for each sample type, and the average for each can be seen below in Table 3-3. This result clearly shows an increase in the toughness of the samples as the repair patch size increases. This ultimately results in more energy required to fracture the sample.

$$Toughness = \int_0^{\varepsilon} \sigma \, d\varepsilon \qquad \textit{Equation 3-3}$$

Table 3-3: Average Toughness and standard deviation for each sample type

Sample Type	Average Toughness (J/m^3)
Undamaged	4.46 ± 0.08
Damaged	0.92 ± 0.07
Repaired 12.5	1.21 ± 0.09
Repaired 25	1.38 ± 0.05
Repaired 50	1.50 ± 0.11

3.3.3 Tensile Strength Results

Figure 3-12 presents a boxplot of the tensile test results, where the median ultimate tensile strength (UTS) is indicated by the central line in each box, and the 25th and 75th percentiles by the top and bottom of the box. The whiskers signify the standard deviation of values in each sample type and show low standard deviation. This is indicative of consistent sample quality. The tabulated results corresponding to the boxplot in Figure 3-12 is presented below in Table 3-4. As anticipated, the undamaged samples exhibited the highest performance in terms of ultimate tensile strength at a value of 553 ± 9.2 MPa. A clear significant difference in ultimate tensile strength is observed when comparing the undamaged samples to the damaged and repaired samples.

Conversely, the damaged samples displayed a noticeable decrease in their average ultimate tensile strength. This emphasizes the critical impact of removing one-quarter of the load-bearing fibers when drilling a hole in the composite. This substantial reduction in strength, totaling 55.7% on average, is due to the stress concentrations created around the hole.

Examining the results of the repair patch's ultimate stress, it is evident that the size of the patch plays a role in the extent of strength recovery. Larger repair patches provide more surface area to distribute shear forces into the repair patch during tensile loading. Based on these results in Figure 3-12, as the repair patch size increases, there is a positive correlation to the degree of strength recovered in the material. However, for all repair patch sizes, there remains a significant reduction in the overall strength of the sample when compared to the undamaged samples. The percent loss of strength in each sample type is calculated and presented in Table 3-4. This was calculated using Equation 3-4, where the difference in average ultimate stress of each sample type compared to the undamaged samples was divided by the average undamaged sample ultimate stress to give the percentage loss in strength.

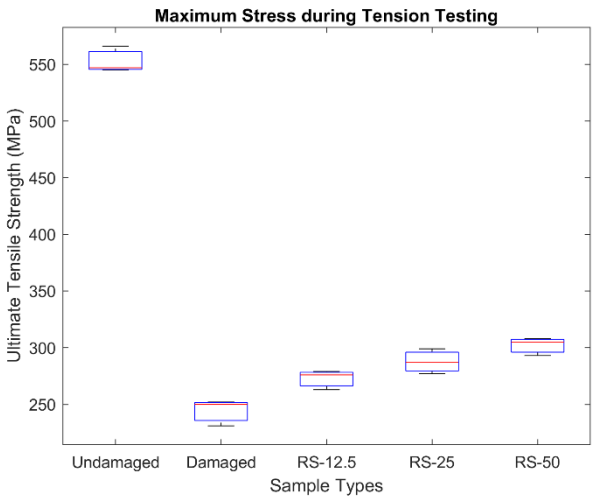

Figure 3-12: Boxplot of ultimate Stress values of each sample type tested

$$\frac{(Undamaged\ Sample\ Strength - Damaged\ Sample\ Type)}{Undamaged\ Sample\ Strength} * 100 = \%\ Loss\ in\ Strength \qquad Equation\ 3\text{-}4$$

Table 3-4: Average of each sample type tensile testing results showing the ultimate stress, the standard deviation in each sample type, and the % loss in strength compared to the original undamaged samples.

Sample Type	**Average Ultimate Stress (MPa)**	**% Loss of Strength**
Undamaged	553.01 ± 9.22	N/A
Damaged	245.04 ± 9.50	55.69
Repaired 12.5 mm (RS-12.5)	272.40 ± 6.82	50.74
Repaired 25 mm (RS-25)	287.77 ± 8.91	47.96
Repaired 50 mm (RS-50)	301.95 ± 6.25	45.40

3.3.4 Failure Modes of Tensile Samples

The primary damage type for all samples was transverse matrix cracking, leading to fibre fracture. In the damaged and repaired samples, tiny cracks begin to form in the matrix near the hole location because of the stress concentrations formed by the hole. These stress concentrations and resulting crack formations can be seen in the DIC images below in Figure 3-13 (a), (b), (c), and (d), which highlight the crack formations that occur moments before fracture. Studies performed on woven carbon fibre composites have indicated that the stress concentration factor formed by a hole can reach a value of 5.3 [48], [49]. Because of this high-stress concentration factor, mitigation is vital when dealing with repairs. The repair patches applied to the damaged samples assist in limiting the stress concentrations formed by the holes. However, they are limited in their ability to resist cracking due to the low shear strength of the plastic welded bond.

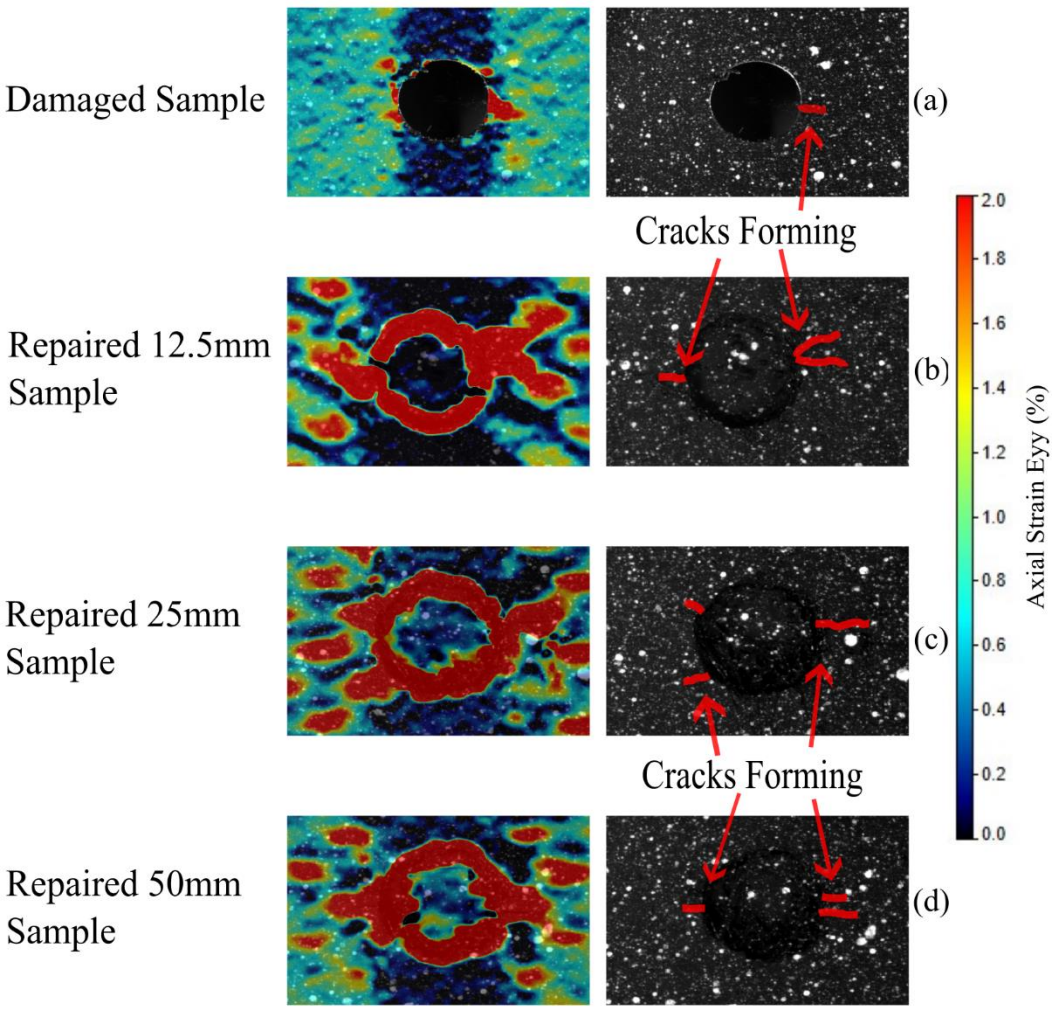

Figure 3-13: Microscopic view of crack formation damaged (a) and repaired samples (b), (c), (d). Cracks are highlighted in red. This image illustrates the initial stages of structural failure, which is a critical aspect in assessing the reparability of these materials.

The three main types of failure for adhesives and welded joints are characterized as adhesive/adherent interface failure, cohesive failure, and adherent failure [42], [50], [51], [52]. A diagram of these failure types can be seen below in Figure 3-14. Figure 3-14 (a) shows adhesive/adherent interface failure and is described as the failure of the layer between the adhesive and the adherent, in this case, the tested sample. This type of failure indicates that the adhesive did not bond well with the adherent and typically results in the lowest shear strength of the three types

of failures. Cohesive failure seen in Figure 3-14 (b) is characterized by a failure of the adhesive through its thickness. This type of failure leads to higher shear stresses and is primarily linked to the shear strength of the adhesive. It also indicates that the bond between the adhesive and the adherent is stronger than that of the adhesive itself. Adherent failure seen in Figure 3-14 (c) is seen when the adhesive bond does not break during testing but the sample fractures. This type of failure is seen with high-strength bonds, indicating that the adhesive bond and the adhesive itself are stronger than the tested sample.

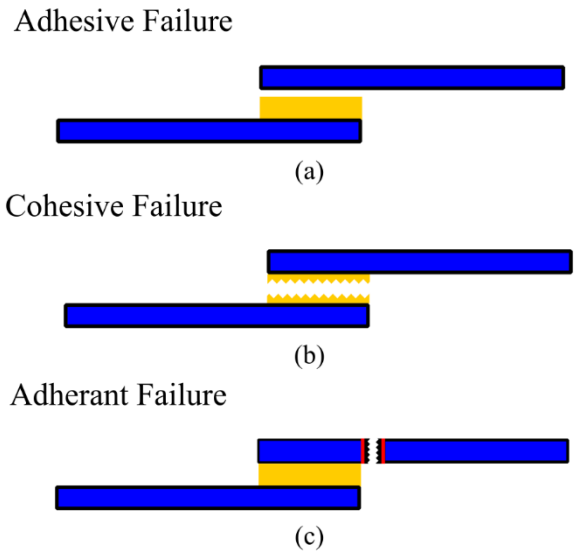

Figure 3-14: Schematic representation of failure modes for adhesive bonds where (a) depicts an adhesive failure where the bond between the adhesive and adherent fails. (b) Shows a cohesive failure in which the adhesive itself fails. (c) Shows an adherent failure where the substrate fails, and the adhesive bond remains intact.

In this study, the repair patches all failed cohesively, and the shear strength of the repair patch bond was a limiting factor in the strength of the repair. Below in Figure 3-15 (a), (b), and (c), the repair patches and samples can be seen after testing. The cohesive failure indicates that the conduction welding performed in this study resulted in the polymer chains in the Elium® resin transitioning into a glassy state and allowing for a good adhesive/adherent bond.

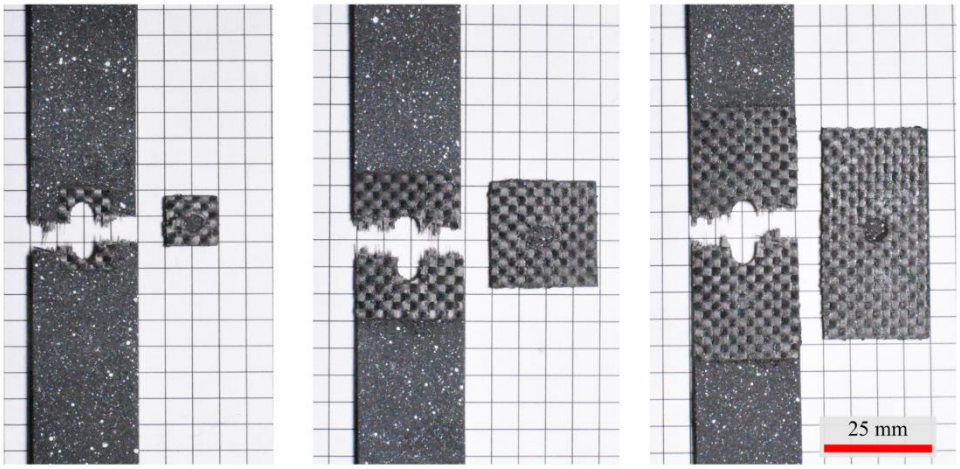

Figure 3-15: Repaired samples post tensile testing showing the cohesive failure of the patches in the (a) 12.5mm patch (b) 25mm patch (c) and 50mm patch (d)

3.3.5 DIC Results

DIC was used to generate full-field strain images of the samples as they underwent tensile testing. The full field strain images at that were generated for the undamaged, damaged, repaired 12.5 mm, repaired 25 mm and repaired 50 mm samples can be seen below in Figure 3-16, Figure 3-17, Figure 3-18, Figure 3-19, and Figure 3-20 respectively. Figure 3-16 - Figure 3-20 (a) and (b) show the strain fields development on the front and back of the samples respectively as the load increases from 2.5 kN to 9kN as well as the final image showing strain at the failure load for each sample. This gives a comparative analysis of the resulting strain for each sample at identical loads. Figure 3-16 - Figure 3-20 (c) plot the axial strain along the central Y axis of the sample in the frame before failure on both sides of the samples while Figure 3-16 - Figure 3-20 (d) illustrate the axial strain along the central x axis of both the front and back side of the samples.

For the undamaged sample, DIC strain map images can be seen in Figure 3-16 (a) and (b), and the strain along the sample is observed to be relatively consistent on the front and back side until

failure. The average strain at failure was around 1%, as seen in Figure 3-16 (c) and (d). Small stress concentrations can be seen forming at the weave interfaces as the sample approaches its ultimate tensile strength. This results from small matrix cracking damage points occurring as the composite reaches its ultimate stress. This damage accumulation determines the ultimate failure of the material, and failure occurs from stress concentrations located at one or more of these damage points.

The damaged sample in Figure 3-17 (a) and (b) shows a lack of strain along the y-axis above and below the hole. This results from the fibres above and below the hole being unable to support the load imparted during testing as they are discontinuous. This can also be seen in Figure 3-17 (c), where axial strain is plotted along the Y-axis and has a noticeable concave shape as it approaches the hole's location. Significant peaks in strain are seen in Figure 3-17 (d), as the plot of strain along the horizontal axis shows the stress concentrations near the hole.

On the front side of the repaired samples in Figure 3-18 - Figure 3-20 (a), the most significant strain experienced was at the patch edges. This is expected as sharp edges lead to considerable stress concentrations. This is further highlighted by the large peaks found in Figure 3-18 - Figure 3-20 (c). However, the average strain over the patch was significantly lower than the average strain on the rest of the sample. This is due to the lack of force transmitted to the repair patch through the bonding interface because of the low shear stress capabilities of the conduction welding technique. On the back side of the samples seen in Figure 3-18 - Figure 3-20 (b), the same lack of strain caused by the discontinuation of fibres occurs, however, it is less pronounced than the damaged sample. This is caused by the repair patch relieving some of the tensile force from the sample. Figure 3-18 - Figure 3-20 (d) highlights the axial strain along the horizontal axis, the peaks

of which are all significantly lower than the peaks on the damaged samples. This indicates a reduction in the stress concentration factor at the holes of the repaired samples.

In all samples, the stress concentrations developed because of the hole, which ultimately led to cracks forming in the composite, resulting in the samples' failure. These findings are consistent with similar research utilizing DIC on open hole composite specimens [48], [53], [54]. This is also evidenced by similar trends in the mechanical behavior of the samples, exhibiting large stress concentrations around the damaged location. This corroborates the established understanding of stress distribution and strength recovery in such materials. The comparative analysis indicates that the results from this study reinforce the conclusions drawn in prior research, demonstrating the reliability of the observed phenomena across different investigations. Furthermore, the agreement with existing studies validates the methodologies employed and the robustness of the conclusions derived from this research.

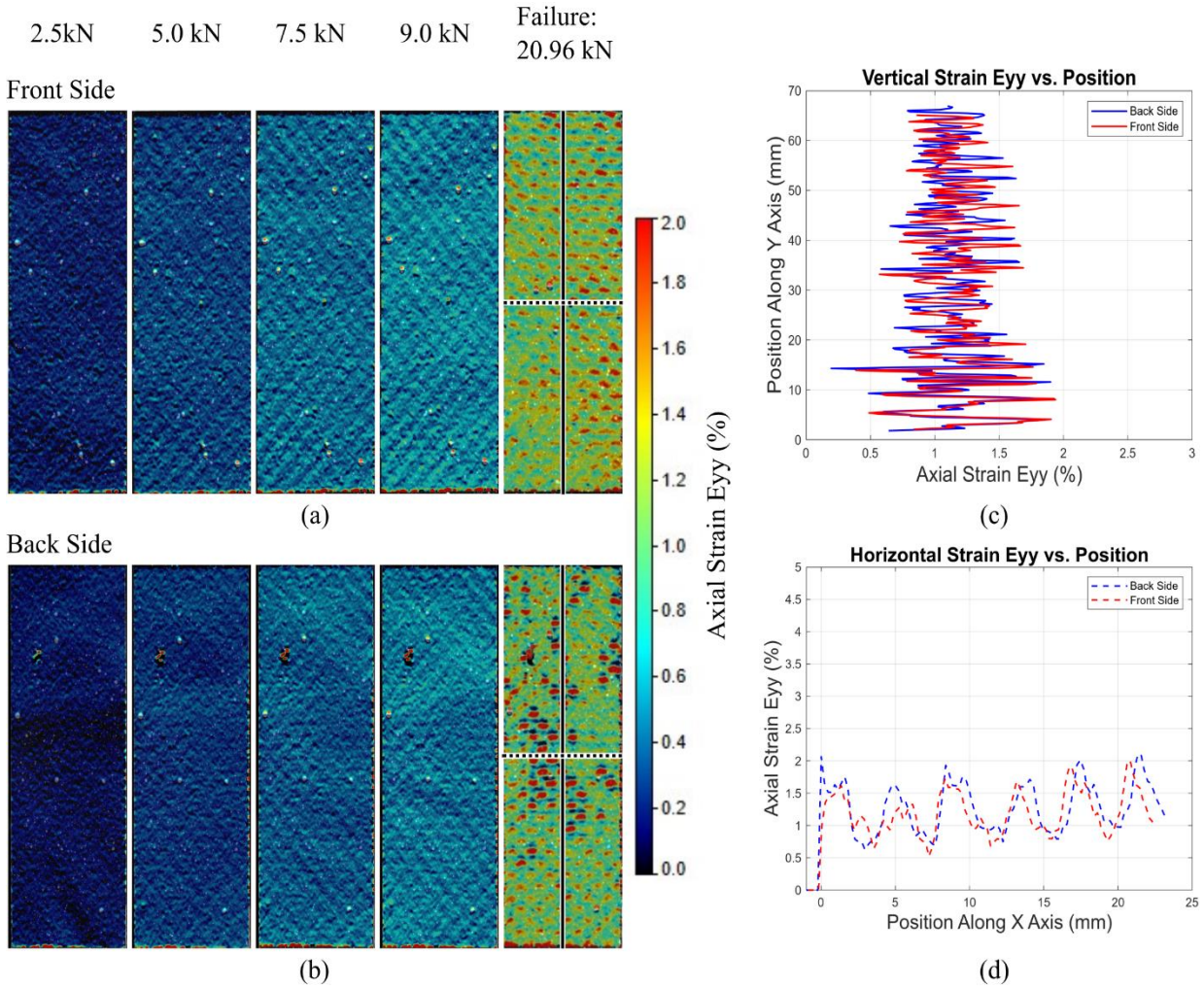

Figure 3-16: DIC axial strain fields of the undamaged sample under loading ranging from 5.0 kN to failure at 20.96 kN, Front side of sample (a) and back side (b). Strain along the center line of the y axis (c) and x axis (d) is plotted, showing strain at failure.

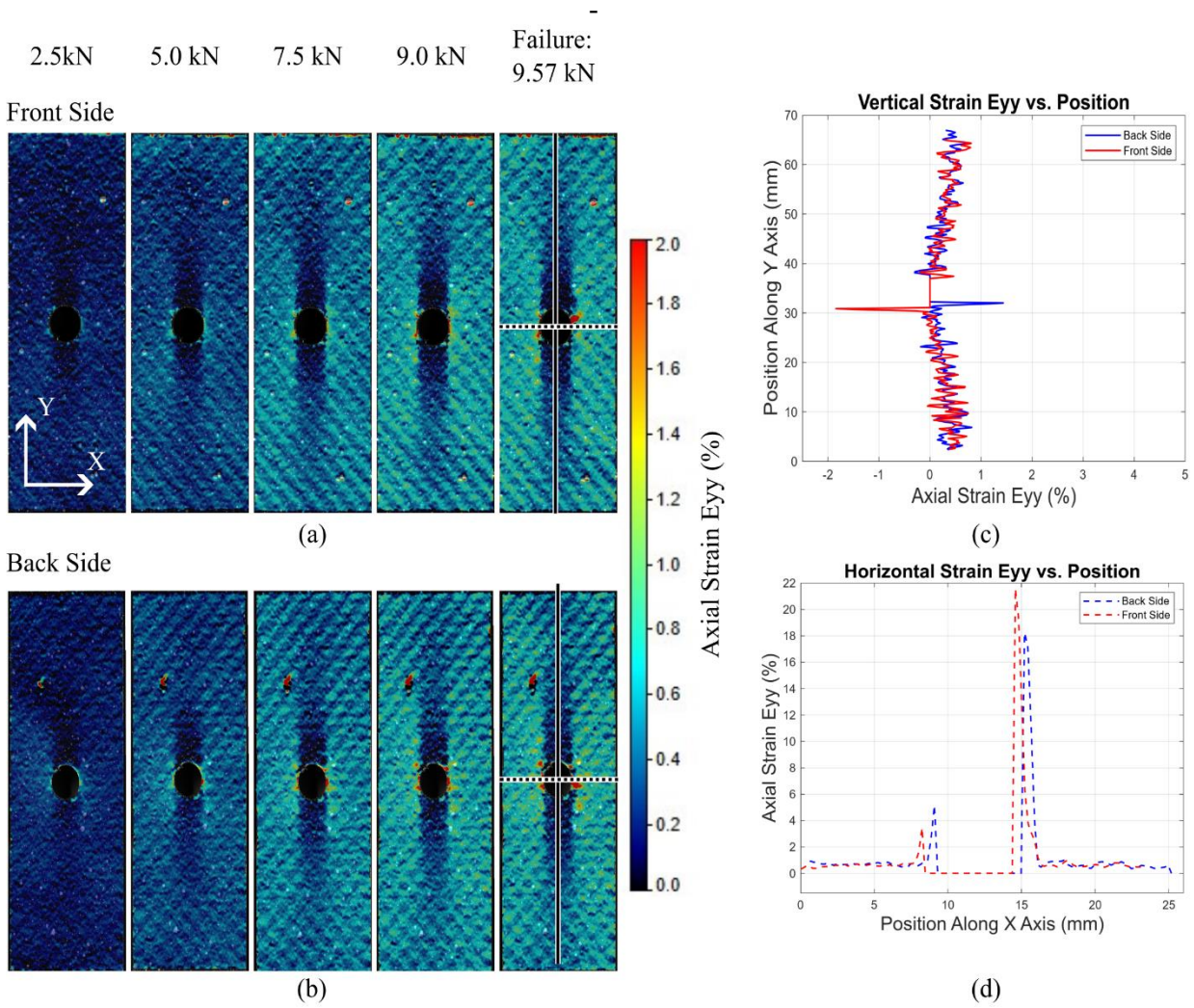

Figure 3-17: DIC axial strain fields of a damaged sample under loading ranging from 2.5 kN to failure at 9.57 kN, Front side of sample (a) and back side (b). Strain along the center line of the y axis (c) and x axis (d) is plotted, showing strain at failure.

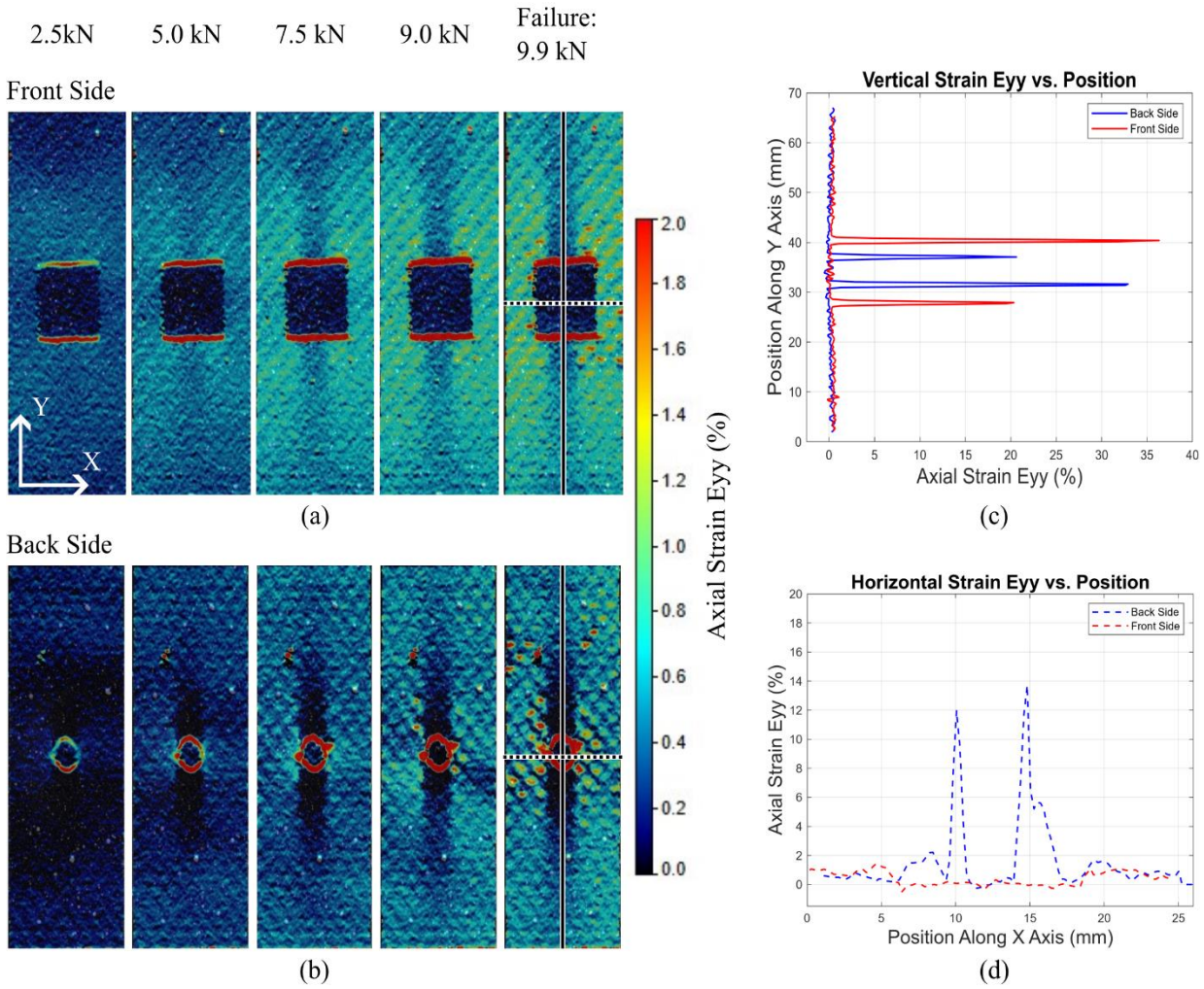

Figure 3-18: DIC axial strain fields of 12.5mm repaired sample under loading ranging from 2.5 kN to failure at 9.9 kN, Front side of sample (a) and back side (b). Strain along the center line of the y axis (c) and x axis (d) is plotted, showing strain at failure.

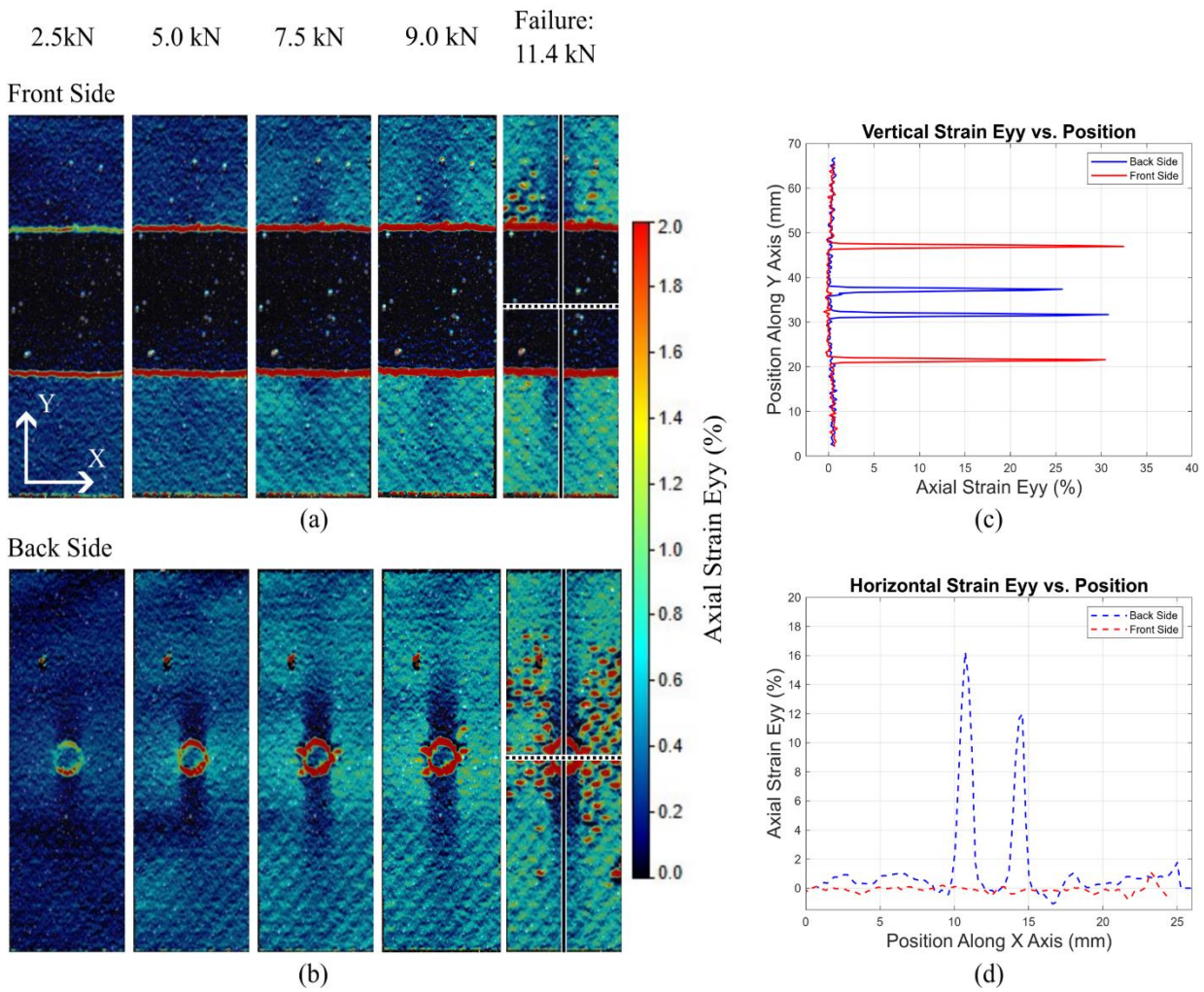

Figure 3-19: DIC axial strain fields of 25mm repaired sample under loading ranging from 2.5 kN to failure at 11.4 kN, Front side of sample (a) and back side (b). Strain along the center line of the y axis (c) and x axis (d) is plotted, showing strain at failure.

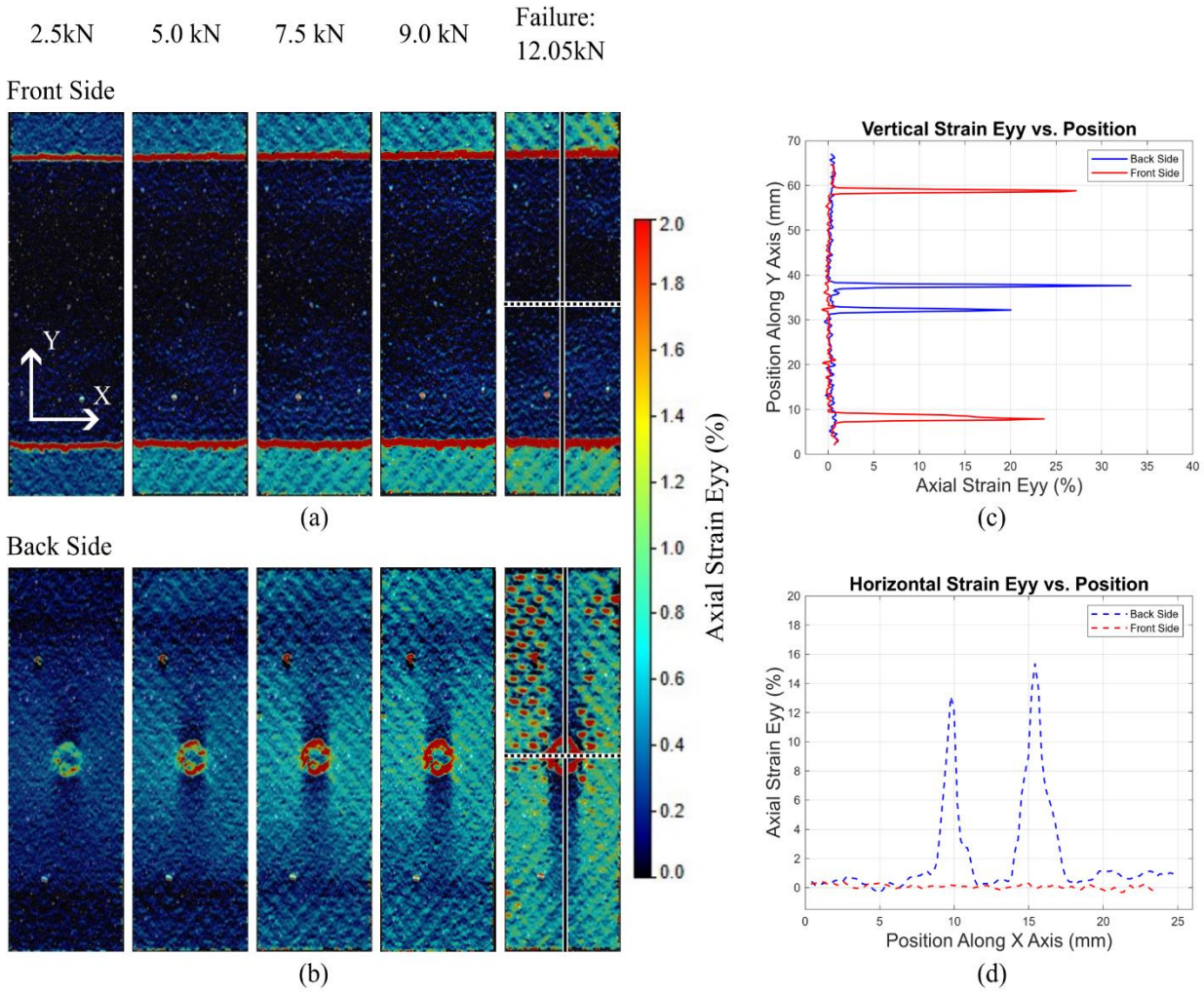

Figure 3-20: DIC axial strain fields of the 50 mm repaired sample under loading ranging from 2.5 kN to failure at 12.05 kN, Front side of sample (a) and back side (b). Strain along the center line of the y axis (c) and x axis (d) is plotted, showing strain at failure.

3.3.6 Statistical Analysis

Analysis of Variance (ANOVA) was employed to assess the significance of repair patch size on the mechanical strength of the samples [55]. It was found that there was a significant difference in tensile strength between the groups at the $p < 0.05$ level with a resulting F value of 18.61 and $p = 0.0006$ Subsequently, the Tukey-Kramer multiple comparison test was conducted, and the results are detailed below in Table 3-5. This test shows that the mean ultimate tensile strength significantly differed between the damaged samples and all other sample types, with a maximum p-value of 0.0365. This result indicates that all repair patch sizes statistically improved the ultimate tensile strength of the samples resulting in an effective repair.

However, when comparing repair patch sizes against each other we see only a statistically significant increase in strength when comparing the 12.5mm repair patch to the 50mm repair patch with a P value of 0.025. There was no statistically significant difference between the 12.5mm patch size and the 25mm patch size, with a P value of 0.29. There was also no significant statistical difference between the 25mm and 50mm patch sizes, with a P value of 0.35.

In summary, we can conclude that the repair patches effectively improved the strength of the sample after it was damaged. However, the small step sizes chosen, in combination with the weak shear strength of the conduction welding process, resulted in the repair patches inability to statistically differentiate themselves from one another. Future work to improve this bonding process as well as optimize the repair patch shape could ultimately lead to drastic improvements in the effectiveness of conduction welded repair patches. The approach demonstrated in this work can also be expanded to other repair methods such as scarfed or stepped repairs.

Table 3-5: Tukey-Kramer multiple comparison test of damaged and repaired samples ultimate tensile strength.

Sample Type A	Sample Type B	Lower Limit	A – B	Upper Limit	P-value
Damaged	Repaired 12.5	-52.938	-27.366	-1.794	0.0365
Damaged	Repaired 25	-68.305	-42.733	-17.161	0.003
Damaged	Repaired 50	-82.472	-56.900	-31.327	0.0005
Repaired 12.5	Repaired 25	-40.938	-15.366	10.205	0.2909
Repaired 12.5	Repaired 50	-55.105	-29.533	-3.961	0.0251
Repaired 25	Repaired 50	-39.738	-14.166	11.405	0.3506

3.4 Conclusion

This study has provided valuable insights into the repairability of Elium® 188 O based thermoplastic composites, a crucial aspect for enhancing the sustainability of composite materials in industrial use. By testing the low-cost repair method of conduction welding, enabled by the use of novel thermoplastic liquid Polymethyl methacrylate (PMMA) resin, this research contributes to the evolving field of composite material repair techniques. Tensile strength testing was performed on a universal testing machine using five types of samples: Undamaged, Damaged, Repaired 12.5mm patch, repaired 25mm patch, and repaired 50mm patch. Notably, the largest repair patches achieved a 55.4% strength recovery, indicating a significant potential for restoring the mechanical properties of damaged composites. Furthermore, lap shear testing results showed an average ultimate shear stress of 8.6 MPa, suggesting room for improvement in the conduction welding process, especially in reducing porosity for stronger repairs. The incorporation of DIC in this study offers in-depth insights into the repair patches' response to loading and provides visual identification of stress concentration points in the tensile samples. The successful repair of Elium®-based composites not only prolongs the lifespan of these materials but also represents a significant step towards reducing waste and negative environmental impacts. This aligns with the broader goal of establishing more sustainable material cycles in industries like aerospace and automotive. Future research should focus on optimizing the conduction welding process and exploring the repairability of other thermoplastic composites, thereby expanding the scope of sustainable practices in material usage. In conclusion, this research underscores the potential of Elium®-based thermoplastic composites as a sustainable choice in the composite material industry. It advocates for a shift towards more repairable and durable material solutions, contributing to the field of material science and aligning with global environmental objectives.

3.5 References

[1] Fortune Business Insights, “Composite Market Size.”

[2] Mordor Intelligence, “Fiber reinforced composites market size & share analysis - growth trends & forecasts (2023 - 2028).”

[3] Y. Yang, R. Boom, B. Irion, D. J. van Heerden, P. Kuiper, and H. de Wit, “Recycling of composite materials,” *Chemical Engineering and Processing: Process Intensification*, vol. 51, pp. 53–68, Jan. 2012, doi: 10.1016/j.cep.2011.09.007.

[4] A. D. La Rosa, D. R. Banatao, S. J. Pastine, A. Latteri, and G. Cicala, “Recycling treatment of carbon fibre/epoxy composites: Materials recovery and characterization and environmental impacts through life cycle assessment,” *Compos B Eng*, vol. 104, pp. 17–25, Nov. 2016, doi: 10.1016/j.compositesb.2016.08.015.

[5] Composites World, “Materials & Processes: Resin matrices for composite.” Accessed: Oct. 01, 2023. [Online]. Available: https://www.compositesworld.com/articles/the-matrix

[6] Painter Paul C. and Coleman Michael M., *Essentials of Polymer Science and Engineering*. 2009.

[7] Chris Martin, “Wind Turbine Blades Can’t Be Recycled, So They’re Piling Up in Landfills,” Bloomberg.

[8] P. Liu and C. Y. Barlow, “Wind turbine blade waste in 2050,” *Waste Management*, vol. 62, pp. 229–240, Apr. 2017, doi: 10.1016/j.wasman.2017.02.007.

[9] M. Valente, I. Rossitti, and M. Sambucci, “Different Production Processes for Thermoplastic Composite Materials: Sustainability versus Mechanical Properties and Processes Parameter,” *Polymers*, vol. 15, no. 1. MDPI, Jan. 01, 2023. doi: 10.3390/polym15010242.

[10] Arkema, “Thermoplastic resin Elium® for recyclable composites.” Accessed: Sep. 05, 2023. [Online]. Available: Thermoplastic resin Elium® for recyclable composites

[11] M. G. Bader, “Selection of composite materials and manufacturing routes for cost-effective performance,” 2002. [Online]. Available: www.elsevier.com/locate/compositesa

[12] D. S. Cousins, Y. Suzuki, R. E. Murray, J. R. Samaniuk, and A. P. Stebner, “Recycling glass fiber thermoplastic composites from wind turbine blades,” *J Clean Prod*, vol. 209, pp. 1252–1263, Feb. 2019, doi: 10.1016/j.jclepro.2018.10.286.

[13] J. Barroeta Robles, M. Dubé, P. Hubert, and A. Yousefpour, “Repair of thermoplastic composites: an overview,” *Advanced Manufacturing: Polymer and Composites Science*, vol. 8, no. 2. Taylor and Francis Ltd., pp. 68–96, 2022. doi: 10.1080/20550340.2022.2057137.

[14] P. Cheng, X. J. Gong, D. Hearn, and S. Aivazzadeh, “Tensile behaviour of patch-repaired CFRP laminates,” *Compos Struct*, vol. 93, no. 2, pp. 582–589, Jan. 2011, doi: 10.1016/j.compstruct.2010.08.021.

[15] X. Liu and G. Wang, “Progressive failure analysis of bonded composite repairs,” *Compos Struct*, vol. 81, no. 3, pp. 331–340, Dec. 2007, doi: 10.1016/j.compstruct.2006.08.024.

[16] T. D. Breitzman, E. V. Iarve, B. M. Cook, G. A. Schoeppner, and R. P. Lipton, “Optimization of a composite scarf repair patch under tensile loading,” *Compos Part A Appl Sci Manuf*, vol. 40, no. 12, pp. 1921–1930, Dec. 2009, doi: 10.1016/j.compositesa.2009.04.033.

[17] S. Mohammadi, M. Yousefi, and M. Khazaei, “A review on composite patch repairs and the most important parameters affecting its efficiency and durability,” *Journal of Reinforced Plastics and Composites*, vol. 40, no. 1–2, pp. 3–15, Jan. 2021, doi: 10.1177/0731684420941602.

[18] A. Yousefpour, M. Hojjati, and J. P. Immarigeon, “Fusion bonding/welding of thermoplastic composites,” *Journal of Thermoplastic Composite Materials*, vol. 17, no. 4, pp. 303–341, Jul. 2004, doi: 10.1177/0892705704045187.

[19] H. Li, C. Chen, R. Yi, Y. Li, and J. Wu, “Ultrasonic welding of fiber-reinforced thermoplastic composites: a review,” *International Journal of Advanced Manufacturing Technology*, vol. 120, no. 1–2. Springer Science and Business Media Deutschland GmbH, pp. 29–57, May 01, 2022. doi: 10.1007/s00170-022-08753-9.

[20] W. P. Seneviratne, J. S. Tomblin, and B. L. Saathoff, “influence of various surface preparation techniques on resistance welded and adhesively bonded unidirectional thermoplastic composite joints,” 2021.

[21] M. J. Troughton, Ed., “Chapter 1 - Heated Tool Welding,” in *Handbook of Plastics Joining (Second Edition)*, Second Edition., Boston: William Andrew Publishing, 2009, pp. 3–13. doi: https://doi.org/10.1016/B978-0-8155-1581-4.50003-2.

[22] D. B. Kline and R. P. Wool, “Polymer welding relations investigated by a lap shear joint method,” *Polym Eng Sci*, vol. 28, no. 1, pp. 52–57, Jan. 1988, doi: 10.1002/pen.760280109.

[23] S. E. Erdogan and U. Huner, “The effect of the welding parameters and the coupling agent on the welding of composites,” *Material in Technologies*, vol. 50, no. 5, pp. 655–662, 2016, doi: 10.17222/mit.2015.059.

[24] V. K. Stokes and K. R. Conway, “A phenomenological study of the hot-tool welding of thermoplastics. 4. Weld strength data for several blends.” [Online]. Available: www.elsevier.nl/locate/polymer

[25] M. A. Caminero, M. Lopez-Pedrosa, C. Pinna, and C. Soutis, “Damage monitoring and analysis of composite laminates with an open hole and adhesively bonded repairs using

digital image correlation," *Compos B Eng*, vol. 53, pp. 76–91, Oct. 2013, doi: 10.1016/j.compositesb.2013.04.050.

[26] M. A. Caminero, S. Pavlopoulou, M. Lopez-Pedrosa, B. G. Nicolaisson, C. Pinna, and C. Soutis, "Analysis of adhesively bonded repairs in composites: Damage detection and prognosis," *Compos Struct*, vol. 95, pp. 500–517, Jan. 2013, doi: 10.1016/j.compstruct.2012.07.028.

[27] M. A. Caminero, S. Pavlopoulou, M. López-Pedrosa, B. G. Nicolaisson, C. Pinna, and C. Soutis, "Using Digital Image Correlation Techniques for Damage Detection on Adhesively Bonded Composite Repairs," *Advanced Composites Letters*, vol. 21, no. 2, p. 096369351202100, Mar. 2012, doi: 10.1177/096369351202100203.

[28] F. Pierron, B. Green, and M. R. Wisnom, "Full-field assessment of the damage process of laminated composite open-hole tensile specimens. Part I: Methodology," *Compos Part A Appl Sci Manuf*, vol. 38, no. 11, pp. 2307–2320, Nov. 2007, doi: 10.1016/j.compositesa.2007.01.010.

[29] M. Grédiac, "The use of full-field measurement methods in composite material characterization: interest and limitations," *Compos Part A Appl Sci Manuf*, vol. 35, no. 7–8, pp. 751–761, Jul. 2004, doi: 10.1016/j.compositesa.2004.01.019.

[30] F. Lagattu, M. C. Lafarie-Frenot, T. Q. Lam, and J. Brillaud, "Experimental characterisation of overstress accommodation in notched CFRP composite laminates," *Compos Struct*, vol. 67, no. 3, pp. 347–357, Mar. 2005, doi: 10.1016/j.compstruct.2004.01.016.

[31] F. Pierron, B. Green, and M. R. Wisnom, "Full-field assessment of the damage process of laminated composite open-hole tensile specimens. Part I: Methodology," *Compos Part A Appl Sci Manuf*, vol. 38, no. 11, pp. 2307–2320, Nov. 2007, doi: 10.1016/j.compositesa.2007.01.010.

[32] M. A. Caminero, M. Lopez-Pedrosa, C. Pinna, and C. Soutis, "Damage assessment of composite structures using digital image correlation," *Applied Composite Materials*, vol. 21, no. 1, pp. 91–106, 2014, doi: 10.1007/s10443-013-9352-5.

[33] H. Wemming, S. B. Lindström, L. Johansson, and Z. Kapidžić, "Identification of bearing failure in composite-aluminium bolted joints using digital image correlation," *Compos Struct*, vol. 300, Nov. 2022, doi: 10.1016/j.compstruct.2022.116072.

[34] J. Holmes, S. Sommacal, R. Das, Z. Stachurski, and P. Compston, "Digital image and volume correlation for deformation and damage characterisation of fibre-reinforced composites: A review," *Composite Structures*, vol. 315. Elsevier Ltd, Jul. 01, 2023. doi: 10.1016/j.compstruct.2023.116994.

[35] "Standard Test Method for Tensile Properties of Polymer Matrix Composite Materials 1", doi: 10.1520/D3039_D3039M-14.

[36] “Tabbing Guide for Composite Test Specimens,” 2002.

[37] Sarah, “5 Things Differential Scanning Calorimetry (DSC) Testing Can Help You Understand About Your Polymers and Composites,” C-Therm Technologies. Accessed: Oct. 06, 2023. [Online]. Available: https://ctherm.com/resources/newsroom/thermal-analysis-labs/5-things-dsc-polymers-composites/

[38] ASTM International, “Standard Test Method for Lap Shear Adhesion for Fiber Reinforced Plastic (FRP) Bonding,” 2023, doi: 10.1520/D5868-01R23.

[39] H. Schreier, J. J. Orteu, and M. A. Sutton, *Image correlation for shape, motion and deformation measurements: Basic concepts, theory and applications*. Springer US, 2009. doi: 10.1007/978-0-387-78747-3.

[40] Y. L. Dong and B. Pan, “A Review of Speckle Pattern Fabrication and Assessment for Digital Image Correlation,” *Exp Mech*, vol. 57, no. 8, pp. 1161–1181, Oct. 2017, doi: 10.1007/s11340-017-0283-1.

[41] S. K. Bhudolia, G. Gohel, J. Kantipudi, K. F. Leong, and R. J. Barsotti, “Ultrasonic welding of novel carbon/ Elium® thermoplastic composites with flat and integrated energy directors: Lap shear characterisation and fractographic investigation,” *Materials*, vol. 13, no. 7, Apr. 2020, doi: 10.3390/ma13071634.

[42] R. E. Murray, J. Roadman, and R. Beach, “Fusion joining of thermoplastic composite wind turbine blades: Lap-shear bond characterization,” *Renew Energy*, vol. 140, pp. 501–512, Sep. 2019, doi: 10.1016/j.renene.2019.03.085.

[43] “Ultrasonic Welding,” in *Handbook of Plastics Joining*, Elsevier, 2009, pp. 15–35. doi: 10.1016/B978-0-8155-1581-4.50004-4.

[44] G. Gardiner, “Welding Thermoplastic Composites,” Sep. 2018. [Online]. Available: https://www.compositesworld.com/articles/welding-thermoplastic-composites

[45] J. Willem Van Ingen, “Thermoplastic Orthogrid Fuselage Shell,” 2016. [Online]. Available: https://www.researchgate.net/publication/307926694

[46] M. Alci and R. Gunes, “A comparison study on experimental characterization of unidirectional fiber reinforced composites using strain-gauges and virtual extensometers,” *Materials Testing*, vol. 65, no. 2, pp. 174–191, Feb. 2023, doi: 10.1515/mt-2022-0274.

[47] Russell C. Hibbeler, *Statics and Mechanics of Materials*, 3rd ed. 2010.

[48] R. M. A. Khan, T. Shafighfard, H. Q. Ali, M. Mieloszyk, and M. Yildiz, “Strength prediction and experimental damage investigations of plain woven CFRPs with interacting holes using multi-instrument measurements,” *Polymer Composites*, vol. 44, no. 6, pp. 3594–3609, Jun. 2023, doi: 10.1002/pc.27347.

[49] Tan Seng C., *Stress Concentrations in Laminated Composites*, 1st ed. Boca Raton: CRC Press, Taylor & Francis Group, 1994.

[50] L. Boriwal, R. M. Sarviya, and & M. M. Mahapatra, “Failure modes of spot welds in quasi-static tensile-shear loading of coated steel sheets,” 2017. [Online]. Available: www.sciencedirect.comwww.materialstoday.com/proceedings

[51] W. Suwanwatana, S. Yarlagadda, and J. W. Gillespie, “Hysteresis heating based induction bonding of thermoplastic composites,” *Compos Sci Technol*, vol. 66, no. 11–12, pp. 1713–1723, Sep. 2006, doi: 10.1016/j.compscitech.2005.11.009.

[52] M. Dubé, A. Chazerain, P. Hubert, A. Yousefpour, and H. E. Bersee, “Characterization of resistance-welded thermoplastic composite double-lap joints under static and fatigue loading,” *Journal of Thermoplastic Composite Materials*, vol. 28, no. 6, pp. 762–776, Jun. 2015, doi: 10.1177/0892705713490714.

[53] Q. Guo, Y. Zhang, D. Li, M. Li, X. Sun, and L. Chen, “Tensile properties and failure mechanism of 3D woven composites containing holes of different geometries,” *Thin-Walled Structures*, vol. 166, Sep. 2021, doi: 10.1016/j.tws.2021.108115.

[54] S. Gupta, S. Pal, and B. C. Ray, “An overview of mechanical properties and failure mechanism of FRP laminates with hole/cutout,” *Journal of Applied Polymer Science*, vol. 140, no. 20. John Wiley and Sons Inc, May 20, 2023. doi: 10.1002/app.53862.

[55] R. Figliola and D. Beasley, *Theory and Design for Mechanical Measurements*, 7th ed. Wiley, 2019.

Chapter 4: Lap Shear Strength Optimization of Conduction Welded Thermoplastic Composites

4.1 Introduction

In the field of composite materials, thermoplastic composites (TPC) are gaining prominence due to their many advantages such as, recyclability, increased impact resistance and toughness, lower storage costs, and their ability to be welded [1] - [7]. However, one of the primary limitations that is preventing further adoption is the difficulties when it comes to the manufacturing of TPCs as they require high temperatures and pressures to process the thermoplastic matrix into a moldable melt material. This limitation has recently been addressed by Arkema with their introduction of a new liquid thermoplastic matrix, Elium® [8]. With the development of liquid thermoplastics, the manufacturability of TPC has expanded to techniques previously reserved exclusively for thermosetting epoxies, such as wet layups and resin infusions [9]. This simplifies the manufacturing process and enables further adoption of more environmentally sustainable materials while offering improved design flexibility due to the remeltability of thermoplastics.

Stemming from the remeltable nature of thermoplastics, the field of fusion bonding poses an innovative approach to joining TPCs without the need for structural adhesives or mechanical fasteners [10] - [12]. This process forms a cohesive polymer bond between thermoplastic laminates by generating heat at the interface which melts the thermoplastic matrix and effectively welds the materials together. This process has been studied extensively in the literature using a variety of techniques such as ultrasonic welding, resistance welding, and induction welding [13] - [18]. Fusion bonding's key advantages are its minimal surface preparation requirements and its rapid processing times [19].

In this study, a novel low-cost method of fusion bonding called conduction welding is investigated. This technique employs a heated press to conduct heat through the TPC laminate to melt and bond the matrix material at the interfaces of two surfaces. This research's objective is to identify the optimal processing parameters of temperature and compaction pressure to maximize the lap shear strength of joints created through the conduction welding of Elium®/Carbon thermoplastic composites. By modifying these parameters, a cost-effective solution for producing high-strength composite bonds is discussed.

4.2 Methodology

The experimental design focused on identifying the main processing parameters that influence conduction welding efficacy, temperature, and compaction pressure. Given that the liquid thermoplastic resin used in the study possesses a glass transition temperature of 76°C, the welding process employed temperatures exceeding this threshold to ensure adequate flow and bonding of the material [20].

4.2.1 Sample Manufacturing

Lap shear samples in this study were manufactured from a panel of 3k 5.7 oz plain weave carbon fibers with an orientation of $[0,90]_6$ and liquid thermoplastic resin (Elium® 188 O, Arkema, Colombes, France) via the resin infusion process that was detailed in chapter 3.2.1.1. Individual samples were then cut from the panel using a waterjet (Flow Mach 2 4020B, Flow International, Washington, USA). The dimensions of the individual samples were based on the ASTM D5868 standard [21], however, to accommodate the limited load capabilities of the universal testing frame used in this study, samples were scaled down to a length, width, and thickness of 60mm by 15mm by 1.5mm, maintaining the same aspect ratio as defined in the standard. The resulting overlap area of the samples was $225mm^2$. End tabs of 1.5mm thick G-10 Fibreglass (Garolite G-10, Accurate

Plastics, New York, USA) were bonded to the samples with epoxy (FIBREGLAST 2000, Fibre Glast Developments, Ohio, USA) and hardener (FIBREGLAST, Fibre Glast Developments, Ohio, USA 2020) at a ratio of 100:23 by weight. A diagram of the lap shear samples used in this study can be seen in Figure 4-1 showing the primary dimensions of the samples.

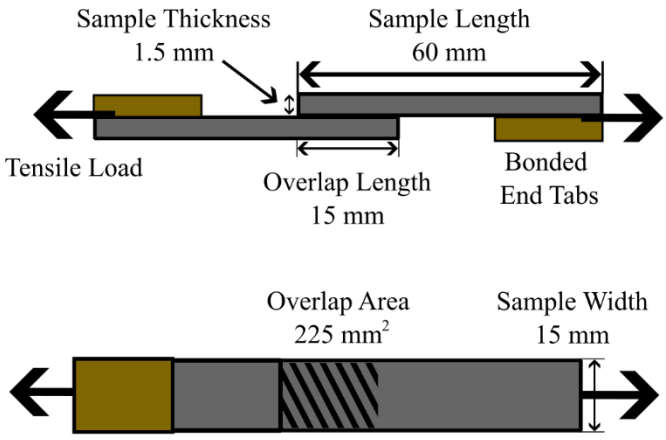

Figure 4-1: Schematic of a single-lap shear test specimen used in this study to evaluate the shear strength of conduction welded joints.

4.2.2 Testing Matrix

The following testing matrix seen in Table 4-1 considers varying temperatures and compaction pressures used in the conduction welding of lap shear joints for this study. Temperatures of 120°C, 150°C, and 180°C, coupled with compaction pressures of 10, 25, and 50 Bar were evaluated. All samples in this study were welded for 60 seconds based on the thermal analysis discussed in section 4.2.4. Preliminary testing included welding temperatures of 210°C but are not included as the increased temperature led to degradation of the Elium® resin, which adversely affected joint performance.

Table 4-1: Testing matrix for lap shear welding conditions

Compaction Pressure (Bar)	Temperature (° Celsius)	Welding Time (Seconds)	Number of Samples Tested
10	120	60	3
25	120	60	3
50	120	60	3
10	150	60	3
25	150	60	3
50	150	60	3
10	180	60	3
25	180	60	3
50	180	60	3

4.2.3 Conduction welding

Prior to the conduction welding process each sample was cleaned with isopropyl alcohol to remove surface residue. Images of the conduction welding process can be seen below in Figure 4-2 where (a) is a diagram of the conduction welding process. Lap shear samples were welded together by a low-cost heated press setup (Heat Press CK220, YaeTek, China) which applied heat to the samples. The heated plates were mounted to a universal testing machine (Electroplus E3000, Instron, Massachusetts, USA) which applied constant compaction pressure during welding seen in (b). A custom aluminum fixture (c) was manufactured to hold the samples in place during welding and (d) shows an image of the final lap shear sample with an overlap area of 225mm^2.

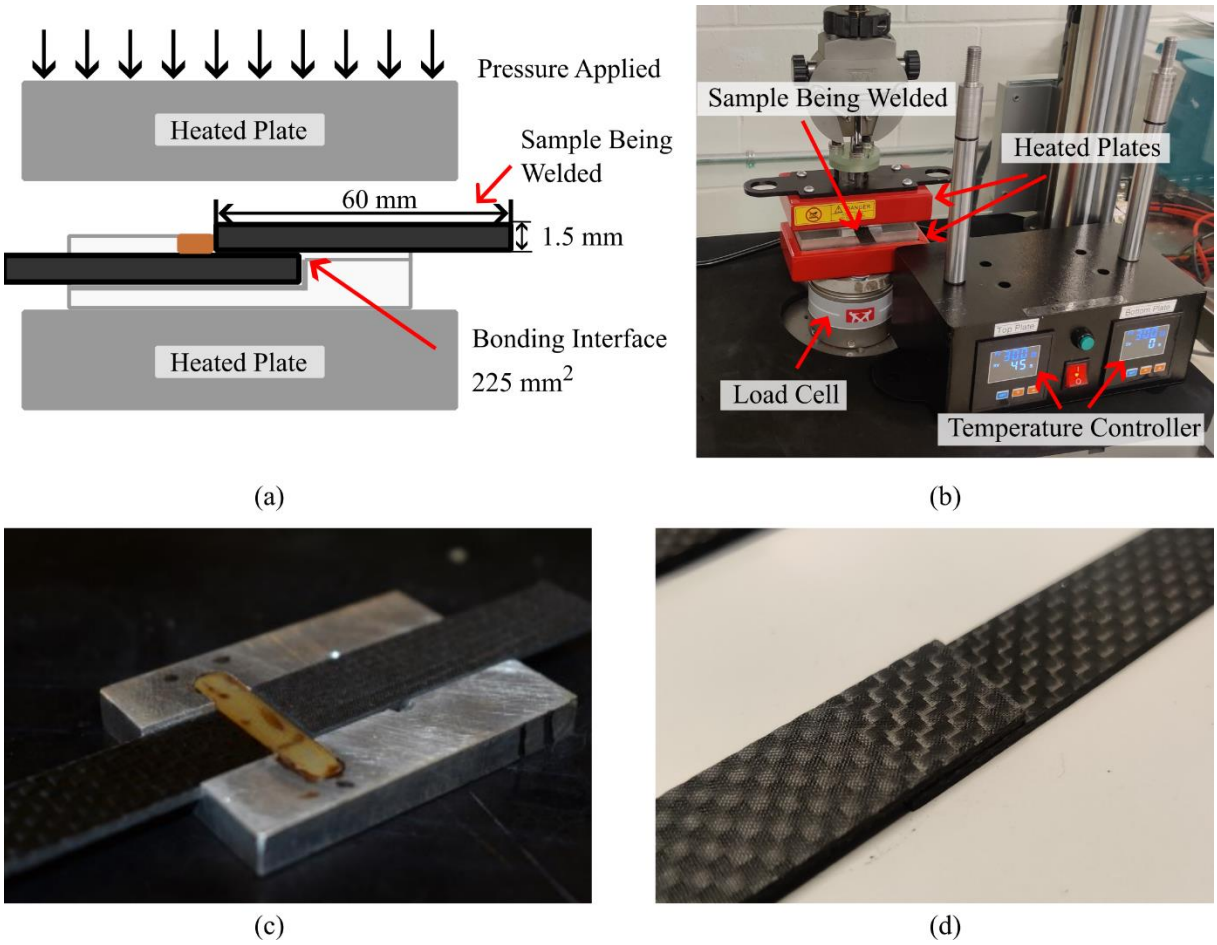

Figure 4-2: Conduction welding process for joining thermoplastic composite samples. (a) Schematic diagram of the welding process, showing the placement of the lap shear samples in an aluminum fixture between the two heated plates. (b) Actual laboratory setup with annotations showing the load cell used to measure compaction pressure and the temperature controller for the heated plates. (c) Custom aluminum fixture for welding lap shear samples. (d) Image of a lap shear joint manufactured using this process.

4.2.4 Thermal Analysis

An analytical model was used to predict the thermal profiles encountered within the bond line during the welding process. Utilizing a single-term approximation for a plane wall, this model predicts the core temperatures of lap shear joints mid-weld, predicated on the assumption of an instantaneously achieved, uniform surface temperature, matching that of the welding plates [22]. Other assumptions made in this thermal model are, neglecting thermal contact resistance, neglecting convective losses, and assuming the material's thermal properties remain constant

throughout the process. The values used in Equation 4-1 and Equation 4-2, calculations can be seen below in Table 4-2. The thermal diffusivity of the material was calculated to be $\alpha = 1.62\,E^{-7}\,\frac{m^2}{s}$ using Equation 4-1, where k is the through thickness thermal conductivity of the Carbon/Elium® composite, ρ is the density of the composite, and C_p is the specific heat capacity of the composite.

Table 4-2: Thermal Properties of Carbon/Elium® Composite

K (W/mK)	ρ (Kg/m^3)	Cp (J/KgK)	Lc (mm)	$A1$	λ_1	T_i (°C)	T_∞ (°C)
0.34 [23]	1500	1200 [23]	1.5 mm	1.2732	1.5708	20°C	120, 150, 180

$$\alpha = \frac{k}{\rho C_p} \qquad \textit{Equation 4-1}$$

The governing equation used to calculate the temperature along the bond line is detailed in Equation 4-3, where $T(x,t)$ is the temperature at any given point x within the material at time t, T_∞ is the boundary temperature which is assumed to be the temperature of the welding plates, T_i is the initial temperature of the material prior to welding which is assumed to be 20°C. L_c is the characteristic length of the system. A_1 and λ_1 are dimensionless constants based on the Biot number and were obtained from Table 4-2 [22]. Finally, τ is the Fourier number and can be seen in Equation 4-2 where α is the thermal diffusivity calculated in Equation 4-1, t is time, and L_c is the characteristic length of the system. To limit error in Equation 4-3 the one term approximation is only calculated for values of $\tau > 0.2$, therefor the analytical solution starts at time t = 2.6 [22].

$$\tau = \frac{\alpha t}{L_c} \qquad \textit{Equation 4-2}$$

$$\frac{T(x,t) - T_\infty}{T_i - T_\infty} = A_1 * e^{-{\lambda_1}^2 \tau} \cos(\lambda_1 * \frac{x}{L_c}) \qquad \textit{Equation 4-3}$$

To corroborate the reliability of the thermal model, temperatures were empirically measured with a thermocouple (K-Type Glass Braided, Adafruit, New York, USA) embedded in the center of a lap shear joint. The empirical data aligns closely with the analytical predictions, as depicted in Figure 4-3. A critical observation from the study is that, across all welding temperatures examined, the bond line attains 95% of the target temperature within 30 seconds of contact. With a welding time of 60 seconds used for all samples, this allows for an additional 30 seconds for the matrix to flow across the bond line and form a cohesive polymer structure.

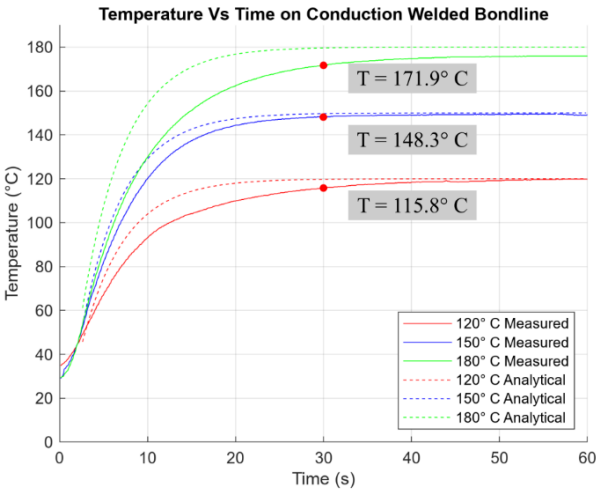

Figure 4-3: Comparison of measured and analytical temperature profiles of the bond line during conduction welding of lap shear joints.

4.2.5 Lap Shear Strength Testing

To assess the integrity and performance of the welded joints, lap shear testing was conducted using a universal testing frame (Electroplus E3000, Instron, Massachusetts, USA). Tension was applied to the samples at a constant rate of 2mm/min until failure.

4.2.6 Microscopy

Optical microscopy analyzed the bond interface of conduction welded samples. Additional lap shear samples welded at temperatures of 120°C, 150°C, and 180°C with 50 Bar pressure were examined to assess temperature effects on the bond line. After welding, samples underwent cross-sectional cutting with a cut-off saw (Presi, Mecatome T260, Grenoble, France) and were then mounted in epoxy (West systems 105, Michigan, USA), and polished to a 0.05-micron finish. An optical microscope (Axio Imager .M2, Zeiss, Oberkochen, Germany) captured images at 2.5x and 10x magnifications to inspect for porosity or incomplete welding along the bond line. This provided insights into the welding quality and the influence of temperature on the resulting bond integrity.

4.3 Results/Discussion

4.3.1 Ultimate Lap shear strength results

Figure 4-4 and Table 4-3 present the ultimate shear strength data of the welded samples across different bonding temperatures and compaction pressures. The data from this test show that higher temperatures and pressures result in higher bonding strength. The elevated temperatures appear to enhance bonding strength by reducing the viscosity of the Elium® thermoplastic resin, promoting better flow across the bond line which forms a cohesive polymer structure when cooled [24], [25]. The higher compaction pressures used in this study affected the bond line thickness of the conduction welded joints which resulted in higher strengths as well.

The 120°C welded samples exhibited the lowest shear strengths, with the highest average recorded at 4.38 ± 0.46 MPa for the 50 Bar condition, also displaying considerable variability indicative of inconsistent bonding. In contrast, welding at 150°C significantly improved shear strength, achieving a peak average of 11.34 ± 0.37 MPa at 50 Bar, due to reduced bond line porosity and

resultant cohesive structure. The highest average lap shear strength was observed in the 50 Bar 180°C samples, yielding 13.72 ± 0.63 MPa.

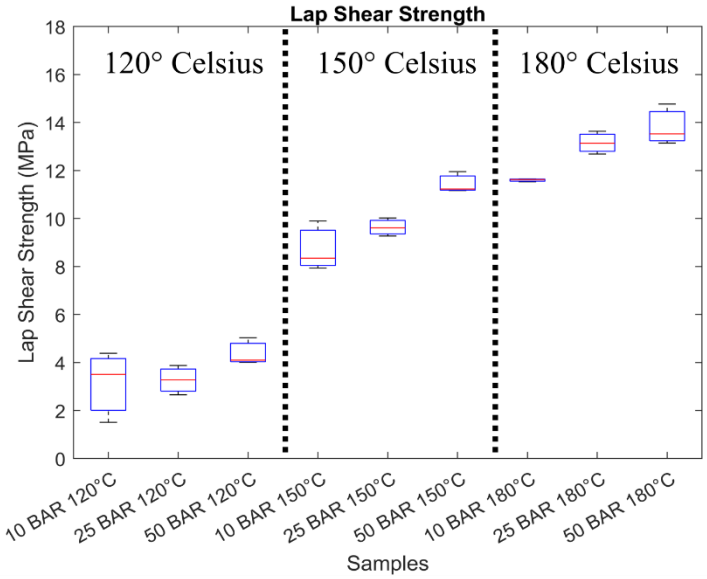

Figure 4-4: Boxplot showing the variation in lap shear strength (MPa) of conduction welded joints across different temperatures and compaction pressures. Each boxplot displays the median, quartiles, and range of the lap shear strength data collected under the specified welding parameters.

Table 4-3: Lap shear strength of each sample type of conduction welded joints in MPa

Sample Type	Lap Shear Strength (MPa)
10 Bar 120°C	3.17 ± 1.2
25 Bar 120°C	3.23 ± 0.49
50 Bar 120°C	4.38 ± 0.46
10 Bar 150°C	8.81 ± 0.87
25 Bar 150°C	9.74 ± 0.34
50 Bar 150°C	11.34 ± 0.37
10 Bar 180°C	11.65 ± 0.14
25 Bar 180°C	13.22 ± 0.36
50 Bar 180°C	13.72 ± 0.63

Comparing these results to the literature, in the paper by Bhudolia et al. [26],Carbon/Elium® composite lap shear joints were manufactured using an ultrasonic welding process with varying integrated energy directors, a method that involves expensive ultrasonic welding techniques and pre-formed energy directors molded into the joints. The lap shear strength of various energy director setups was evaluated, and the authors achieved lap shear strengths ranging from 11.2 MPa to 18.8 MPa, the latter figure underscoring the potential of their optimized approach. Furthermore, Bhudolia et al. concluded that increasing thickness in the bond line of the welds adversely affected the lap shear strength. This observation is consistent with other studies that explore the impact of bond line thickness on the lap shear strength of fusion bonded joints [27], further emphasizing the significance of optimizing welding parameters to achieve optimal joint strength.

4.3.2 Statistical Analysis

The influence of temperature and compaction pressure on the lap shear strength of conduction welded joints was examined through a two-way Analysis of Variance (ANOVA) calculated in MATLAB, the results of which are detailed in Table 4-4 [28]. The significance level used in this analysis to is $p < 0.05$. The analysis showed that temperature ($p < 0.001$) and compaction pressure ($p < 0.001$) both have statistically significant effects and are required to produce high lap shear strength joints. In contrast, the interaction between temperature and compaction pressure was not found to be statistically significant ($p = 0.3705$), indicating their effects are independent of each other. This independence implies that each parameter can be optimized separately to enhance the welding process.

To calculate the contribution percentage that each of the independent variables had on the lap shear strength the sum of squares of each variable is divided by the total sum of squares [29]. This calculation reveals that temperature is responsible for 93% of the variability in lap shear strength,

while compaction pressure contributes 3.89%. Given these findings, it is evident that temperature is the most influential parameter in the conduction welding process, making it a primary target for further optimization efforts.

Subsequent investigations into the conduction welding of other thermoplastic composites should therefore prioritize temperature control to maximize joint strength, which could lead to more efficient manufacturing processes and improved structural performance.

Table 4-4: Analysis of Variance result table

ANOVA Results	DOF	SS	MS	F	P	%
Temperature	2	404.70	202.35	344.63	<0.001	93.06
Compaction Pressure	2	16.94	8.47	14.42	<0.001	3.89
Temperature and Compaction Pressure	4	2.67	0.67	1.14	0.37	0.61
Error	18	10.57	0.59	-	-	2.43
Total	26	434.88	-	-	-	100.00

4.3.3 Bond Line Microscopy Images

Optical microscopy offers valuable insights into the impact of welding temperatures on thermoplastic composites, as shown in Figure 4-5 (a-f). In addition to this, Figure 4-5 (g-i) displays the fracture surfaces of the lap shear samples post-testing, revealing the variability in bonding quality as a result of variations in temperature. Figure 4-5 (g) demonstrates an obvious lack of bonding attributed to lower temperatures used in the welding process while Figure 4-5 (h) and (i) present cohesive fractures of the joints. These images, in tandem with the cross-sectional analyses, highlight the significant role of temperature in attaining a robust and uniform bond, with optimal

conditions minimizing porosity and achieving a suitable bond line thickness for enhanced joint integrity.

At 120°C under 50 Bar pressure, Figure 4-5 (a) and (d) reveal incomplete fusion at the bond line, characterized by pronounced porosity. This suggests that the temperature was insufficient to adequately lower the viscosity of the thermoplastic matrix, impeding the formation of a uniform and cohesive structure upon cooling.

At elevated temperatures of 150°C the welding outcomes differ significantly. Figure 4-5 (b), captured at 2.5X magnification, reveals a marked decrease in porosity compared to the lower temperature samples. The bond line integrity, as seen in Figure 4-5 (e), demonstrates a more uniform adhesion, indicating enhanced cohesive bonding between the thermoplastic matrix. The reduction in porosity can be attributed to a more fluid thermoplastic matrix at this temperature, allowing for better interlaminar diffusion and bonding and is ultimately responsible for the increased lap shear strength observed during testing.

Further increasing the temperature to 180°C, the samples presented in Figure 4-5 (c) and (f) continue the trend of porosity reduction. The bond line at this temperature appears to be homogenous, suggesting that a higher temperature facilitates a more effective thermoplastic flow and upon cooling, the resulting bond line shows very minimal porosity. Of note, in Figure 4-5 (c) the weft tows in the carbon fiber fabric appear to be displaced, squeezing out of the composite structure. This is theorized to result from the reduced viscosity of the matrix and high pressures applied to the samples during the welding process as only samples welded at 180°C with pressures of 25 Bar and above exhibit this deformation.

These observations underscore the critical role that temperature plays in determining the quality of welds in thermoplastic composites. Specifically, the weld quality is significantly influenced by two main factors: porosity and bond line thickness. It is clear that minimizing porosity is essential, as it helps to reduce stress concentrations and microcracks within the bond line, which are detrimental to the integrity of the joint. Furthermore, research by Gleich et al. [30] has highlighted the importance of bond line thickness, demonstrating that thicker bond lines can weaken the joint by increasing peak shear and peel stresses under load. They suggest an optimal bond line thickness of 0.2 mm to balance these effects.

The improvement in welding quality with increasing temperature—from a porous and incomplete bond to a smooth, cohesive interface—sheds light on the thermal dynamics of the welding process. This change suggests the presence of a temperature-dependent mechanism that promotes the diffusion and entanglement of polymer chains across the weld interface. Such a mechanism is key to forming a strong and uniform joint. By understanding the interplay between temperature, porosity, and bond line thickness, the welding processes can be optimized for various thermoplastic composites, aiming for the ideal conditions that produce the most durable and reliable bonds. Future work in this area to advance understanding could include the use of advanced imaging techniques such as micro computed tomography to precisely quantify the porosity and bond line thickness through the full bonding area. The long-term performance and durability of these welds also warrants further examination through fatigue testing to evaluate the lifespan of joints fabricated using the conduction welding method. Finally, the conduction welding process could be explored with different thermoplastic materials to compare their weldability and resulting performance characteristics.

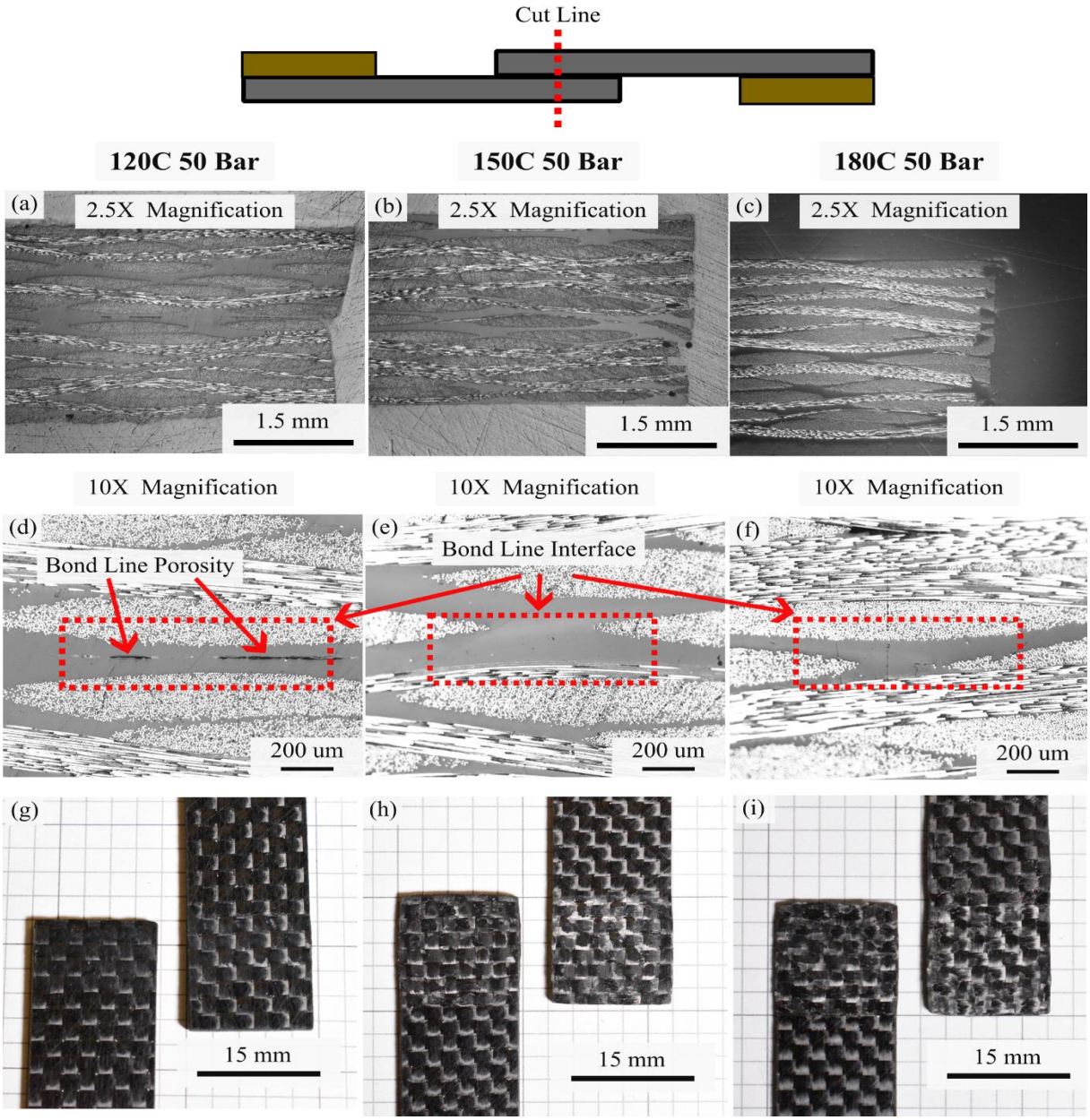

Figure 4-5: Examination of thermoplastic composite welds at various temperatures. (a)-(c) show the welds at 2.5X magnification for temperatures of 120°C, 150°C, and 180°C respectively under a constant pressure of 50 Bar, showing increased cohesion at the bond line for 150°C and 180°C samples. (d)-(f) shows 10X magnification of the bond line, highlighting porosity and interface quality at the different welding temperatures. (g)-(i) presents images of the samples after lap shear testing, displaying the surface textures. Each sample corresponds to the respective conditions above.

4.4 Conclusion

Fusion bonding of thermoplastic composites offers a rapid solution for joining composite materials, circumventing the traditional reliance on adhesives or mechanical fasteners. This study delves into the lap shear strength of joints between woven Carbon/Elium® composites that are fusion bonded, introducing a novel and cost-effective conduction welding technique. The investigation reveals that the welding parameters, specifically temperature and compaction pressure, significantly impact the strength of the resulting joints. Through careful analysis, optimal welding parameters have been identified, which are critical for maximizing joint efficacy. The study's findings underscore the potential of fusion bonding for joining thermoplastic composites. The following are the important findings from this research:

1. The optimal welding parameters found in this study were 50 Bar 180°C that produced an average lap shear strength of 13.72 ± 0.63 MPa.
2. High welding temperatures of 150 - 180°C ensure the thermoplastic matrix is sufficiently fluid allowing for polymer diffusion across the bonding line and result in a cohesive polymer matrix with minimal porosity.
3. High compaction pressures of 50 Bar promote polymer diffusion and decrease the bond line thickness, resulting in the increase of the lap shear strength.
4. Optical microscopy shows that low welding temperatures of 120°C produce incomplete welds with significant porosity found along the bond line.

4.5 References

[1] A. D. La Rosa, D. R. Banatao, S. J. Pastine, A. Latteri, and G. Cicala, "Recycling treatment of carbon fibre/epoxy composites: Materials recovery and characterization and environmental impacts through life cycle assessment," *Compos B Eng*, vol. 104, pp. 17–25, Nov. 2016, doi: 10.1016/j.compositesb.2016.08.015.

[2] D. S. Cousins, Y. Suzuki, R. E. Murray, J. R. Samaniuk, and A. P. Stebner, "Recycling glass fiber thermoplastic composites from wind turbine blades," *J Clean Prod*, vol. 209, pp. 1252–1263, Feb. 2019, doi: 10.1016/j.jclepro.2018.10.286.

[3] I. O. Oladele *et al.*, "Modern Trends in Recycling Waste Thermoplastics and Their Prospective Applications: A Review," *Journal of Composites Science*, vol. 7, no. 5. MDPI, May 01, 2023. doi: 10.3390/jcs7050198.

[4] N. Ramawat, N. Sharma, P. Yamba, and M. A. T. Sanidhi, "Recycling of polymer-matrix composites used in the aerospace industry-A comprehensive review," *Mater Today Proc*, Jun. 2023, doi: 10.1016/j.matpr.2023.05.386.

[5] S. K. Bhudolia and S. C. Joshi, "Low-velocity impact response of carbon fibre composites with novel liquid Methylmethacrylate thermoplastic matrix," *Compos Struct*, vol. 203, pp. 696–708, Nov. 2018, doi: 10.1016/j.compstruct.2018.07.066.

[6] R. Manaii, L. Guillaumat, S. Terekhina, and D. Duriatti, "behaviour and repair of flax/Elium biocomposites loaded in low velocity impact", doi: 10.5075/epfl-298799_978-2-9701614-0-0.

[7] G. Kinvi-Dossou *et al.*, "Innovative acrylic thermoplastic composites versus conventional composites: Improving the impact performances," *Compos Struct*, vol. 217, pp. 1–13, Jun. 2019, doi: 10.1016/j.compstruct.2019.02.090.

[8] Arkema, "Thermoplastic resin Elium® for recyclable composites." Accessed: Sep. 05, 2023. [Online]. Available: Thermoplastic resin Elium® for recyclable composites

[9] M. E. Kazemi, L. Shanmugam, D. Lu, X. Wang, B. Wang, and J. Yang, "Mechanical properties and failure modes of hybrid fiber reinforced polymer composites with a novel liquid thermoplastic resin, Elium®," *Compos Part A Appl Sci Manuf*, vol. 125, Oct. 2019, doi: 10.1016/j.compositesa.2019.105523.

[10] A. Yousefpour, M. Hojjati, and J. P. Immarigeon, "Fusion bonding/welding of thermoplastic composites," *Journal of Thermoplastic Composite Materials*, vol. 17, no. 4, pp. 303–341, Jul. 2004, doi: 10.1177/0892705704045187.

[11] C. Ageorges, L. Ye, and M. Hou, "Advances in fusion bonding techniques for joining thermoplastic matrix composites: a review," *Compos Part A Appl Sci Manuf*, vol. 32, no. 6, pp. 839–857, Jun. 2001, doi: 10.1016/S1359-835X(00)00166-4.

[12] J. Barroeta Robles, M. Dubé, P. Hubert, and A. Yousefpour, "Repair of thermoplastic composites: an overview," *Advanced Manufacturing: Polymer and Composites Science*,

vol. 8, no. 2. Taylor and Francis Ltd., pp. 68–96, 2022. doi: 10.1080/20550340.2022.2057137.

[13] R. Rudolf, P. Mitschang, and M. Neitzel, “Induction heating of continuous carbon-fibre-reinforced thermoplastics.” [Online]. Available: www.elsevier.com/locate/compositesa

[14] I. F. Villegas, L. Moser, A. Yousefpour, P. Mitschang, and H. E. N. Bersee, “Process and performance evaluation of ultrasonic, induction and resistance welding of advanced thermoplastic composites,” *Journal of Thermoplastic Composite Materials*, vol. 26, no. 8, pp. 1007–1024, Sep. 2013, doi: 10.1177/0892705712456031.

[15] K. Panneerselvam, S. Aravindan, and A. Noorul Haq, “Study on resistance welding of glass fiber reinforced thermoplastic composites,” *Mater Des*, vol. 41, pp. 453–459, Oct. 2012, doi: 10.1016/j.matdes.2012.05.025.

[16] M. Dubé, P. Hubert, J. N. A. H. Gallet, D. Stavrov, H. E. N. Bersee, and A. Yousefpour, “Metal mesh heating element size effect in resistance welding of thermoplastic composites,” *J Compos Mater*, vol. 46, no. 8, pp. 911–919, Apr. 2012, doi: 10.1177/0021998311412986.

[17] S. K. Bhudolia, G. Gohel, K. F. Leong, and A. Islam, “Advances in ultrasonic welding of thermoplastic composites: A review,” *Materials*, vol. 13, no. 6, Mar. 2020, doi: 10.3390/ma13061284.

[18] I. F. Villegas and G. Palardy, “Ultrasonic welding of thermoplastic composite coupons for mechanical characterization of welded joints through single lap shear testing,” *Journal of Visualized Experiments*, vol. 2016, no. 108, Feb. 2016, doi: 10.3791/53592.

[19] W. P. Seneviratne, J. S. Tomblin, and B. L. Saathoff, “influence of various surface preparation techniques on resistance welded and adhesively bonded unidirectional thermoplastic composite joints.”

[20] Arkema, “ELIUM ® 188 LIQUID THERMOPLASTIC RESIN TECHNICAL DATA SHEET.” [Online]. Available: http://www.arkema.com/en/products/product-safety/disclaimer/index.html

[21] ASTM International, “Standard Test Method for Lap Shear Adhesion for Fiber Reinforced Plastic (FRP) Bonding,” 2023, doi: 10.1520/D5868-01R23.

[22] Y. Cengel and A. Ghajar, *Heat and Mass Transfer Fundamentals and Applications*, vol. 5th. 2015.

[23] N. Han, I. Baran, J. S. M. Zanjani, O. Yuksel, L. L. An, and R. Akkerman, “Experimental and computational analysis of the polymerization overheating in thick glass/Elium® acrylic thermoplastic resin composites,” *Compos B Eng*, vol. 202, Dec. 2020, doi: 10.1016/j.compositesb.2020.108430.

[24] P. E. Baillagou and D. S. Soong, “a viscosity constitutive equation for pmma—mma solutions,” *Chem Eng Communications*, vol. 33, no. 1–4, pp. 125–134, Feb. 1985, doi: 10.1080/00986448508911164.

[25] C. B. Martinez and M. C. Williams, “Viscosity and Microstructure of Polyethylene-Poly(Methyl Methacrylate) Melt Blends: Some Simple Interpretations,” *J Rheol (N Y N Y)*, vol. 24, no. 4, pp. 421–450, Aug. 1980, doi: 10.1122/1.549595.

[26] S. K. Bhudolia, G. Gohel, J. Kantipudi, K. F. Leong, and R. J. Barsotti, “Ultrasonic welding of novel carbon/ Elium® thermoplastic composites with flat and integrated energy directors: Lap shear characterisation and fractographic investigation,” *Materials*, vol. 13, no. 7, Apr. 2020, doi: 10.3390/ma13071634.

[27] A. J. Smiley, M. Chao, and J. W. Gillespie, “Influence and control of bondline thickness in fusion bonded joints of thermoplastic composites,” *Composites Manufacturing*, vol. 2, no. 3–4, pp. 223–232, Jan. 1991, doi: 10.1016/0956-7143(91)90144-6.

[28] I. Milosan, “statistical processing of experimental data using analysis of variance,” *scientific research and education in the air force*, vol. 18, no. 1, pp. 489–496, Jun. 2016, doi: 10.19062/2247-3173.2016.18.1.67.

[29] D. Dairabayeva, A. Perveen, and D. Talamona, “Influence of Fused Filament Fabrication parameters on the flexural strength of Nylon-NC-ND,” 2023. [Online]. Available: www.sciencedirect.com

[30] D. M. Gleich, M. J. L. Van Tooren, and A. Beukers, “Analysis and evaluation of bondline thickness effects on failure load in adhesively bonded structures,” *J Adhes Sci Technol*, vol. 15, no. 9, pp. 1091–1101, 2001, doi: 10.1163/156856101317035503.

Chapter 5: Conclusions and Future Work

5.1 Conclusions

This thesis aimed to investigate the repairability of thermoplastic composites by utilizing conduction welding to apply repair patches. Thermoplastic composites exhibit a compelling alternative to traditional thermoset composite materials stemming from their environmental benefits and recyclability while retaining the advantages of composite materials such as their high strength to weight ratio. Furthermore, with the advent of liquid thermoplastic resins there now exists simplistic manufacturing methods that can be used to manufacture these more sustainable composite materials.

First this thesis presented a detailed literature review of the fundamentals of composite materials, their properties, and classifications. Next, a review of composite manufacturing techniques as well as composite repair methods was conducted investigating the differences in approach between thermoset and thermoplastic composites. Owing to the remeltable nature of thermoplastics, fusion bonding has become a new area of research in thermoplastic composites focusing on the joining of these materials without the use of adhesives. The various forms of fusion bonding are explored in depth to create a list of advantages and disadvantages for each technique. Relevant mechanical testing techniques were then explored, discussing tensile testing, open hole testing, and lap shear testing and the mechanical properties that they evaluate. DIC and its use in mechanical testing has grown in popularity in recent years because of its ability to measure strain on non-homogenous materials and generate full field strain maps over the surface of a sample. The literature review discussed this strain measurement technique in detail and reviewed current papers published on the topic. Finally, based on the literature study conducted, current gaps were identified. These gaps include defining the optimal size of the repair patch, quantifying what types of damage can be

repaired, how these repair patches can be applied, as well as detailed processing parameters for the conduction welding process. These parameters include the welding temperature, compaction pressure, and cycle time.

Chapter 3 assesses the repairability of a novel liquid thermoplastic (Elium® 188 O) in order to further enhance the sustainability of thermoplastic composites. In this chapter tensile testing was conducted to compare the strength of five types of samples, undamaged, damaged, repaired 12.5, repaired 25 and repaired 50. These samples were manufactured using the resin infusion technique, highlighting the benefits of liquid thermoplastics and their ability to be used with manufacturing techniques previously reserved for thermosets. The samples had a hole drilled in the center and then repair patches were applied using the conduction welding method. During tensile testing DIC was performed to provide full field strain measurements enabling a detailed analysis of the repair patches response to loading. It was found that the largest repair patch performed the best with a 55.4% strength recovery compared to the undamaged samples. Further lap shear testing was performed showing an average ultimate shear strength of 8.6 MPa. The fracture behavior of the conduction welded regions were analyzed and determined to fail cohesively, indicating a strong bond between the sample and repair patch. These results led to further analysis of the conduction welding process in an attempt to increase the shear strength of the conduction welded samples. This was further evaluated in chapter 4 in order to fill gaps in the existing literature surrounding the conduction welding process.

Chapter 4 aimed to optimize the welding process to increase the lap shear strength of liquid thermoplastic composites (Carbon/Elium®) joined through conduction welding. To accomplish this, the investigation explored welding temperatures of 120°C, 150°C, and 180°C, along with compaction pressures of 10, 25, and 50 Bar, to fabricate nine different types of lap shear samples.

Among these parameters, temperature emerged as the critical factor and the combination of 180°C and 50 Bar yielding the highest lap shear strength of 13.72 ± 0.63 MPa. Optical microscopy conducted on the bonded joints illuminated the impact of temperature on the welding process, revealing how variations in welding temperatures significantly influence the integrity of the welds. Low welding temperatures were seen to produce incomplete welds with significant porosity along the bond line and diminished lap shear strength. Conversely, joints manufactured under higher welding temperatures and pressures displayed a cohesive polymer matrix along the bond line with minimal void content, which resulted in significantly higher lap shear strengths. The effectiveness of high temperatures and pressures in the welding process can be attributed to the resultant lower viscosity of the polymer melt, which facilitates polymer diffusion along the bond line and ensures a high-strength joint.

5.2 Future Work

This thesis explores the process of conduction welding liquid thermoplastic composites to apply repair patches in a straightforward and economic way. Despite the progress made, there still exists research gaps in this field that can be explored in future work.

One promising avenue for further research is in the optimization of the shape of the applied repair patch. The overarching aim of this area of research would be to devise a patch design that not only covers the damaged area but also significantly mitigates stress concentrations at the repair site, thereby improving the overall efficacy of the repair. While the concept of stress concentration reduction has been previously explored, as noted in studies by Mahandi et al [1], these investigations primarily concentrated on halting crack progression in thermoset composites. Therefore, there exists room for future work to extend this theory to thermoplastic composites, examining how different patch shapes and sizes influence the stress distribution and integrity of the repaired area. This research could be performed through a combination of computational modeling and experimental validation, aiming to identify optimal patch geometries that work with the unique properties of thermoplastic materials. Additionally, this research could assist in developing standardized guidelines for patch shape optimization in various industrial applications, and ultimately making a significant contribution to the field of composite material repair.

Further investigation into the Elium® resin and its mechanical properties presents a promising avenue for research, particularly as it fills significant gaps in current academic literature regarding this new material. Specifically, thermogravimetric analysis could be utilized to characterize its thermal properties and ascertain the degradation temperature. This property would assist in determining the maximum processing temperatures allowable during various fusion bonding processes. Additionally, rheological studies could be conducted to measure the viscosity of the

resin melt and analyze its behavior under various shear rates. Additionally, employing Fourier-transform infrared spectroscopy would aid in identifying the chemical structure and composition of the Elium® resin. These investigative approaches would collectively advance the current understanding of this resin and fill important gaps in the literature regarding this material.

Another area of research that could be further expanded is the conduction welding of various other thermoplastic composite materials. This study focused on the welding of PMMA based liquid thermoplastic composites, however, the conduction welding process could be expanded to a host of other thermoplastic materials used in thermoplastic composites to such as Polyethylene, Polyamide, and PAEK. This research could assist in filling gaps in the literature regarding the process of conduction welding and provide guidance for optimal processing parameters to achieve high strength joints.

Finally, the recyclability of thermoplastic composites is another important area that will require further research to truly enable the replacement of thermoset composite materials. While the feasibility of recycling thermoplastic composites on the lab scale has been demonstrated by researchers such as Cousins et al [2], there remains a need to expand this to a larger industrial scale. This expansion of scale is necessary to understand the viability and efficiency of recycling processes in real world scenarios. One promising approach to this recyclability is through chemical dissolution, enabling recovery of both fibers and matrix materials. This process not only facilitates the recycling of these components but holds economic benefits as the materials can be resold to generate profits for the recyclers. The expansion of this research would assist in reducing the environmental impact of composite materials through the reuse of these materials by reducing waste materials.

5.3 References

[1] M. Rachid, B. Serier, B. Bachir Bouiadjra, and M. Belhouari, “Numerical analysis of the patch shape effects on the performances of bonded composite repair in aircraft structures,” *Compos B Eng*, vol. 43, no. 2, pp. 391–397, Mar. 2012, doi: 10.1016/j.compositesb.2011.08.047.

[2] D. S. Cousins, Y. Suzuki, R. E. Murray, J. R. Samaniuk, and A. P. Stebner, “Recycling glass fiber thermoplastic composites from wind turbine blades,” *J Clean Prod*, vol. 209, pp. 1252–1263, Feb. 2019, doi: 10.1016/j.jclepro.2018.10.286.